

THE RESPONSE TO TIDAL FLUCTUATIONS OF TWO
NON-HOMOGENEOUS COASTAL AQUIFER MODELS

by
John A. Williams
and
Ta-Chiang Liu

Technical Report No. 51

September 1971

Partial Project Completion Report

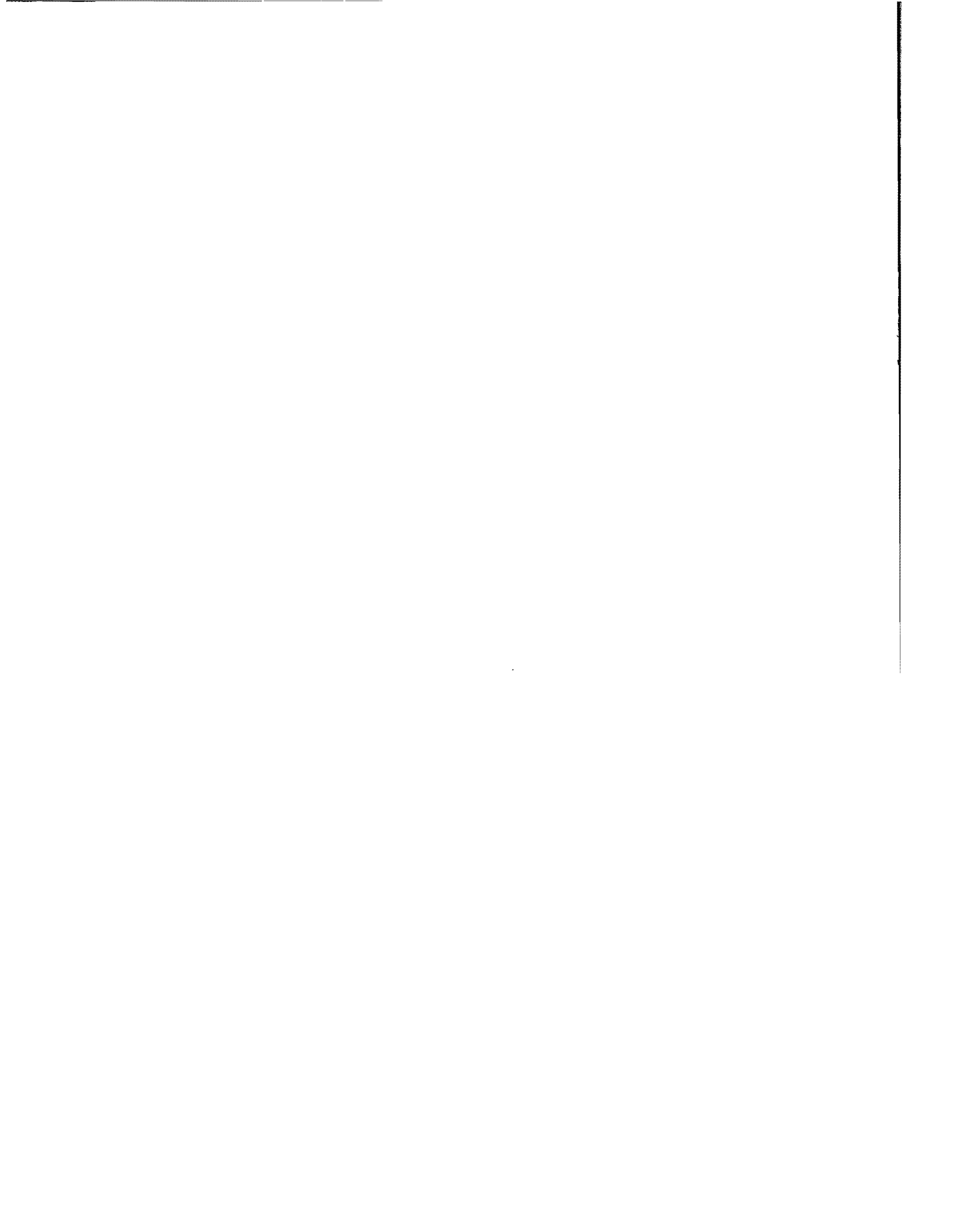
of

ANALOG SIMULATION OF TIDAL EFFECTS ON GROUND WATER AQUIFERS
OWRR PROJECT NO. A-020-HI, GRANT AGREEMENT NO. 14-31-0001-3211

PRINCIPAL INVESTIGATORS: JOHN A. WILLIAMS, DOAK C. COX,
AND L. STEPHEN LAU

PROJECT PERIOD: JULY 1, 1969 to JUNE 30, 1972

The programs and activities described herein were supported in part by funds provided by the United States Department of the Interior as authorized under the Water Resources Act of 1964, Public Law 88-379.

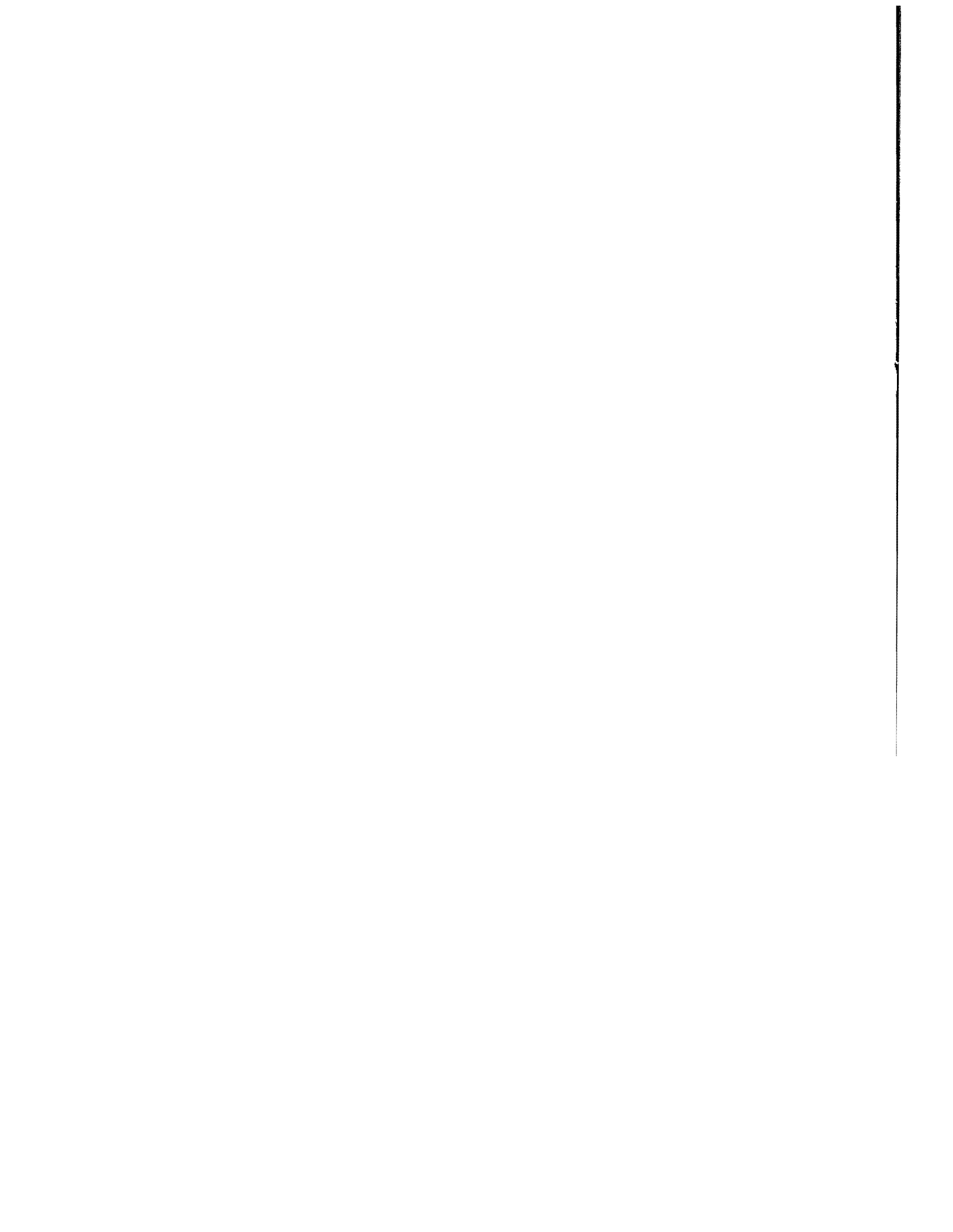


ABSTRACT

Mathematical and electric analog (R-C circuit) models for two one-dimensional non-homogeneous coastal aquifers have been developed. The first is a semi-infinite aquifer having a discontinuous change in permeability at a distance L from the coastline and the second is an aquifer of length L whose permeability changes linearly with distance from the coastline and whose interior boundary represents either a constant head or a no-flow condition. Both models were subjected to a sinusoidal tidal input.

Results, in the form of graphs of amplitude and phase angle vs position, show excellent agreement between the outputs of the mathematical and electric analog models. In the case of a discontinuous permeability, these graphs indicate a positive or negative reflection from the discontinuity for a decrease or increase, respectively, in the permeability. In the case of the linearly varying permeability model, the graphs of amplitude indicate that energy is attenuated at a greater rate near the coastline when $K_L/K_0 < 1$ for both types of boundary condition. Graphs of the phase angle are concave downwards for the constant-head boundary condition but for the no-flow condition they exhibit a point of inflection whose position depends on t_0 and K_L/K_0 .

Electric analog model results show that for the semi-infinite aquifer no significant error will result from the circuit configuration if $a \leq \lambda/50$ and the circuit length is equivalent to 2λ , furthermore, "lumped" components, i.e., $a = \lambda/5$, may be used to extend the circuit beyond $x = -.4\lambda$ if measurements are restricted to $x \geq -.2\lambda$.



CONTENTS

LIST OF FIGURES.....	v
LIST OF TABLES.....	vii
INTRODUCTION.....	1
THEORETICAL CONSIDERATIONS.....	1
The Mathematical Model.....	1
The Electric Analog Model.....	8
EXPERIMENTAL CONSIDERATIONS.....	9
Experimental Set-up.....	9
Experimental Procedure.....	10
PRESENTATION OF THE RESULTS.....	13
DISCUSSION OF THE RESULTS AND THE CONCLUSIONS.....	37
ACKNOWLEDGEMENTS.....	43
REFERENCES.....	44
APPENDICES.....	45

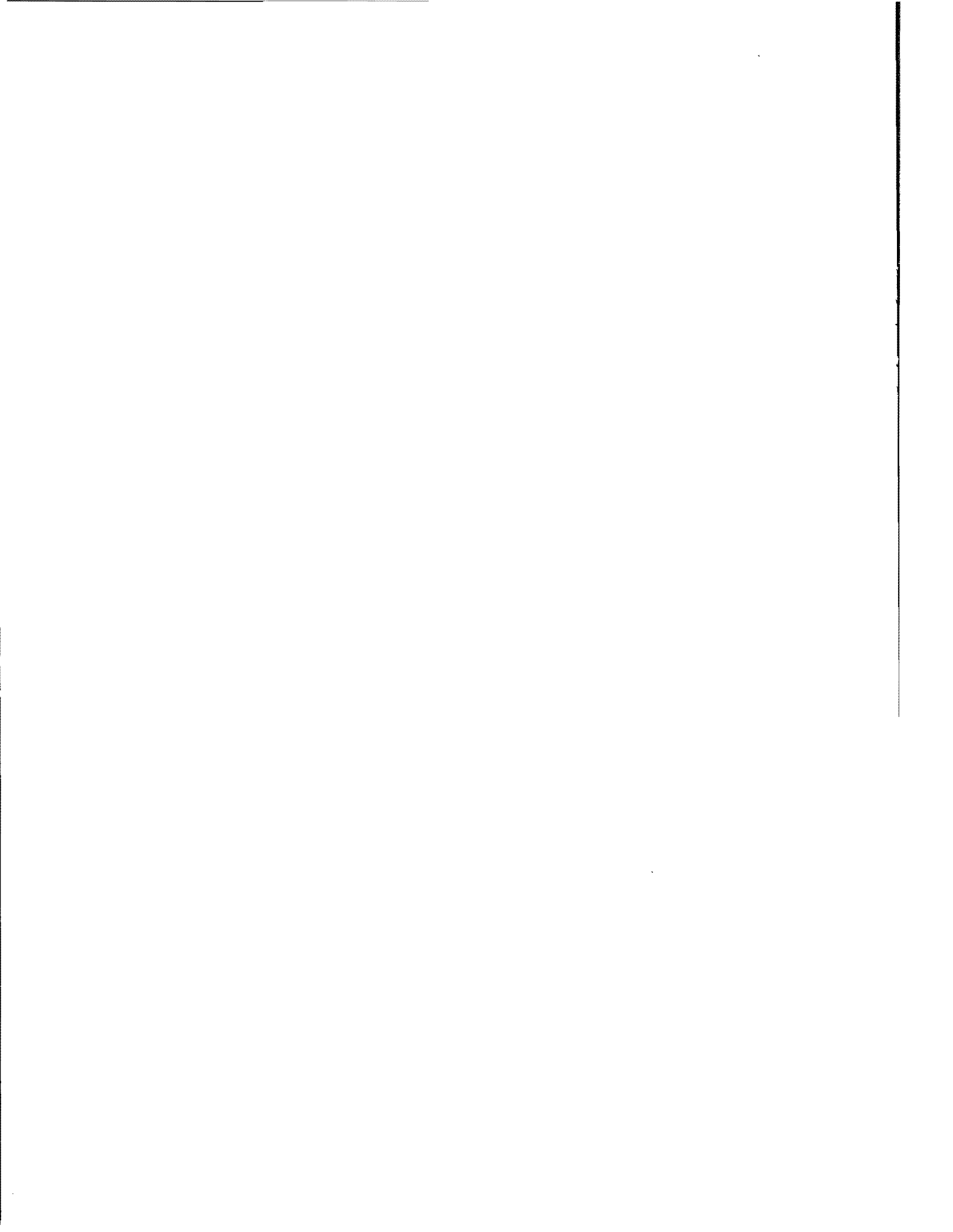
LIST OF FIGURES

1. Photographs of the experimental apparatus.....	11
2. Circuit diagrams for the discontinuous permeability and the linearly varying permeability electric analog models.....	12
3. Amplitude and phase angle v_s x/L for a coastal aquifer with a discontinuous permeability: $r^2 = 0.5$	15
4. Amplitude and phase angle v_s x/L for a coastal aquifer with a discontinuous permeability: $r^2 = 0.8$	16
5. Amplitude and phase angle v_s x/L for a coastal aquifer with a discontinuous permeability: $r^2 = 1.25$	17
6. Amplitude and phase angle v_s x/L for a coastal aquifer with a discontinuous permeability: $r^2 = 1.5$	18
7. Comparison of the math model for an aquifer of infinite extent (equations 8, with $r = 1$) with electric analog model results for several open-end circuit configurations.....	19
8. Amplitude and phase angle v_s x/L for a coastal aquifer with a no-flow boundary condition at $x = 0$ and a linearly varying permeability: $K = 0.1(1+(1/2)x)$ ft/sec.....	21

9.	Amplitude and phase angle <i>vs</i> x/L for a coastal aquifer with a no-flow boundary condition at $x = 0$ and a linearly varying permeability: $K = 0.3(1-(1/6)x)$ ft/sec.....	22
10.	Amplitude and phase angle <i>vs</i> x/L for a coastal aquifer with a no-flow boundary condition at $x = 0$ and a linearly varying permeability: $K = 0.1(1+(3/4)x)$ ft/sec.....	23
11.	Amplitude and phase angle <i>vs</i> x/L for a coastal aquifer with a no-flow boundary condition at $x = 0$ and a linearly varying permeability: $K = 0.4(1-(3/16)x)$ ft/sec.....	24
12.	Amplitude and phase angle <i>vs</i> x/L for a coastal aquifer with a no-flow boundary condition at $x = 0$ and a linearly varying permeability: $K = 0.1(1+x)$ ft/sec.....	25
13.	Amplitude and phase angle <i>vs</i> x/L for a coastal aquifer with a no-flow boundary condition at $x = 0$ and a linearly varying permeability: $K = 0.5(1-(1/5)x)$ ft/sec.....	26
14.	Amplitude and phase angle <i>vs</i> x/L for a coastal aquifer with a constant-head boundary condition at $x = 0$ and a linearly varying permeability: $K = 0.1(1+(1/2)x)$ ft/sec.....	27
15.	Amplitude and phase angle <i>vs</i> x/L for a coastal aquifer with a constant-head boundary condition at $x = 0$ and a linearly varying permeability: $K = 0.3(1-(1/6)x)$ ft/sec.....	28
16.	Amplitude and phase angle <i>vs</i> x/L for a coastal aquifer with a constant-head boundary condition at $x = 0$ and a linearly varying permeability: $K = 0.1(1+(3/4)x)$ ft/sec.....	29
17.	Amplitude and phase angle <i>vs</i> x/L for a coastal aquifer with a constant-head boundary condition at $x = 0$ and a linearly varying permeability: $K = 0.4(1-(3/16)x)$ ft/sec.....	30
18.	Amplitude and phase angle <i>vs</i> x/L for a coastal aquifer with a constant-head boundary condition at $x = 0$ and a linearly varying permeability: $K = 0.1(1+x)$ ft/sec.....	31
19.	Amplitude and phase angle <i>vs</i> x/L for a coastal aquifer with a constant-head boundary condition at $x = 0$ and a linearly varying permeability: $K = 0.5(1-(1/5)x)$ ft/sec.....	32
20.	Comparison of math model results for aquifers having $K = 0.1(1+mx)$ ft/sec: $m = 1/2, 0, -1/6$, for $t_0 = 1.5$ sec and a no-flow boundary condition.....	33
21.	A comparison of the phase angle <i>vs</i> position relation for several values of r and t_0 for the discontinuous permeability model.....	34
22.	Comparison of electric analogs having an image circuit and an open circuit to simulate a no-flow boundary condition with math model DAMP for $r = 0$ and $r = 1$	35
A-1.	Sketch defining the aquifer models analyzed.....	49

LIST OF TABLES

1. Summary of conditions for discontinuous permeability model.....14
2. Summary of conditions for linearly changing permeability model....14
3. Penetration lengths for semi-infinite aquifer in region 2.....39



INTRODUCTION

Model studies of the response to tidal fluctuations of isotropic and homogeneous coastal aquifers having a simple boundary geometry have been made by Williams, *et al.* (1970). These studies indicated that diffusion theory could be used as the basis for analytical representation of the physical phenomenon provided that the correct diffusion coefficient was used. This result in turn justified the use of the electric analog model as a research tool for the confined aquifer and for unconfined aquifers where the Dupuit assumptions hold.

The generally good results from the model studies provided the motivation for this current research which is being conducted in several phases. This report presents the results of Phase I, which have concentrated on the development of mathematical and electric analog models for two non-homogeneous, one-dimensional coastal aquifers, since it is the non-homogeneous condition which is most likely to be encountered in practice. The two types considered here are a semi-infinite aquifer having a discontinuous change in permeability at a distance L from the coastline and a finite aquifer of length L with a permeability which varies linearly with distance from the coastline.

THEORETICAL CONSIDERATIONS

The Mathematical Model

Laminar flow through a porous media when streamline curvatures in any vertical plane are small is represented by the expressions

$$\nabla \cdot (Kz\nabla h) = zS_s \frac{\partial h}{\partial t} \quad (1a)$$

and

$$\nabla \cdot (Kz\nabla h) = \epsilon' \frac{\partial h}{\partial t} \quad (1b)$$

where equations (1a) and (1b) apply to a confined and unconfined upper water surface, respectively. In the above equations $z(x, y)$ is the thickness of the saturated zone, $h(x, y)$ is the piezometric head, $K(x, y)$ is the Darcy coefficient of permeability, ϵ' is an apparent porosity, and S_s is the specific storage (*i.e.*, $w_0 (\alpha + \epsilon/\beta)$).

If the flow does not vary in the y direction, if the thickness of the saturated zone is a constant \bar{z} for a confined upper surface or

varies only slightly from an average value \bar{z} for an unconfined upper surface, and if the time variation is periodic, *i.e.*, $h(x, t) = R (\eta(x) e^{i\sigma t})$, then equations (1a) and (1b) reduce to

$$\frac{d}{dx} \left(\bar{z} K(x) \frac{d}{dx} \eta(x) \right) - i\bar{z}\sigma D\eta = 0 \quad (2)$$

Here, D is either S_s for the confined condition or ε'/\bar{z} for the unconfined condition. Equation (2) provides a basis for the investigation of one-dimensional flows where the medium is non-homogeneous. A list of definitions of the symbols used together with sketches of the aquifer models analyzed is included in Appendix A.

First, consider the case where the Darcy permeability changes suddenly. Thus, in region 1, $0 \leq x \leq L$, $K = K_1$ and in region 2, $-\infty \leq x \leq 0$, $K = K_2$ and the "coastline" is located at $x = L$. Equation (2) must be solved in both regions with the conditions that the piezometric head must be continuous at $x = 0$ and that conservation of mass at $x = 0$ is satisfied. That is, in both regions 1 and 2

$$\frac{d^2}{dx^2} \eta_j - i\sigma \frac{D_j}{K_j} \eta_j = 0, \quad j = 1 \text{ or } 2 \quad (3a)$$

and at $x = 0$

$$\eta_1 = \eta_2 \quad (3b)$$

and

$$\left(K\bar{z} \frac{d\eta}{dx} \right)_1 = \left(K\bar{z} \frac{d\eta}{dx} \right)_2 \quad (3c)$$

The additional boundary condition at $x = L$ is

$$\eta_1(L) = \zeta_0 \sin \sigma t = R \left(-i\zeta_0 e^{i\sigma t} \right) \quad (3d)$$

The solution to equation (3a) is known (Williams, *et al.*, 1970) to be

$$\eta_j(x) = C_{j1} e^{\sqrt{i\alpha_j}x} + C_{j2} e^{-\sqrt{i\alpha_j}x}$$

where

$$C_{j1} = a_{j1} + ib_{j1}; \quad C_{j2} = a_{j2} + ib_{j2}; \quad \alpha_j = \sigma \frac{D_j}{K_j} = 2\psi_j^2 \quad ^1$$

¹ This latter definition is introduced for convenience in writing the lengthy equations which follow.

Thus, the expression for the piezometric head becomes

$$\begin{aligned}
 h(x,t) &= R (\eta(x) e^{i\sigma t}) \\
 &= \left\{ e^{\psi_j x} (a_{j1} \cos \psi_j x - b_{j1} \sin \psi_j x) + e^{-\psi_j x} (a_{j2} \cos \psi_j x \right. \\
 &\quad \left. + b_{j2} \sin \psi_j x) \right\} \cos \sigma t - \left\{ e^{\psi_j x} (a_{j1} \sin \psi_j x + b_{j1} \cos \psi_j x) \right. \\
 &\quad \left. + e^{-\psi_j x} (-a_{j2} \sin \psi_j x + b_{j2} \cos \psi_j x) \right\} \sin \sigma t \quad (4)
 \end{aligned}$$

In region 2 the position variable x may approach negative infinity, hence, $a_{22} = b_{22} = 0$. This leaves six constants of integration, a_{11} , a_{12} , b_{11} , b_{12} , a_{21} , and b_{21} , to be determined from the three boundary conditions given by equations (3b), (3c), and (3d). Application of these boundary conditions generates the following set of equations:

$$a_{11} + a_{12} + 0 + 0 - a_{21} + 0 = 0 \quad (5a)$$

$$0 + 0 + b_{11} + b_{12} + 0 - b_{21} = 0 \quad (5b)$$

$$a_{11} - a_{12} - b_{11} + b_{12} - r a_{21} + r b_{21} = 0 \quad (5c)$$

$$a_{11} - a_{12} + b_{11} - b_{12} - r a_{21} - r b_{21} = 0 \quad (5d)$$

$$\begin{aligned}
 e^{\psi_1 L} C(\psi_1 L) a_{11} + e^{-\psi_1 L} C(\psi_1 L) a_{12} - e^{\psi_1 L} S(\psi_1 L) b_{11} + e^{-\psi_1 L} S(\psi_1 L) b_{12} \\
 + 0 + 0 = 0 \quad (5e)
 \end{aligned}$$

$$\begin{aligned}
 e^{\psi_1 L} S(\psi_1 L) a_{11} - e^{-\psi_1 L} S(\psi_1 L) a_{12} + e^{\psi_1 L} C(\psi_1 L) b_{11} + e^{-\psi_1 L} C(\psi_1 L) b_{12} \\
 + 0 + 0 = -\zeta_0 \quad (5f)
 \end{aligned}$$

where $C \equiv$ cosine, $S \equiv$ sine, and $r = (K_2 \bar{z}_2 / K_1 \bar{z}_1)^{1/2}$. Equations (5a) and (5b) follow from equation (3b), (5c) and (5d) from (3c), and (5e) and (5f) from 3d).

Solving this system for the unknown coefficients yields the relations:

$$a_{21} = \frac{2}{r+1} a_{11} \quad (6a)$$

$$b_{21} = \frac{2}{r+1} b_{11} \quad (6b)$$

$$a_{12} = \frac{1-r}{1+r} a_{11} \quad (6c)$$

$$b_{12} = \frac{1-r}{1+r} b_{11}$$

$$a_{11} = \frac{-\zeta_0 Q}{p^2 + Q^2} \quad (6e)$$

$$b_{11} = \frac{-\zeta_0 P}{p^2 + Q^2} \quad (6f)$$

where P and Q are given by

$$P = C(\psi_1 L) \left(e^{\psi_1 L} + \frac{1-r}{1+r} e^{-\psi_1 L} \right)$$

$$Q = S(\psi_1 L) \left(e^{\psi_1 L} - \frac{1-r}{1+r} e^{-\psi_1 L} \right)$$

If equations (6c, d, e, f) are substituted into equation (4) the result for region 1 is

$$h_1(x,t) = \left\{ \zeta_0 / (P^2 + Q^2) \right\} \left\{ e^{\psi_1(x+L)} \sin(\psi_1(x-L) + \sigma t) \right. \\ \left. + \left(\frac{1-r}{1+r} \right) e^{\psi_1(x-L)} \sin(\psi_1(x+L) + \sigma t) \right. \\ \left. - \left(\frac{1-r}{1+r} \right) e^{-\psi_1(x-L)} \sin(\psi_1(x+L) - \sigma t) \right. \\ \left. - \left(\frac{1-r}{1+r} \right)^2 e^{-\psi_1 L(x+L)} \sin(\psi_1(x-L) - \sigma t) \right\}. \quad (7)$$

From equation (7) it is apparent that as r approaches 1, only a single left-traveling disturbance of amplitude $\zeta_0 e^{\psi_1(x-L)}$ remains, which is consistent with previous results (Williams, *et al.*, 1970) for uniform aquifers of infinite length.

A second form of equation (7) which is more convenient to use and to interpret may be formed by substituting equation (6) into equation (4), and expressing $h(x,t)$ in terms of an amplitude and phase angle. After considerable algebraic manipulation, the result is

$$h_1(x,t) = \zeta_0 \rho(x,r,L) \sin(\sigma t - \theta_p), \quad (8a)$$

where

$$\rho(x,r,L) = \sqrt{\frac{A_0 + A_1 r + A_2 r^2 + A_3 r^3 + A_4 r^4}{[(C^2(\psi_1 L) + \text{Sh}^2(\psi_1 L)) + 2r \text{Ch}(\psi_1 L) \text{Sh}(\psi_1 L) + r^2 (S^2(\psi_1 L) + \text{Sh}^2(\psi_1 L))]}^2} \quad (8b)$$

with

$$A_0 = (C^2(\psi_1 x) + \text{Sh}^2(\psi_1 x)) (C^2(\psi_1 L) + \text{Sh}^2(\psi_1 L)) \equiv (A_0, x) (A_0, L)$$

$$A_1 = 2\text{Ch}(\psi_1 x) \text{Sh}(\psi_1 x) (A_0, L) + 2\text{Ch}(\psi_1 L) \text{Sh}(\psi_1 L) (A_0, x)$$

$$A_2 = 4\text{Ch}(\psi_1 x) \text{Ch}(\psi_1 L) \text{Sh}(\psi_1 x) \text{Sh}(\psi_1 L) + (A_4, x) (A_0, L) + (A_4, L) (A_0, x)$$

$$A_3 = 2\text{Ch}(\psi_1 x) \text{Sh}(\psi_1 x) (A_4, L) + 2\text{Ch}(\psi_1 L) \text{Sh}(\psi_1 L) (A_4, x)$$

$$A_4 = (S^2(\psi_1 x) + \text{Sh}^2(\psi_1 x)) (S^2(\psi_1 L) + \text{Sh}^2(\psi_1 L)) \equiv (A_4, x) (A_4, L) \quad (8c)$$

and

$$\tan \theta_p = \frac{A_0 + A_1 r + A_2 r^2}{\beta_0 + \beta_1 r + \beta_2 r^2} \quad (8d)$$

with

$$\begin{aligned}
 A_0 &= C(\psi_1 x) \operatorname{Ch}(\psi_1 x) S(\psi_1 L) \operatorname{Sh}(\psi_1 L) - C(\psi_1 L) \operatorname{Ch}(\psi_1 L) S(\psi_1 x) \operatorname{Sh}(\psi_1 x), \\
 A_1 &= C(\psi_1 x) S(\psi_1 L) \operatorname{Sh}(\psi_1 x) \operatorname{Sh}(\psi_1 L) + C(\psi_1 x) \operatorname{Ch}(\psi_1 x) \operatorname{Ch}(\psi_1 L) S(\psi_1 L) \\
 &\quad - C(\psi_1 L) S(\psi_1 x) \operatorname{Sh}(\psi_1 x) \operatorname{Sh}(\psi_1 L) - C(\psi_1 L) \operatorname{Ch}(\psi_1 x) \operatorname{Ch}(\psi_1 L) S(\psi_1 x), \\
 A_2 &= C(\psi_1 x) \operatorname{Ch}(\psi_1 L) S(\psi_1 L) \operatorname{Sh}(\psi_1 x) - C(\psi_1 L) \operatorname{Ch}(\psi_1 x) S(\psi_1 x) \operatorname{Sh}(\psi_1 L), \\
 \beta_0 &= S(\psi_1 x) \operatorname{Sh}(\psi_1 x) S(\psi_1 L) \operatorname{Sh}(\psi_1 L) + C(\psi_1 x) \operatorname{Ch}(\psi_1 x) C(\psi_1 L) \operatorname{Ch}(\psi_1 L), \\
 \beta_1 &= C(\psi_1 x) C(\psi_1 L) \operatorname{Ch}(\psi_1 x) \operatorname{Sh}(\psi_1 L) + C(\psi_1 x) C(\psi_1 L) \operatorname{Ch}(\psi_1 L) \operatorname{Sh}(\psi_1 x) \\
 &\quad + \operatorname{Ch}(\psi_1 L) S(\psi_1 x) S(\psi_1 L) \operatorname{Sh}(\psi_1 x) + \operatorname{Ch}(\psi_1 x) S(\psi_1 x) S(\psi_1 L) \operatorname{Sh}(\psi_1 L), \\
 \beta_2 &= C(\psi_1 x) C(\psi_1 L) \operatorname{Sh}(\psi_1 x) \operatorname{Sh}(\psi_1 L) + \operatorname{Ch}(\psi_1 x) \operatorname{Ch}(\psi_1 L) S(\psi_1 x) S(\psi_1 L), \\
 &\hspace{15em} (8e)
 \end{aligned}$$

where Sh and Ch represent the hyperbolic sine and hyperbolic cosine, respectively.

Note that equations (7) and (8) apply not only to aquifers with a discontinuous change in permeability, but also to unconfined aquifers which have a discontinuous change in their average depth or a change in both depth and permeability at the same point, since $r = (K_2 \bar{z}_2 / K_1 \bar{z}_1)^{1/2}$.

Equations (8a to 8e) may be checked by investigating several limiting cases:

Case 1. Let r approach 0. Then either K_2 is very small compared with K_1 or \bar{z}_2 is very small compared with \bar{z}_1 . This corresponds to an aquifer which is permeable on the range $0 \leq x \leq L$ and which has a no-flow condition at $x = 0$. Equations (8a to 8e) reduce to the appropriate solution for these conditions (see Williams, *et al.*, 1970).

Case 2. Let r approach infinity. Then either K_2 is very large compared to K_1 or \bar{z}_2 is very large compared to \bar{z}_1 . This corresponds to an aquifer which is permeable on the range $0 \leq x \leq L$ and has a constant-head boundary condition at $x = 0$. Equations (8) reduce to the appropriate solution for these conditions (see Williams, *et al.*, 1970).

Case 3. Let r approach unity. This corresponds to a single, semi-infinite aquifer of uniform thickness and permeability, as mentioned above. Equations (8) reduce to the appropriate solution for this case.

It should be pointed out that equation (7) also reduces to the appropriate forms when the above-mentioned limits are taken.

If equations (6a and 6b) are substituted into equation (4) with $C_{22} = a_{22} + ib_{22} = 0$, the result gives the piezometric head as a function of (x,t) in region 2. That is,

$$h_2(x,t) = \left\{ 2\zeta_0 / [(1+r)(P^2 + Q^2)] \right\} \left\{ e^{\psi_2(x+rL)} \sin(\psi_2(x-rL) + \sigma t) + \frac{1-r}{1+r} e^{\psi_2(x-rL)} \sin(\psi_2(x+rL) + \sigma t) \right\}. \quad (9)$$

The alternative form of this expression in terms of amplitude and phase angles is

$$h_2(x,t) = \zeta_0 \rho(x,r,L) \sin(\sigma t - \theta_p), \quad (10a)$$

where

$$\rho(x,r,L) = \frac{\zeta_0 e^{\psi_2 x}}{[(C^2(\psi_1 L) + \text{Sh}^2(\psi_1 L)) + 2r \text{Ch}(\psi_1 L) \text{Sh}(\psi_1 L) + r^2 (S^2(\psi_1 L) + \text{Sh}^2(\psi_1 L))]^{1/2}} \quad (10b)$$

and

$$\tan \theta_p = \frac{C(\psi_2 x) S(\psi_1 L) \text{Sh}(\psi_1 L) - C(\psi_1 L) \text{Ch}(\psi_1 L) S(\psi_2 x) + r(C(\psi_2 x) \text{Ch}(\psi_1 L) S(\psi_1 L) - C(\psi_1 L) S(\psi_2 x) \text{Sh}(\psi_1 L))}{C(\psi_2 x) C(\psi_1 L) \text{Ch}(\psi_1 L) + S(\psi_2 x) S(\psi_1 L) \text{Sh}(\psi_1 L) + r(C(\psi_2 x) C(\psi_1 L) \text{Sh}(\psi_1 L) + \text{Ch}(\psi_1 L) S(\psi_2 x) S(\psi_1 L))} \quad (10c)$$

Again, several limiting cases can be investigated to check equations (9) and (10):

Case 1. Let r approach infinity. Then $h(x,t)$ vanishes as it should for a "constant head" condition at $x = 0$.

Case 2. Let r approach unity. Then $h(x,t)$ again reduces to a single left-traveling wave of amplitude $\zeta_0 e^{\psi_2(x-L)}$.

Case 3. Let r approach zero for $x = 0$. Equations (8b, 8d) and (10b, 10c) yield consistent values for the amplitude and the phase angles.

A second problem which can be analyzed is one where the permeability varies linearly with position. If

$$K = K_0 + m'x = K_0(1 + mx) \quad (11)$$

for $0 \leq x \leq 1$ and if a new variable is defined by

$$\xi = 1 + mx \quad (12)$$

then equation (2) takes the form

$$\frac{d}{d\xi} \left(\xi \frac{d\eta}{d\xi} \right) - \frac{i\sigma D}{m^2 K_0} \eta = 0 \quad (13)$$

Equation (13) is a modified Bessel's Equation and has a solution of the form

$$\eta(\xi) = C_1 I_0(i^{1/2}\sqrt{4\alpha\xi}) + C_2 K_0(i^{1/2}\sqrt{4\alpha\xi}), \quad (14)$$

where

$$\alpha = \frac{\sigma D}{m^2 K_0}, \text{ and } C_1 \text{ and } C_2 \text{ are complex constants.}$$

The following boundary conditions

$$\left. \frac{\partial h}{\partial x} \right|_{x=0} = 0 \text{ or } C_1 I_1(i^{1/2}\sqrt{4\alpha}) + C_2 K_1(i^{1/2}\sqrt{4\alpha}) = 0 \quad (15a)$$

and

$$h(L,t) = \zeta_0 \sin \sigma t \text{ or } \eta(L) = -i\zeta_0, \quad L = 1 + mL \quad (15b)$$

require that a no-flow condition exist at the internal boundary ($x = 0$) and that the piezometric surface vary as $\sin \sigma t$ at the "coastline" where ζ_0 is the amplitude of the tidal change.

Imposing these conditions on equation (14) gives the following expression for η :

$$\eta(x) = \frac{-i\zeta_0 [-K_1(i^{1/2}\sqrt{4\alpha}) I_0(i^{1/2}\sqrt{4\alpha\xi}) + I_1(i^{1/2}\sqrt{4\alpha}) K_0(i^{1/2}\sqrt{4\alpha\xi})]}{[I_1(i^{1/2}\sqrt{4\alpha}) K_0(i^{1/2}\sqrt{4\alpha L}) - K_1(i^{1/2}\sqrt{4\alpha}) I_0(i^{1/2}\sqrt{4\alpha L})]} \quad (16)$$

The functions K_0 and I_0 are complex quantities and may be expressed by the equations:

$$I_0(i^{1/2}x) = M_0(x) e^{i\theta_0(x)} \quad (17a)$$

$$K_0(i^{1/2}x) = N_0(x) e^{i\phi_0(x)} \quad (17b)$$

Substituting equations (17) into equation (16), multiplying the results by $e^{i\sigma t}$ and taking the real part of the product produces the desired expression for the piezometric surface. That is,

$$h(\xi, t) = \zeta_0 \rho(\xi, L) \sin(\sigma t + \theta p) \quad (18a)$$

where

$$\rho(\xi, L) = \sqrt{\frac{N_1^2(\bar{\psi})M_0^2(\psi) + M_1^2(\bar{\psi})N_0^2(\psi) - 2M_1(\bar{\psi})N_1(\bar{\psi})M_0(\psi)N_0(\psi) \cos \left\{ \begin{array}{l} \theta_0(\psi) \\ -\theta_1(\bar{\psi}) - (\phi_0(\psi) - \phi_1(\bar{\psi})) \end{array} \right\}}{N_1^2(\bar{\psi})M_0^2(\bar{\psi}_1) + M_1^2(\bar{\psi})N_0^2(\bar{\psi}_1) - 2M_1(\bar{\psi})N_1(\bar{\psi})M_0(\bar{\psi}_1)N_0(\bar{\psi}_1) \cos \left\{ \begin{array}{l} \theta_0(\bar{\psi}_1) \\ -\theta_1(\bar{\psi}) - (\phi_0(\bar{\psi}_1) - \phi_1(\bar{\psi})) \end{array} \right\}}}} \quad (18b)$$

$$\tan\theta_p = \frac{-A\sin[(\theta_0(\psi)-\theta_1(\bar{\psi}))-(\phi_0(\bar{\psi}_1)-\phi_1(\bar{\psi}))]+B\sin[\phi_0(\psi)-\phi_0(\bar{\psi}_1)]}{+C\sin[\theta_0(\psi)-\theta_0(\bar{\psi}_1)]-D\sin[(\phi_0(\psi)-\phi_1(\bar{\psi}))-(\theta_0(\bar{\psi}_1)-\theta_1(\bar{\psi}))]} \\ -A\cos[(\theta_0(\psi)-\theta_1(\bar{\psi}))-(\phi_0(\bar{\psi}_1)-\phi_1(\bar{\psi}))]+B\cos[\phi_0(\psi)-\phi_0(\bar{\psi}_1)] \\ +C\cos[\theta_0(\psi)-\theta_0(\bar{\psi}_1)]-D\cos[(\phi_0(\psi)-\phi_1(\bar{\psi}))-(\theta_0(\bar{\psi}_1)-\theta_1(\bar{\psi}))]} \quad (18c)$$

with

$$\begin{aligned} A &= M_0(\psi) N_0(\bar{\psi}_1) M_1(\bar{\psi}) N_1(\bar{\psi}) \\ B &= M_1^2(\bar{\psi}) N_0(\bar{\psi}_1) N_0(\psi) \\ C &= M_0(\bar{\psi}_1) M_0(\psi) N_1^2(\bar{\psi}) \\ D &= M_0(\bar{\psi}_1) M_1(\bar{\psi}) N_0(\psi) N_1(\bar{\psi}) \end{aligned}$$

and $\psi = \sqrt{4\alpha\xi}$, $\bar{\psi} = \sqrt{4\alpha}$, $\bar{\psi}_1 = \sqrt{4\alpha l}$

A constant head boundary condition at $x = 0$ ($\xi = 1$) requires that

$$\eta(1) = C_1 I_0(i^{1/2}\sqrt{4\alpha}) + C_2 K_0(i^{1/2}\sqrt{4\alpha}) = 0 \quad (19)$$

Thus, for this boundary condition, the piezometric surface is expressed by equations (18), provided all the "1" subscripts are replaced with "0" subscripts.

In the preceding, $h(x,t)$ is referenced from its equilibrium surface.

The Electric Analog Model

The electric analog model is based on the analogy between electric current flowing in a resistance-capacitance circuit and water flowing through a resistive porous media. An analysis (see Williams, *et al.*, 1970 or Walton and Prickett, 1963) gives the following relation for the time scale ratio between the two systems:

$$K_4 = \frac{a^2 S}{CRT} \quad (20)$$

Here, K_4 is the ratio of time in the hydraulic system to time in the electrical system, S is the storage, T is the transmissability (ft^2/sec), R is the electrical resistance (ohms), C is the capacitance (farads) and a is a length in the hydraulic model.

In the case of a linear variation of K with position the transmissability becomes

$$T = \bar{z}K = \bar{z}K_0(1 + mx), \quad m = (K_L/K_0 - 1)/L \quad (21)$$

where K_0 and K_L are the permeabilities at the internal boundary and the coastline, respectively, and \bar{z} and L are the thickness and length of the aquifer, respectively. Then, the value of T at any one of N evenly spaced points along the aquifer is

$$T_n = \bar{z}K_0 \left[\frac{2N + mL(2n-1)}{2N} \right] ; n = 1, \dots, N \quad (22)$$

Expressing $\bar{z}K_0$ in terms of T_N , equation (22) can be written

$$T_n = T_N \left[\frac{2N + mL(2n-1)}{2N + mL(2N-1)} \right] ; n = 1, \dots, N \quad (22a)$$

As R is inversely proportional to T , then

$$R_n = R_N \left[\frac{2N + mL(2N-1)}{2N + mL(2n-1)} \right] ; n = 1, \dots, N \quad (23)$$

Therefore, the product RT in equation (20) is a constant and can be taken as $R_N T_N$. Equation (23) may be used to calculate the R_n for a given R_N where R_N in the electric analog model corresponds to the resistance encountered in a particular length $L/N = a$ in the porous media.

For the discontinuous aquifer, the product RT is the same for both regions 1 and 2; therefore

$$R_2 = (T_1/T_2) R_1 = \left(\frac{1}{r^2}\right) R_1 \quad (24)$$

EXPERIMENTAL CONSIDERATIONS

Experimental Set-Up

The electric analog model of the aquifer of linearly varying permeability consisted of a set of 20, single-turn, 0 to 300 ohm, 2 watt, potentiometers mounted on a piece of 8 1/2" x 17" vector board. The potentiometers were placed in series with a .01 μ f capacitor connecting the junction between two adjacent potentiometers to ground, except at the first and last (nineteenth) junction where .015 μ f capacitors were used. The circuit was excited with a General Radio (#1310-A) audio oscillator and a Hewlett-Packard (#122a) dual-trace oscilloscope monitored the input at the "coastline" and the response at a given point ($x_n = na$). For a no-flow boundary condition at $x = 0$, the first half of the circuit (*i.e.*, the first ten potentiometers and corresponding capacitors) constituted the aquifer

while the second half provided an "image" aquifer in which that portion of the input reflected from the no-flow boundary could be developed. For the constant-head boundary condition, only the first half of the circuit was used.

The analog circuit for the discontinuous aquifer utilized the same piece of hardware described above to model that portion of the aquifer extending from $x = -L$ to the coastline at $x = L$ with the location of the discontinuity at $x = 0$. This circuit was then extended to $x = -2L$ with an array of components similar to those representing the aquifer on $-L \leq x \leq L$ and from $-10L \leq x \leq -2L$ with eight resistors and capacitors, each representing the resistance and storage encountered in a length L of region 2 in the aquifer. This circuit was also excited with the audio oscillator and the input and output monitored on the dual-trace oscilloscope.

Figure 1 presents photographs of the experimental apparatus. Figure 2 shows the circuit diagrams for the two electric analog models described above.

Experimental Procedure

The experimental procedure for both models was essentially identical. For the linearly varying permeability model, R_N was selected first, then the remainder of the variable resistances were adjusted according to equation (23). Next, the time scale factor was determined from equation (20) for a selected value of ϵ/T and the electrical frequencies calculated for a selected tidal period. The final step involved adjusting the audio-oscillator to the calculated frequency, and then observing on the oscilloscope the amplitude of the input and the amplitude and the phase of the response at the desired point ($x_n = an$).

For the discontinuous permeability model, R_2 was fixed first and R_1 determined from equation (24). The remainder of the procedure was identical to that described above.

For both models the values of N and a were 10 and 0.4 feet,

¹This method of simulating the no-flow boundary condition was used here for comparison with the simpler technique of leaving an open circuit at the interior end of the analog model (see Fig. 22). Both techniques give similar results, but the open circuit is more practical, especially when two or three dimensions are involved (see for example, Walton and Prickett, 1963).

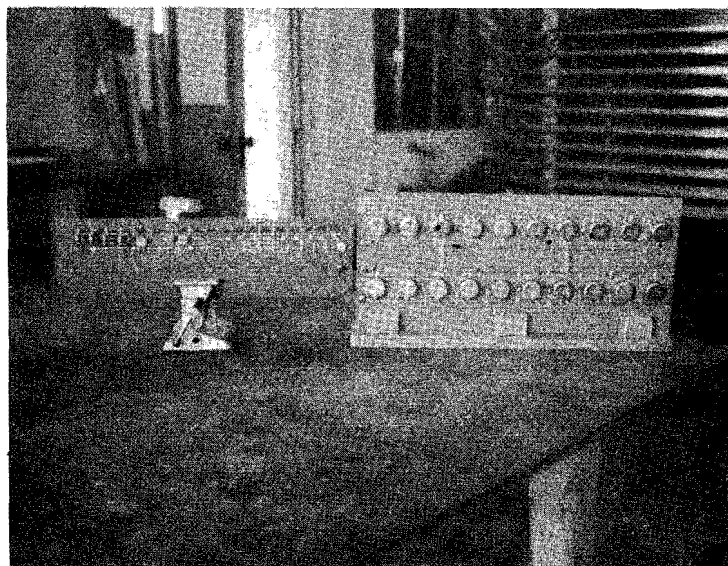
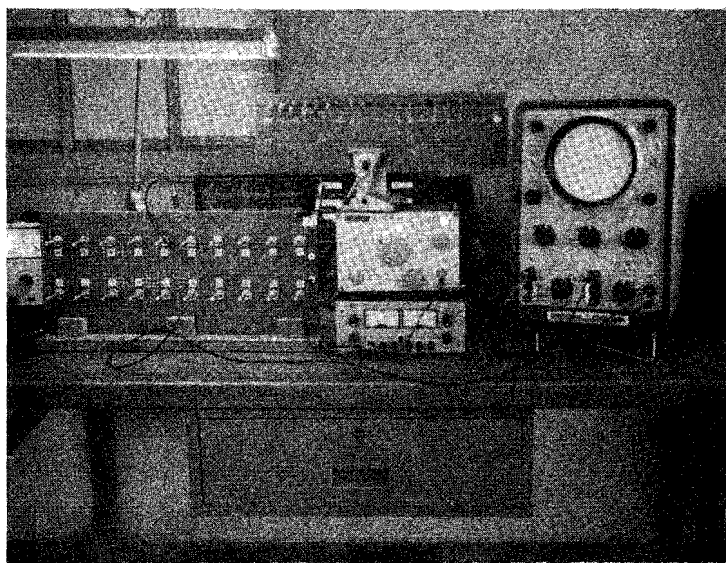
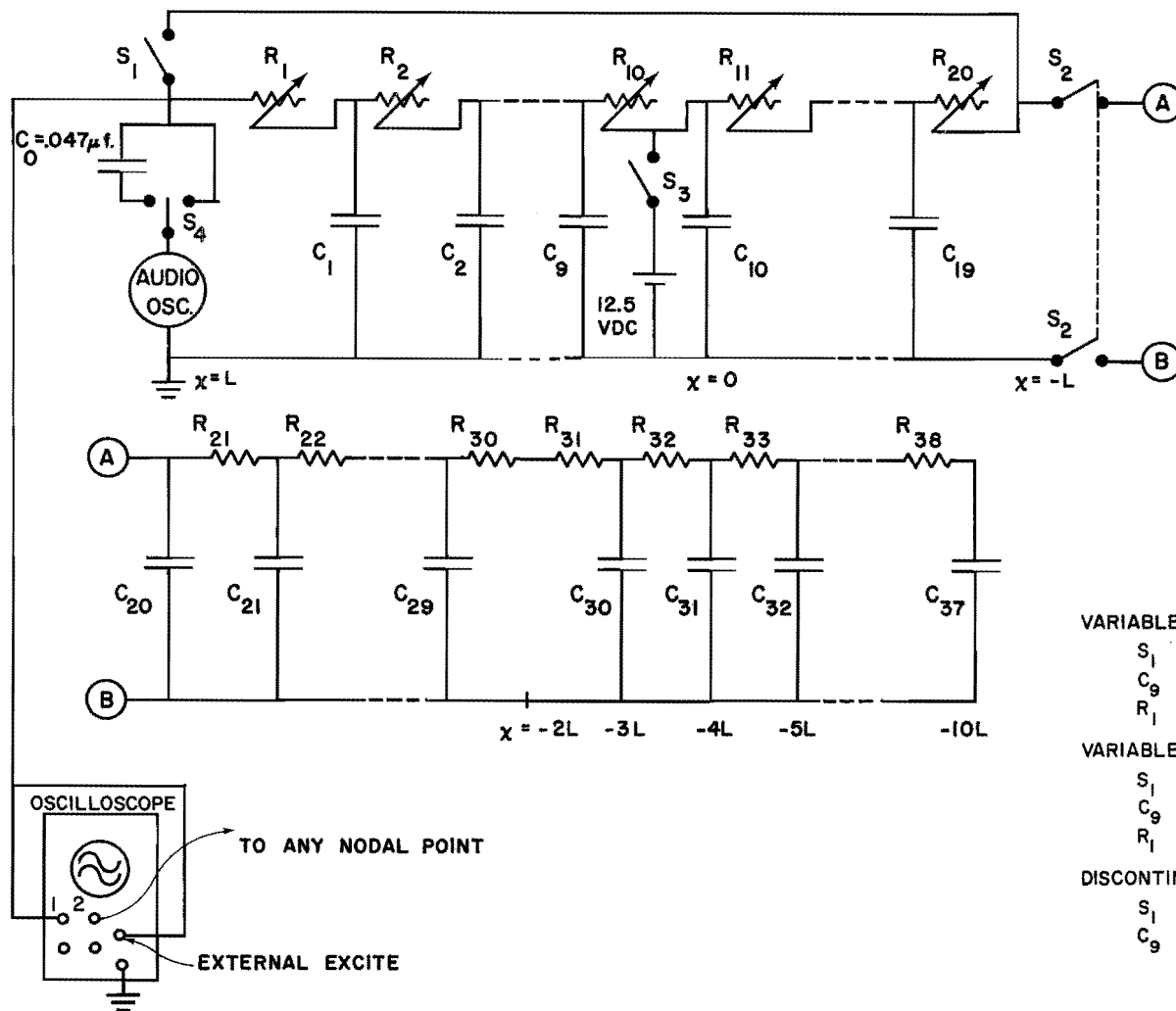


FIGURE 1. PHOTOGRAPHS OF THE
EXPERIMENTAL APPARATUS.



- S_1 = SINGLE POLE SWITCH
 S_2 = DOUBLE POLE SWITCH
 S_3 = SINGLE POLE SWITCH
 S_4 = TWO POSITION SWITCH
 $C_1 = C_{29} = 0.015 \mu f.$
 $C_2 = \dots = C_8 = C_{10} = \dots = C_{18} = 0.01 \mu f.$
 $C_{20} = \dots = C_{28} = 0.01 \mu f.$
 $C_{30} = \dots = C_{37} = 0.1 \mu f.$
 $R_{21} = \dots = R_{30} = 200 \Omega$
 $R_{31} = \dots = R_{38} = 2000 \Omega$

VARIABLE PERMEABILITY MODEL, NO FLOW B.C.

S_1 CLOSED, S_2 AND S_3 OPEN.

$C_9 = 0.01 \mu f.$, $C_{19} = 0.015 \mu f.$; C_0 OUT OF CIRCUIT

R_1 TO R_{20} FROM EQUATION 23.

VARIABLE PERMEABILITY MODEL, CONSTANT HEAD B.C.

S_1 AND S_2 OPEN, S_3 CLOSED.

$C_9 = 0.015 \mu f.$, C_0 IN CIRCUIT.

R_1 TO R_{10} FROM EQUATION 23.

DISCONTINUOUS PERMEABILITY MODEL

S_1 AND S_3 OPEN, S_2 CLOSED, C_0 OUT OF CIRCUIT.

$C_9 = C_{19} = 0.01 \mu f.$; R_1 TO R_{10} FROM EQUATION 24,

R_{11} TO $R_{20} = 200 \Omega.$

FIGURE 2. CIRCUIT DIAGRAMS FOR THE DISCONTINUOUS PERMEABILITY AND THE LINEARLY VARYING PERMEABILITY ELECTRIC ANALOG MODELS.

respectively, and the amplitude of the "tide" was set at 3.5 volts for all tests.

PRESENTATION OF THE RESULTS

The results are presented as plots of the dimensionless amplitude ρ and the phase angle θ_p versus the dimensionless position x/L .

Experimental values of ρ were determined by taking the ratio of the double amplitude of the voltage fluctuation at each x_n to the double amplitude of the input at the coastline. Both amplitudes were scaled off the wave form traces on the oscilloscope. Similarly, the phase angles were determined as the ratio of the distance between the peaks of the input and the response fluctuations to the distance separating two successive peaks of the input. Distances on the oscilloscope screen could be estimated to within ± 1 mm which corresponds to an accuracy of ± 0.1 volts for the amplitudes and ± 6 degrees for the phase angles.

The mathematical models were evaluated on the IBM 360 digital computer, which calculated ρ and θ_p at predetermined values of x for each tidal period selected. Amplitudes and phase angles for the discontinuous aquifer, represented by equations (8b), (8d), (10b), and (10c) were calculated only to $x = -L$ in region 2, and are plotted in Figures 3 through 6 as the solid line curves. Figure 7 shows the effect of extending the circuit to include the region $x \leq -L$ and of the "lumping" together of the individual resistors and capacitors corresponding to a length L of the media for $r = 1$ and a tidal period $t_0 = 3$ sec.

The results for the linearly varying permeability model represented by equations (18b), (18c), and (19) are presented as the solid line curves in Figures 8 through 19. Figures 8 through 13 pertain to the no-flow boundary condition at $x = 0$ and Figures 14 through 19 pertain to the constant-head boundary condition at $x = 0$. The corresponding electric analog results are indicated on these same plots by the individual data points at each x_n . Since the amplitude curves for the constant-head boundary condition are so close together, only the electric analog results for the two extreme periods used have been included in Figures 14 to 19.

Figure 20 presents a comparison of the variation of the amplitude and phase angle with x/L for $K_L/K_0 = 0.3/0.1$, $K_L/K_0 = 0.1/0.1$ and $K_L/K_0 = 0.1/0.3$ for $t_0 = 1.5$ sec.

Figure 21 shows the effect on the phase angle of the value of r , *i.e.*, of the amount of positive or negative reflection at the section where K changes discontinuously.

Finally, Figure 22 shows the effect of using both an open circuit and an image circuit to simulate a no-flow boundary condition and compares these results with DAMP for $r = 1.0$, a semi-infinite aquifer, and for $r = 0$, an aquifer of length $2L$ with a no-flow boundary.

Summaries of the values of the significant parameters are given in Tables 1 and 2. The following quantities and their indicated

TABLE 1. SUMMARY OF CONDITIONS* FOR DISCONTINUOUS PERMEABILITY MODEL.

K_1 FT/SEC	K_2 FT/SEC	r^2	R_1 OHMS	R_2 OHMS	K_4	t_0 SEC	FIG. NO.
0.1	0.05	0.5	100	200	16,000	0.75, 1.5, 3, 6, 9	3
0.1	0.08	0.8	160	200	10,000	0.75, 1.5, 3, 6, 9	4
0.1	0.125	1.25	250	200	6,400	0.75, 1.5, 3, 6, 9	5
0.1	0.150	1.50	300	200	5,333	0.75, 1.5, 3, 6, 9	6
0.1	0.1	1.0	200	200	8,000	3	7

* THE INDICATED VALUES FOR THE FOLLOWING QUANTITIES WERE USED IN ALL CALCULATIONS:
 $D = \epsilon'/\bar{z} = .01$, $a = 0.4$ FT., $L = 4.0$ FT., $C = .01\mu\text{f}$.

TABLE 2. SUMMARY OF CONDITIONS* FOR LINEARLY CHANGING PERMEABILITY MODEL.

K_0 FT/SEC	K_1 FT/SEC	m FT ⁻¹	R_0 OHMS	R_1 OHMS	K_4	t_0 SEC	B.C. AT X = 0	
							NO-FLOW	CONST. HEAD
0.1	0.3	1/2	264	100	5517	1.5, 3, 6, 9	FIG. 8	FIG. 14
0.3	0.1	-1/6	100	264	5517	1.5, 3, 6, 9	" 9	" 15
0.1	0.4	3/4	268	80	5200	1.5, 3, 6, 9	" 10	" 16
0.4	0.1	-3/16	80	268	5200	1.5, 3, 6, 9	" 11	" 17
0.1	0.5	1	280	70	4762	1.5, 3, 6, 9	" 12	" 18
0.5	0.1	-1/5	70	280	4762	1.5, 3, 6, 9	" 13	" 19
0.1	0.1	0	264	264	6060	1.5, 3, 6	" 20	

* THE INDICATED VALUES FOR THE FOLLOWING QUANTITIES WERE USED IN ALL CALCULATIONS:
 $D = \epsilon'/\bar{z} = .01$, $a = 0.4$ FT., $L = 4.0$ FT., $C = .01\mu\text{f}$.

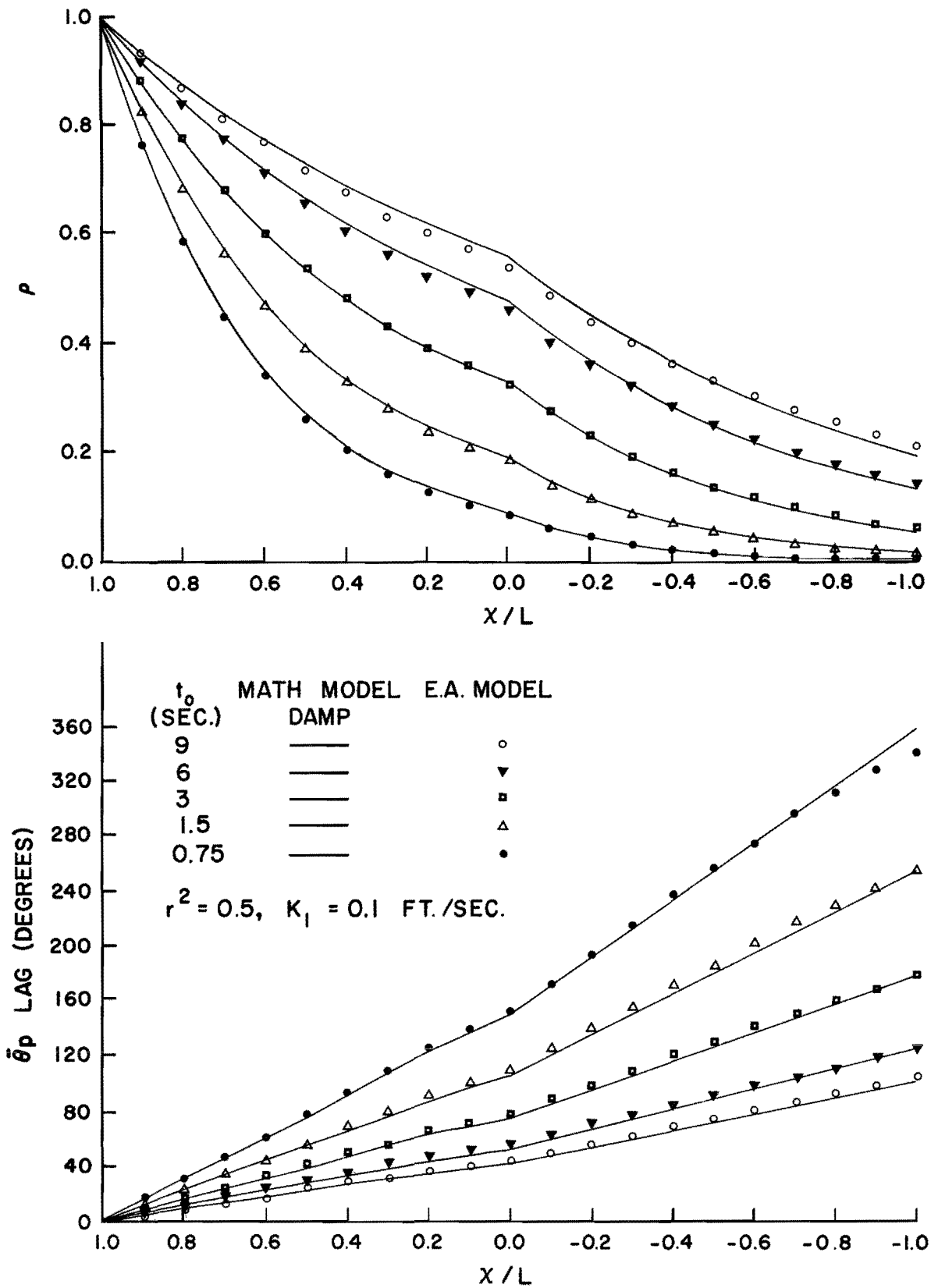


FIGURE 3. AMPLITUDE AND PHASE ANGLE VS x/L FOR A COASTAL AQUIFER WITH A DISCONTINUOUS PERMEABILITY: $r^2 = 0.5$.

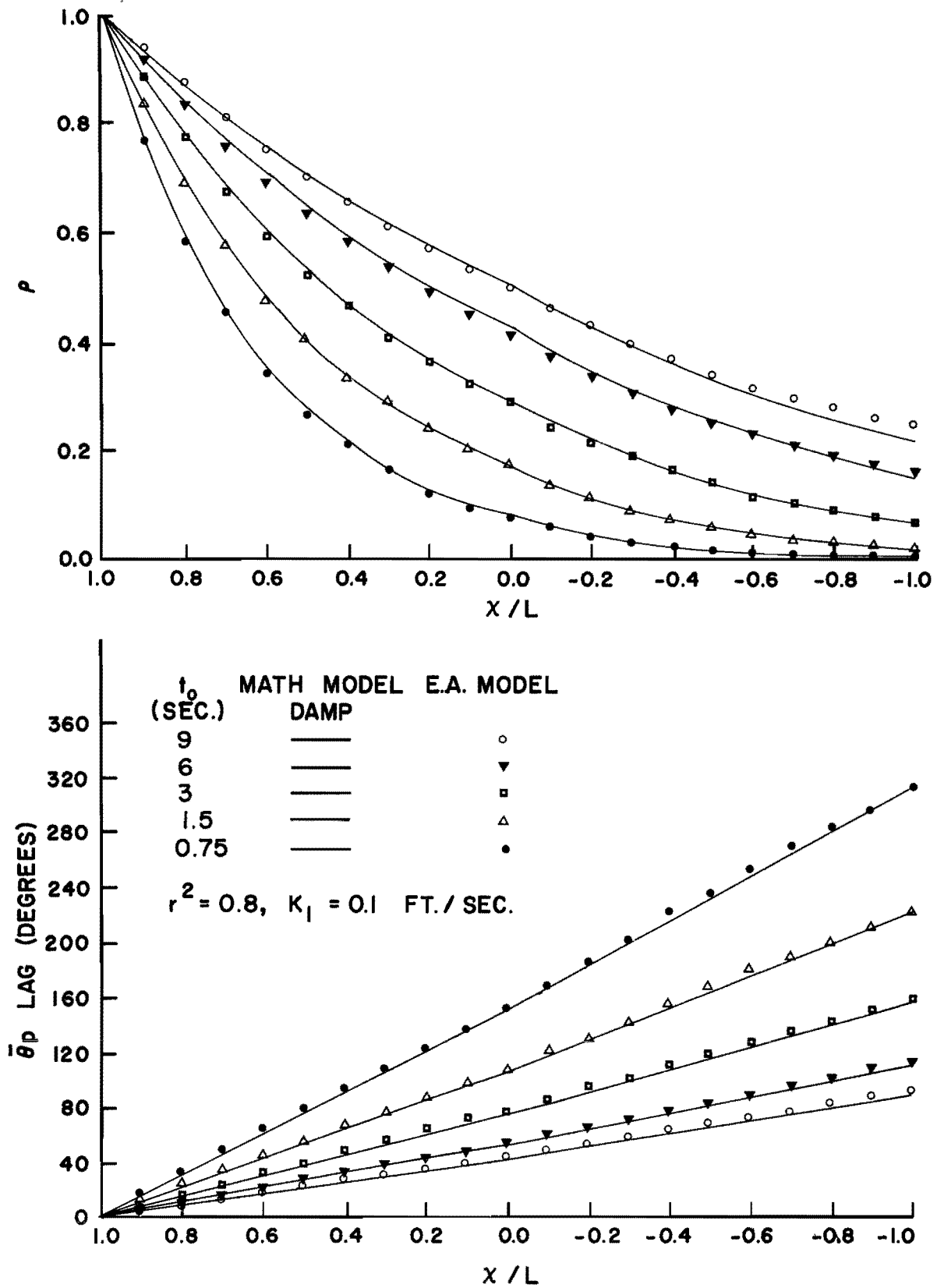


FIGURE 4. AMPLITUDE AND PHASE ANGLE $\bar{\theta}_p$ VS x/L FOR A COASTAL AQUIFER WITH A DISCONTINUOUS PERMEABILITY: $r^2 = 0.8$.

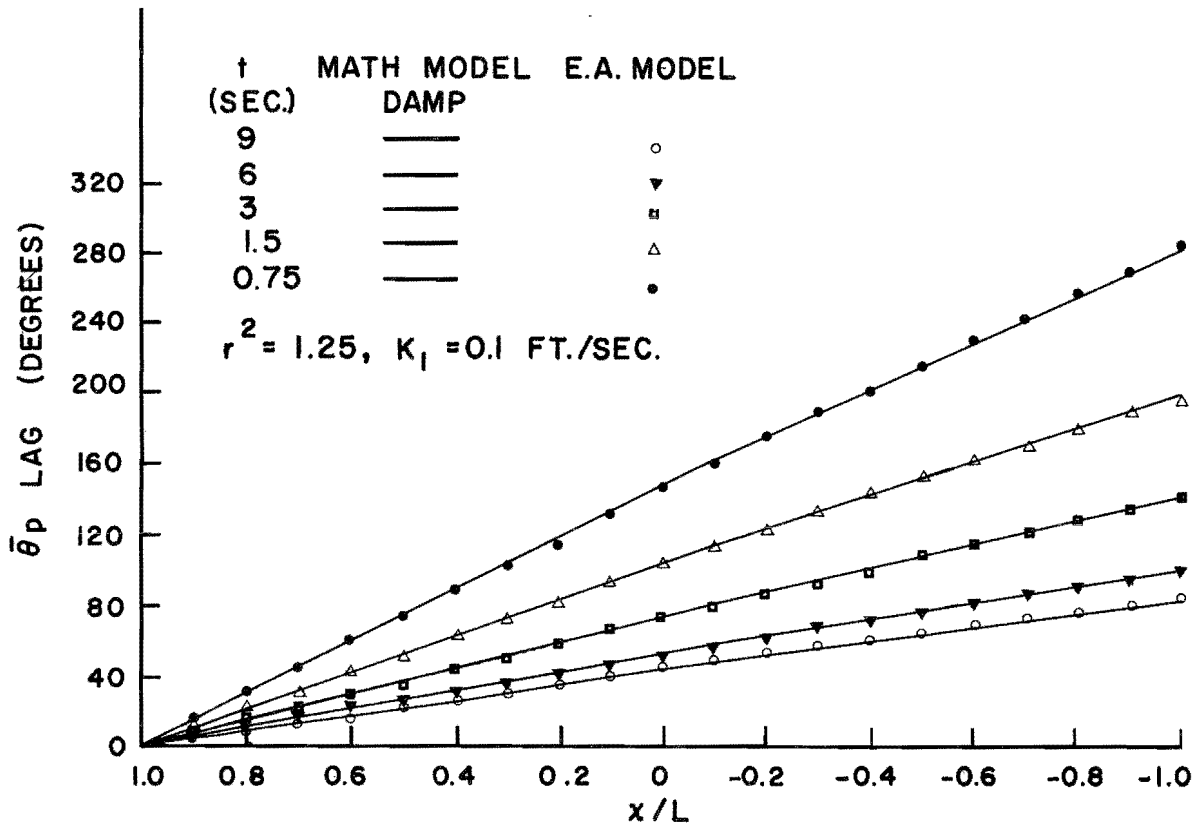
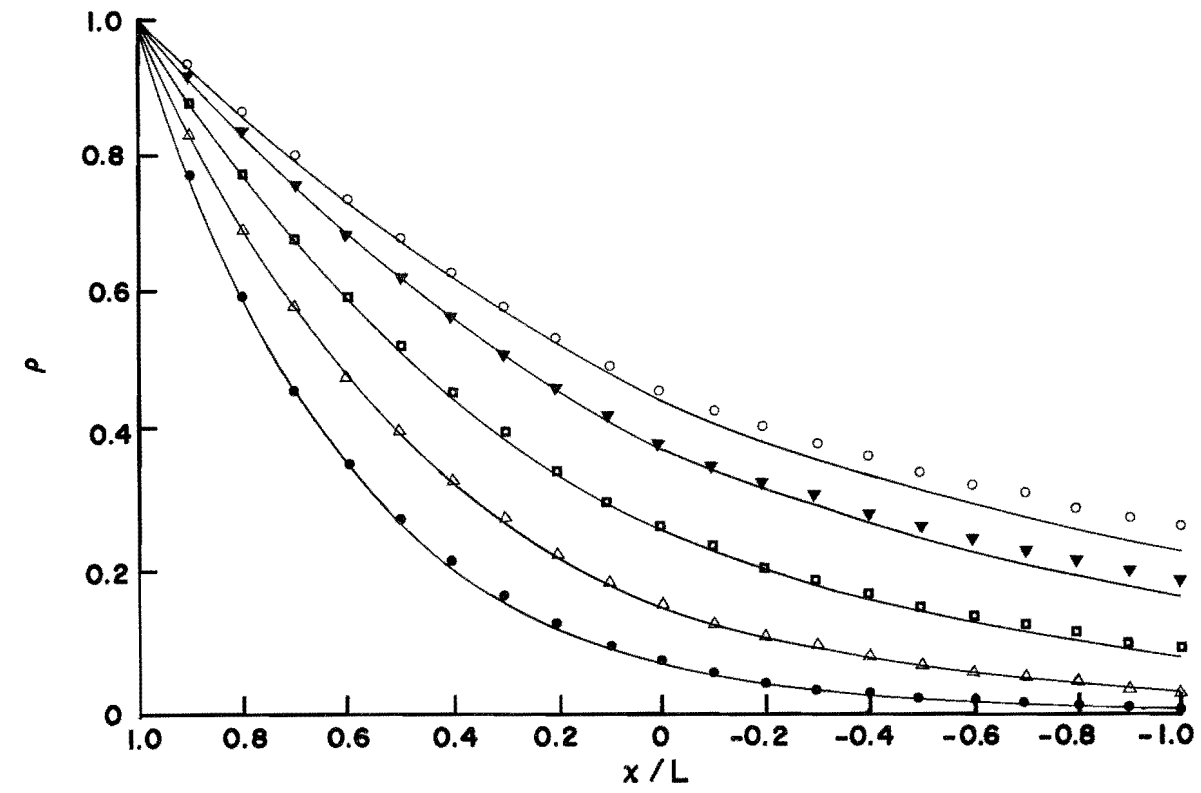


FIGURE 5. AMPLITUDE AND PHASE ANGLE $\bar{\theta}_p$ VS x/L FOR A COASTAL AQUIFER WITH A DISCONTINUOUS PERMEABILITY: $r^2 = 1.25$.

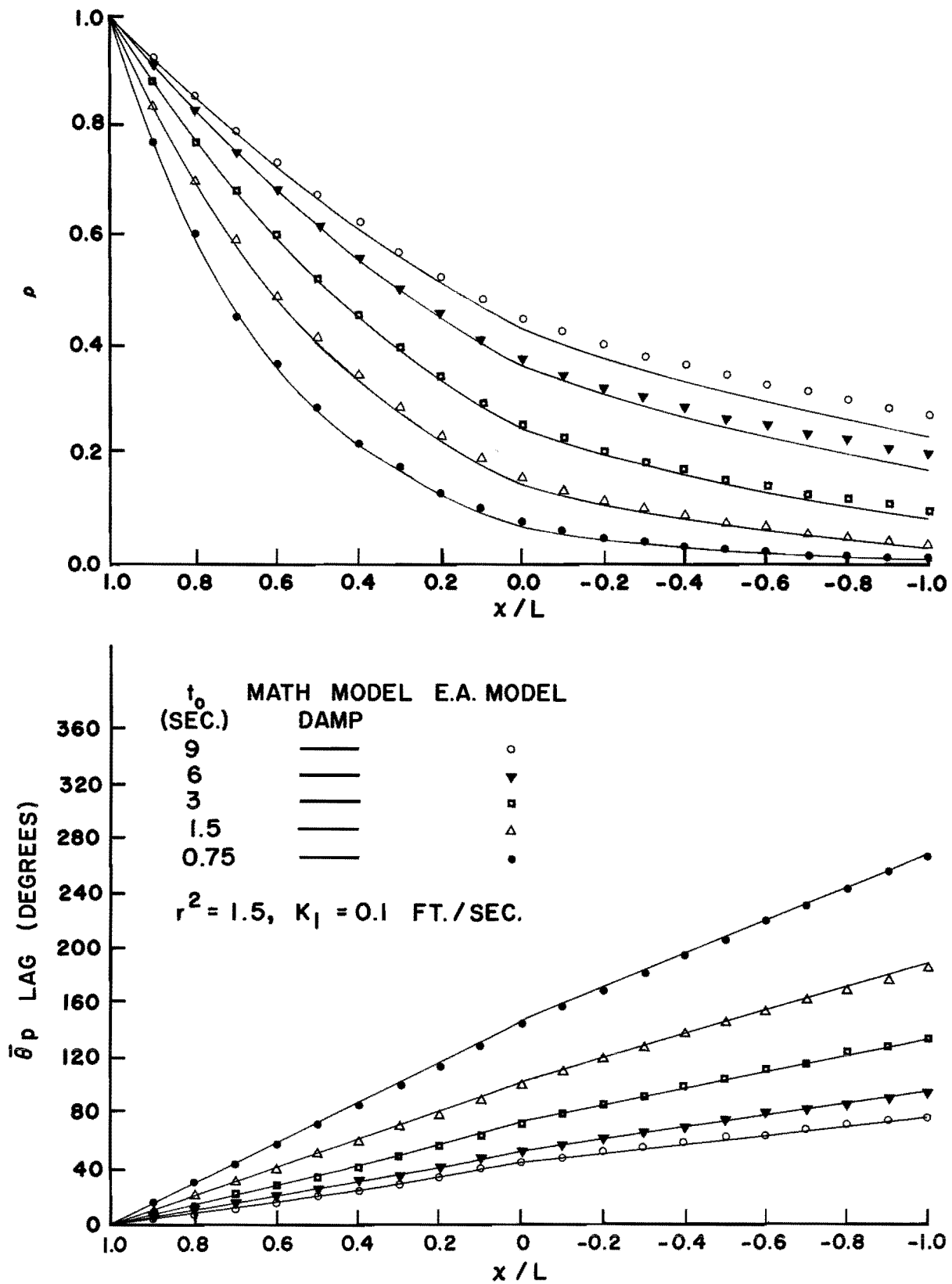


FIGURE 6. AMPLITUDE AND PHASE ANGLE $\bar{\theta}_p$ VS x/L FOR A COASTAL AQUIFER WITH A DISCONTINUOUS PERMEABILITY: $r^2 = 1.5$.

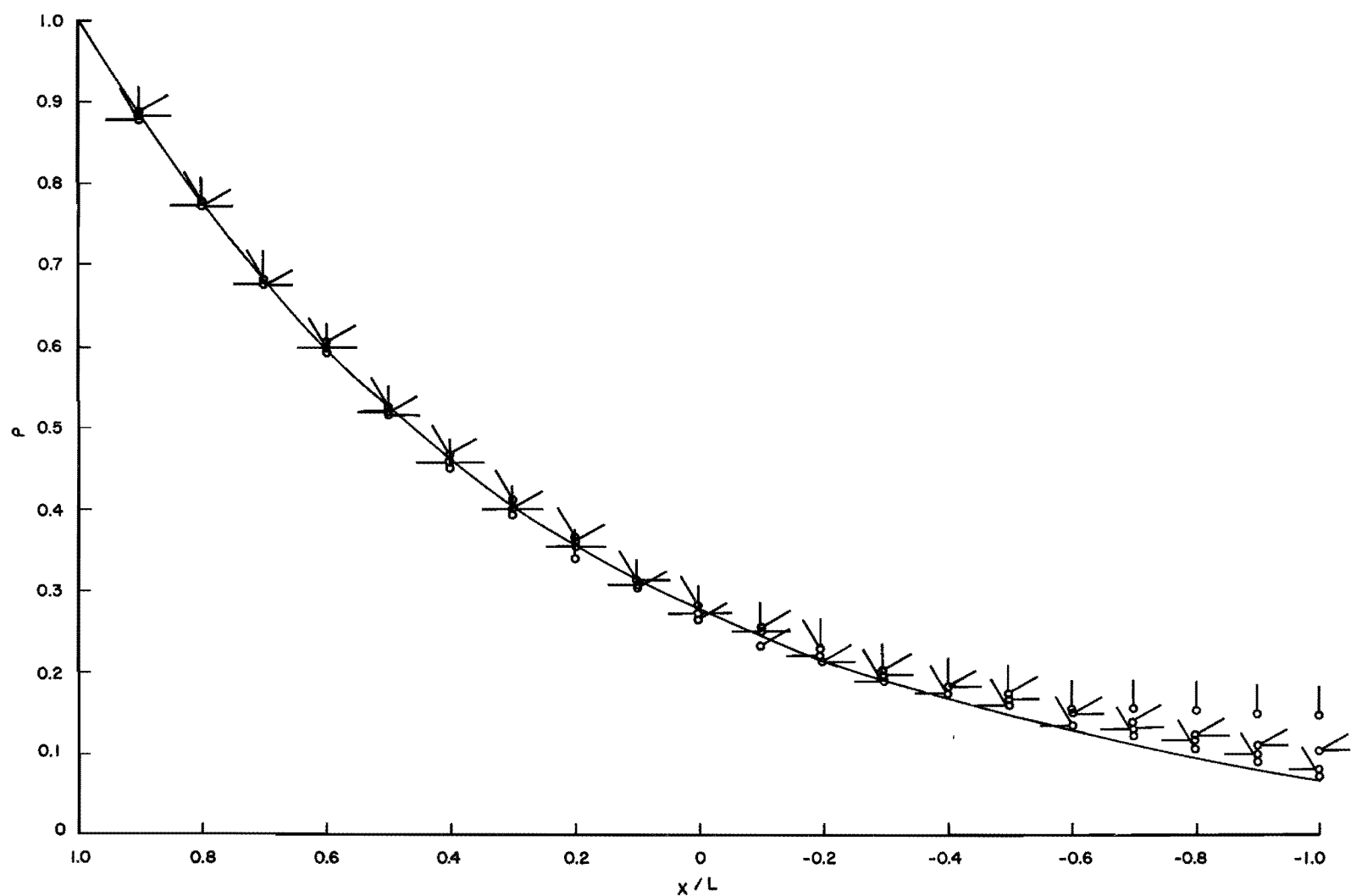
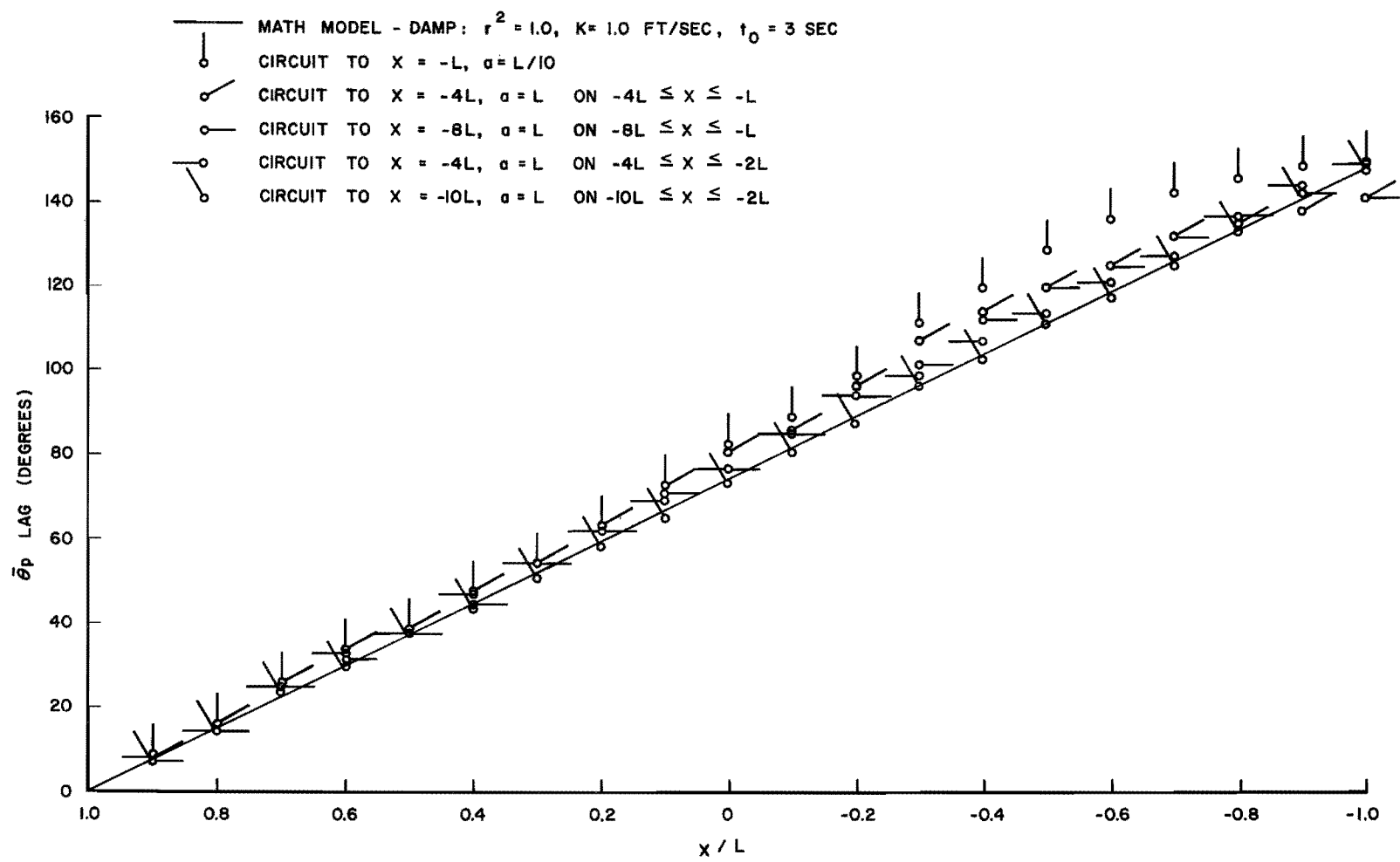
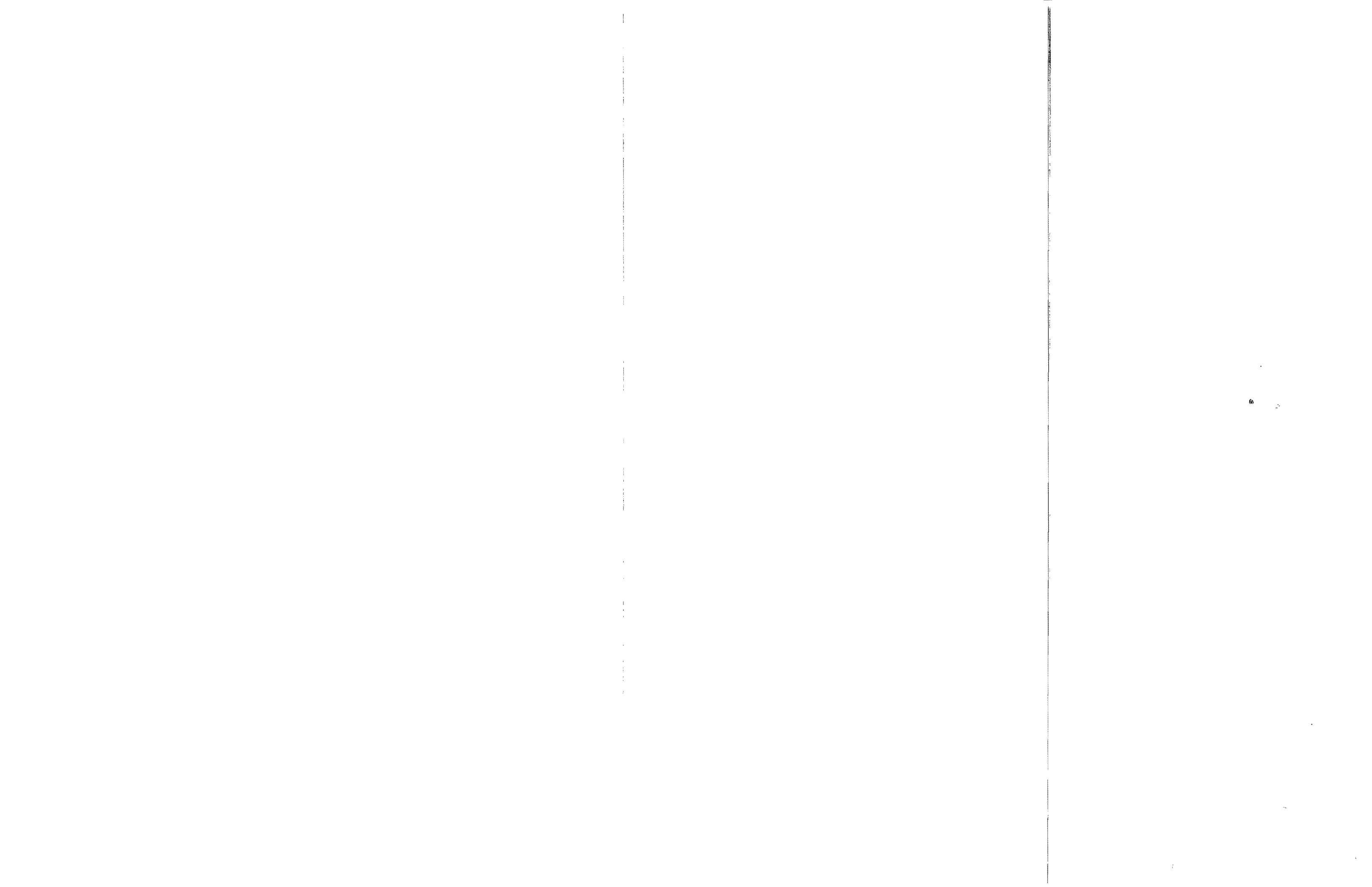


FIGURE 7. COMPARISON OF THE MATH MODEL FOR AN AQUIFER OF INFINITE EXTENT (EQUATIONS 8, WITH $r = 1$) WITH ELECTRIC ANALOG MODEL RESULTS FOR SEVERAL OPEN-END CIRCUIT CONFIGURATIONS.



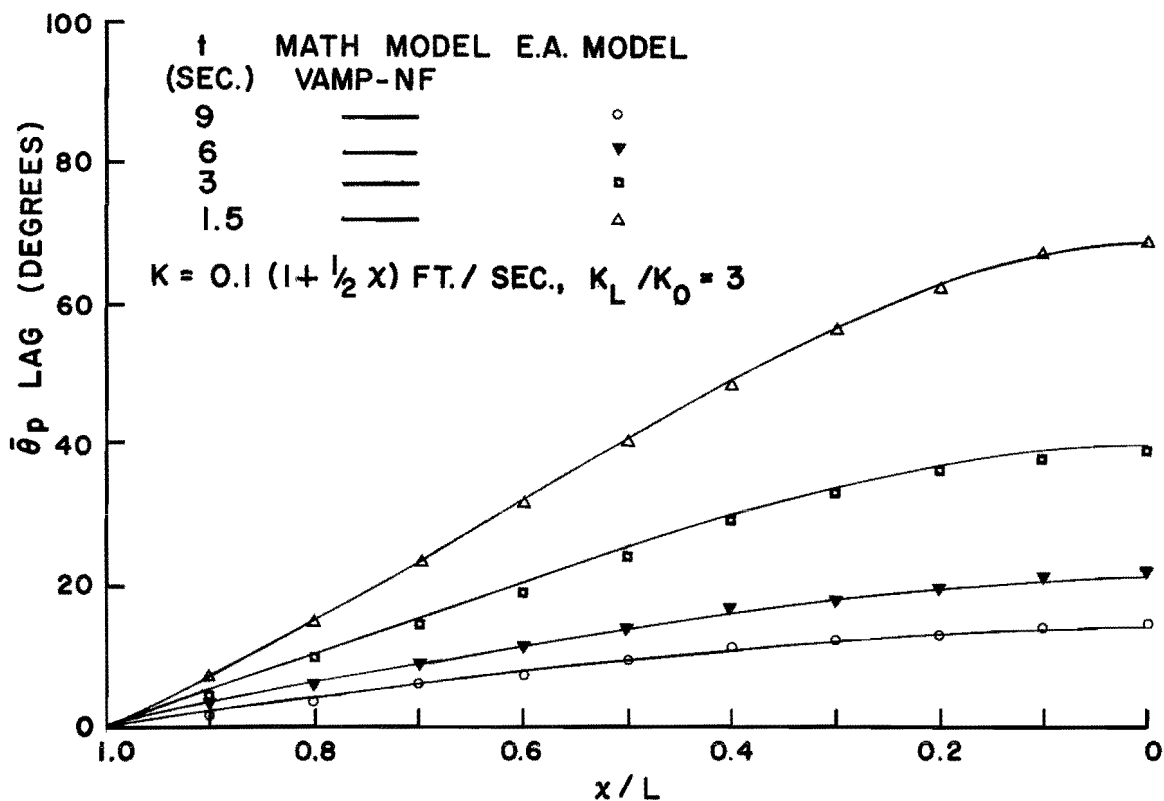
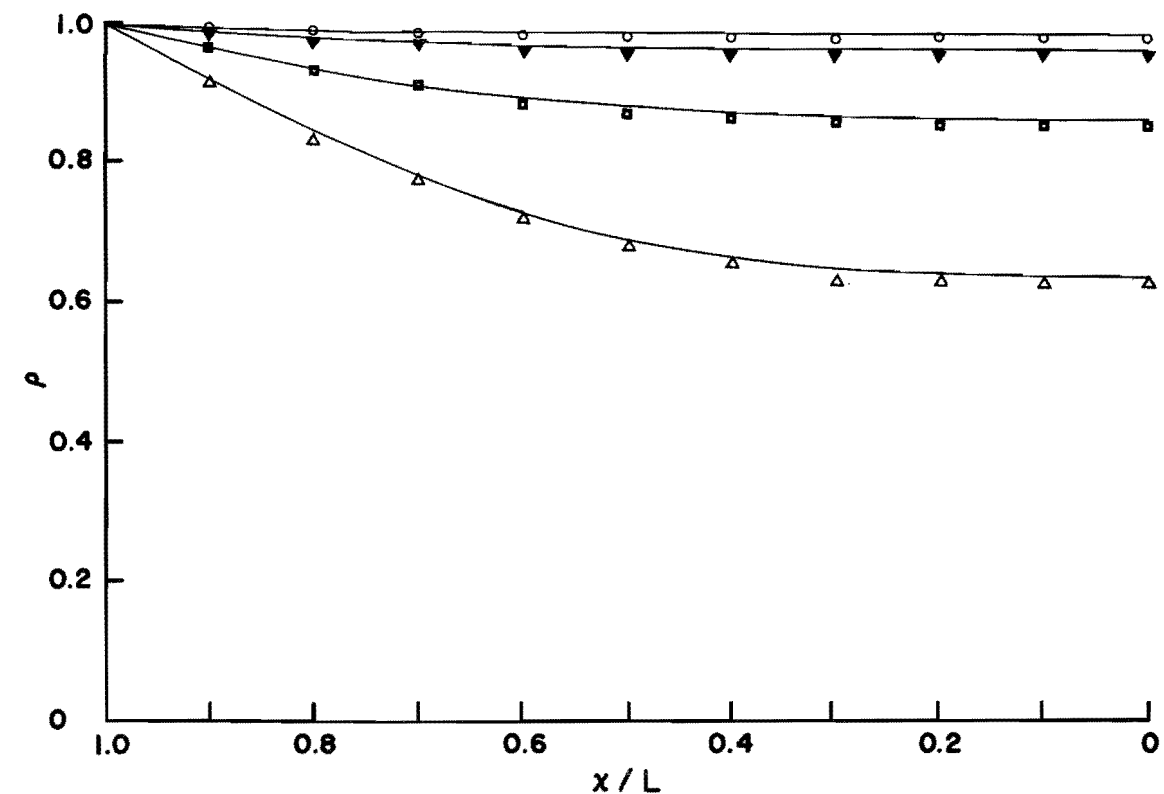


FIGURE 8. AMPLITUDE AND PHASE ANGLE VS x/L FOR A COASTAL AQUIFER WITH A NO-FLOW BOUNDARY CONDITION AT $x = 0$ AND A LINEARLY VARYING PERMEABILITY: $K = 0.1(1 + (1/2)x)$ FT/SEC.

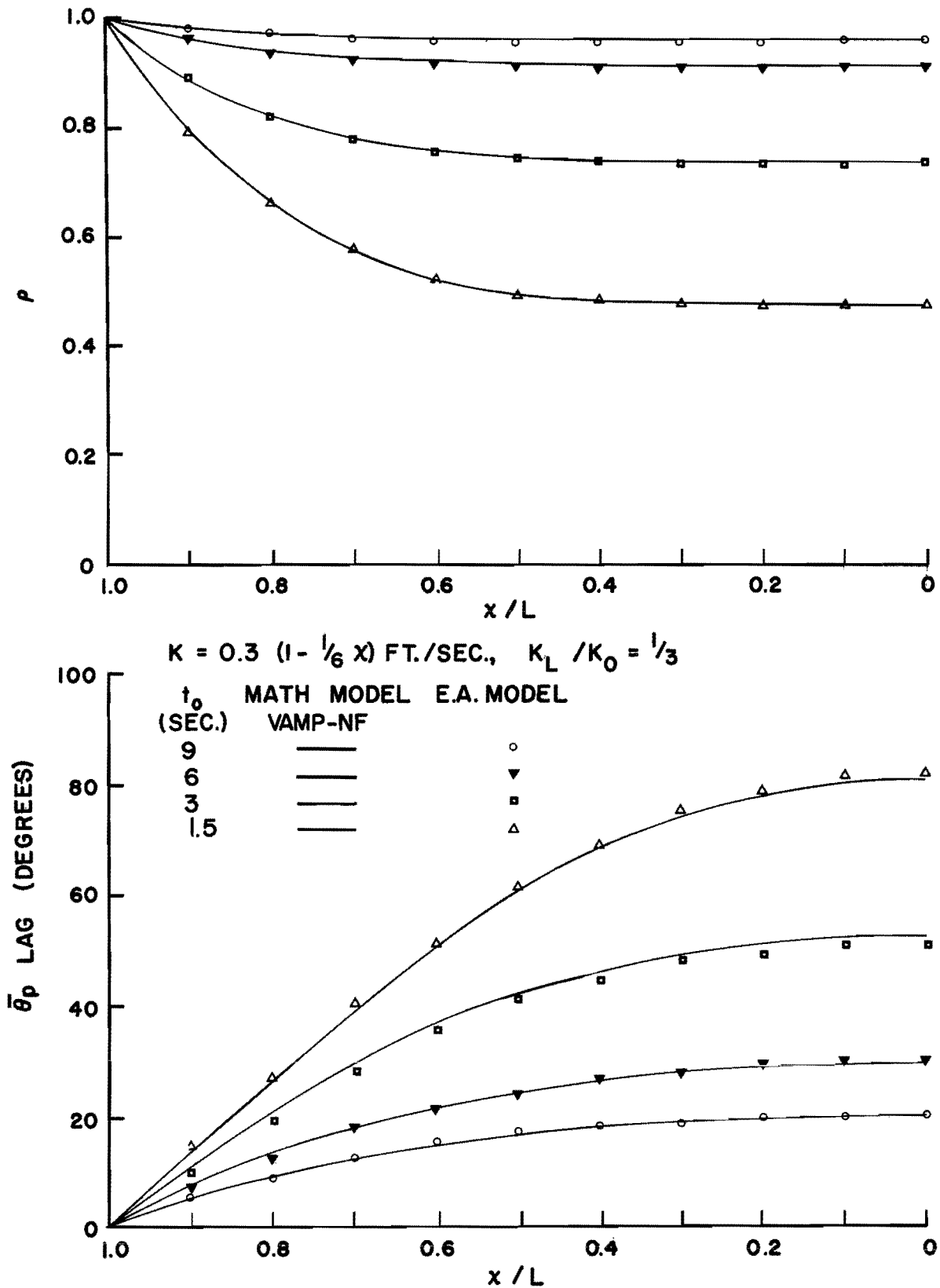


FIGURE 9. AMPLITUDE AND PHASE ANGLE VS x/L FOR A COASTAL AQUIFER WITH A NO-FLOW BOUNDARY CONDITION AT $x = 0$ AND A LINEARLY VARYING PERMEABILITY: $K = 0.3(1 - (1/6)x)$ FT/SEC.

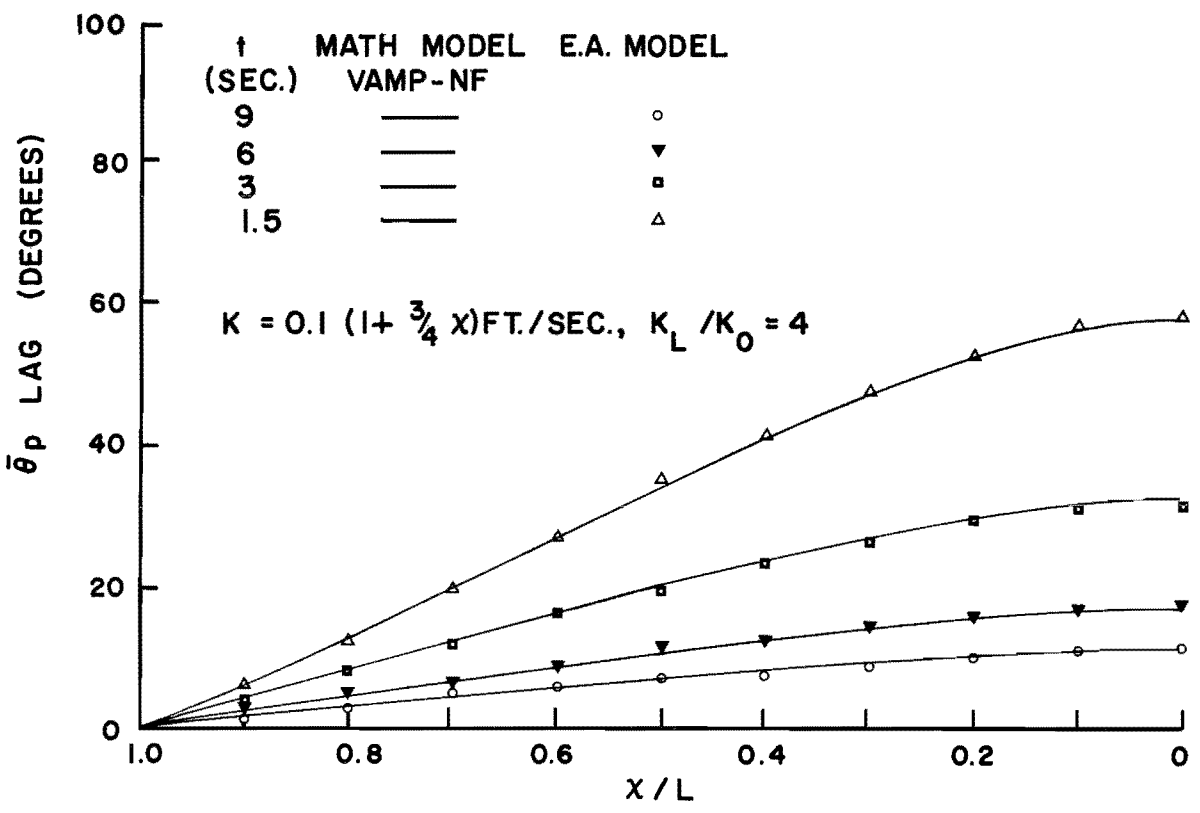
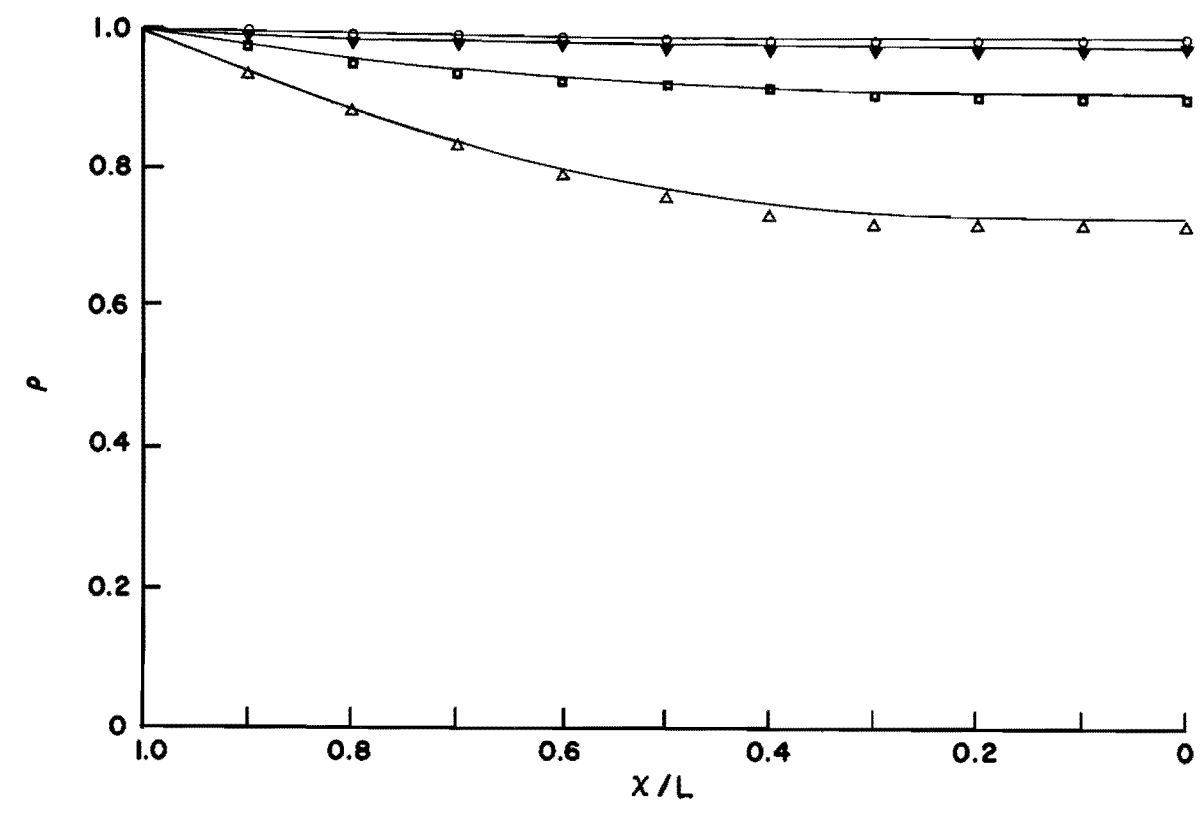


FIGURE 10. AMPLITUDE AND PHASE ANGLE VS x/L FOR A COASTAL AQUIFER WITH A NO-FLOW BOUNDARY CONDITION AT x = 0 AND A LINEARLY VARYING PERMEABILITY: $K = 0.1(1+(3/4)x)$ FT SEC.

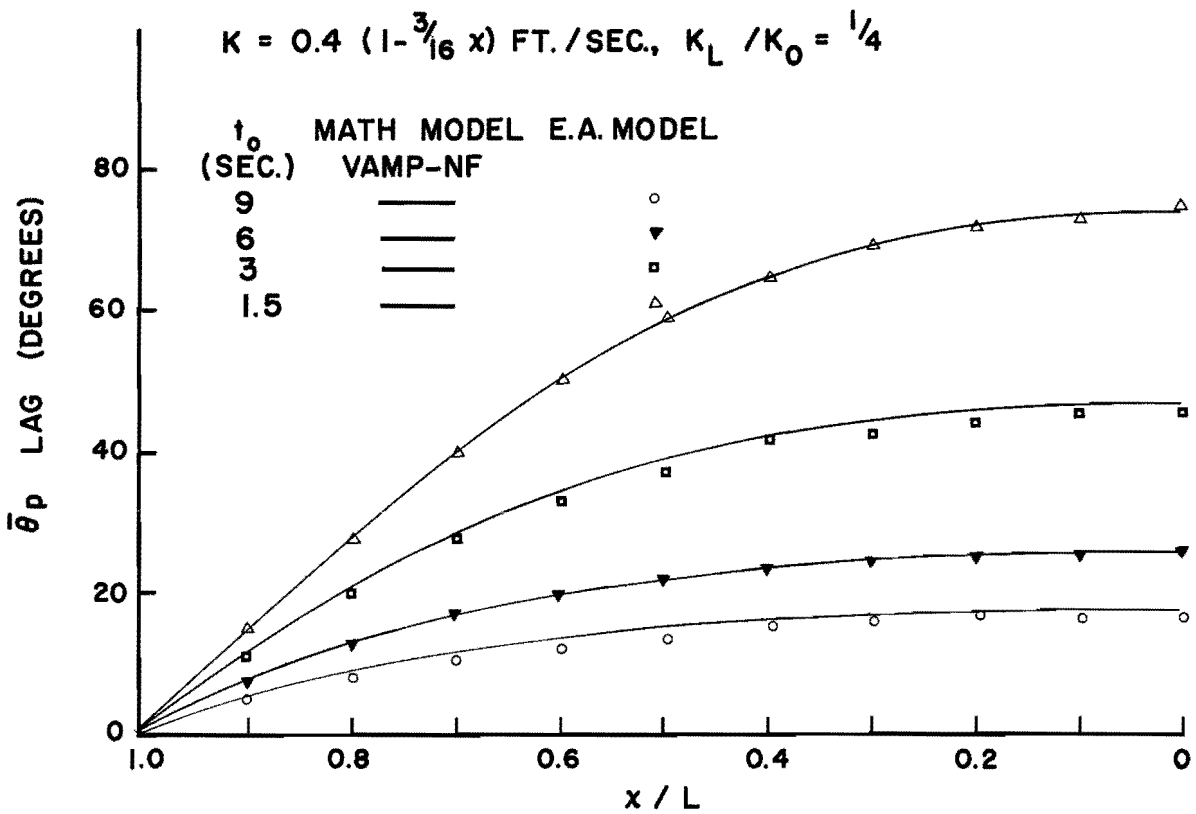
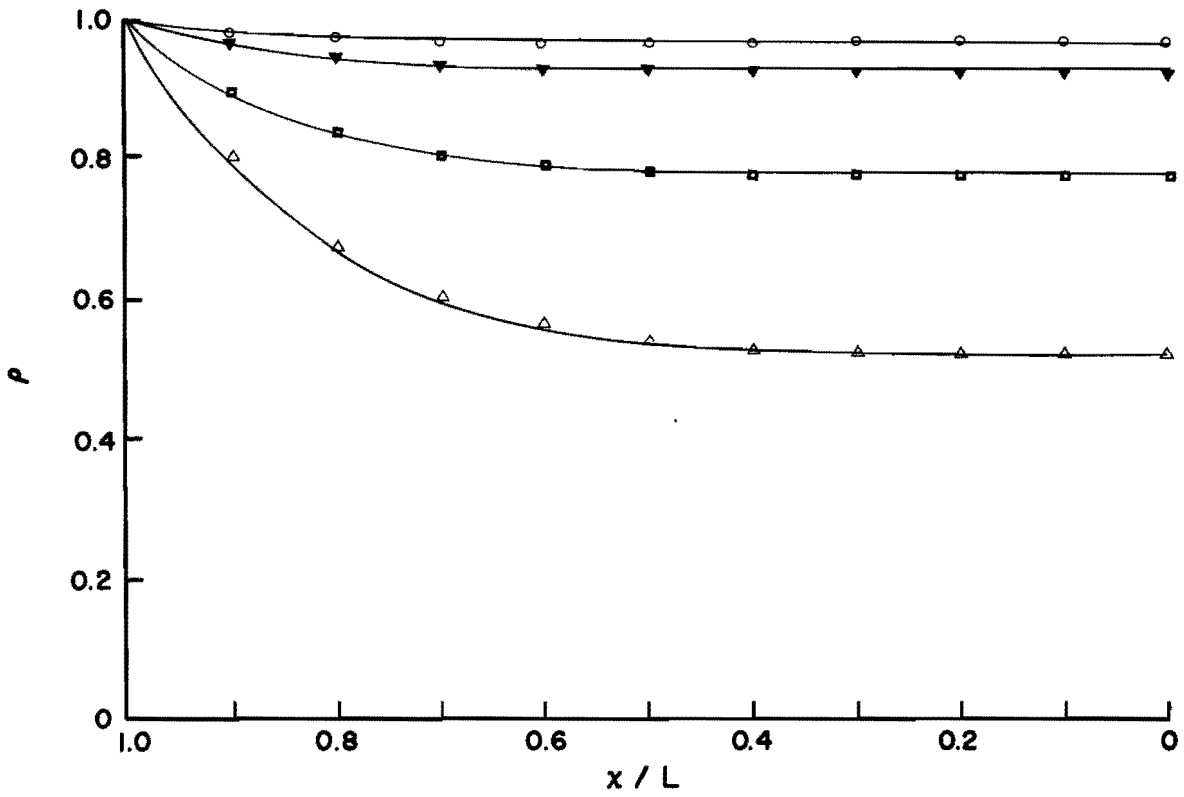


FIGURE 11. AMPLITUDE AND PHASE ANGLE VS x/L FOR A COASTAL AQUIFER WITH A NO-FLOW BOUNDARY CONDITION AT $x = 0$ AND A LINEARLY VARYING PERMEABILITY: $K = 0.4(1 - (3/16)x)$ FT/SEC.

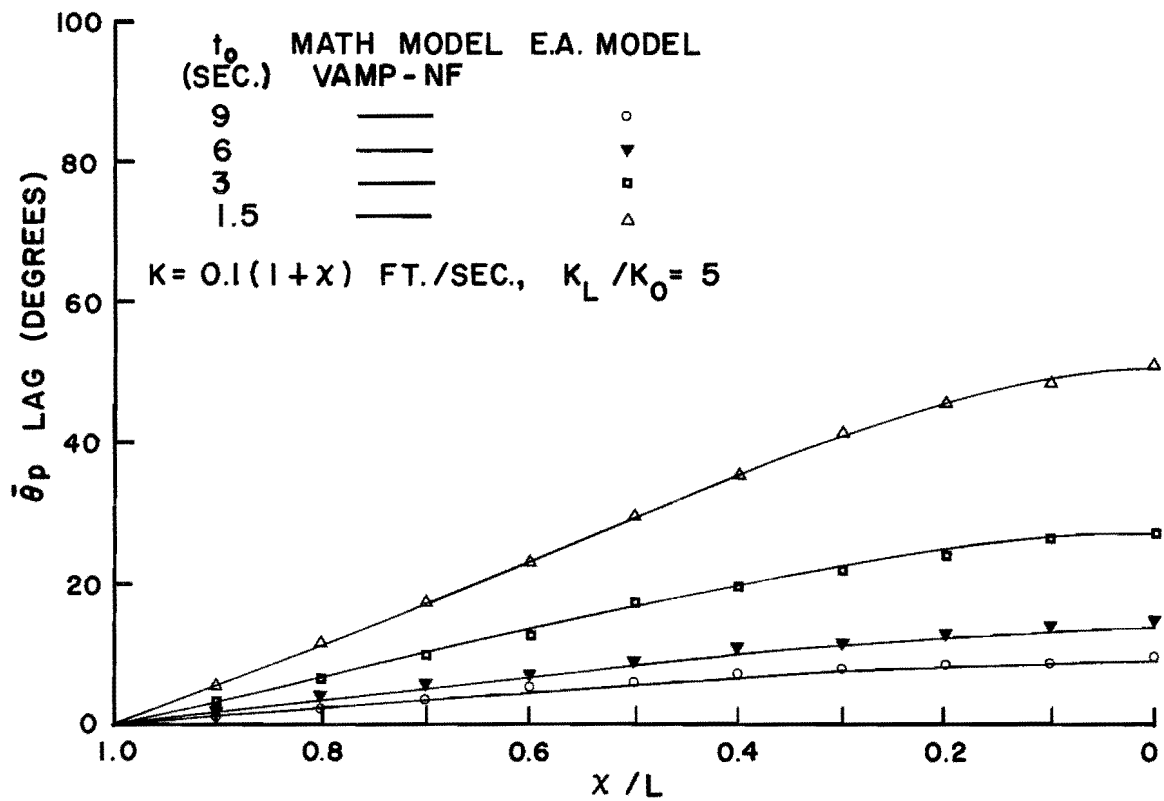
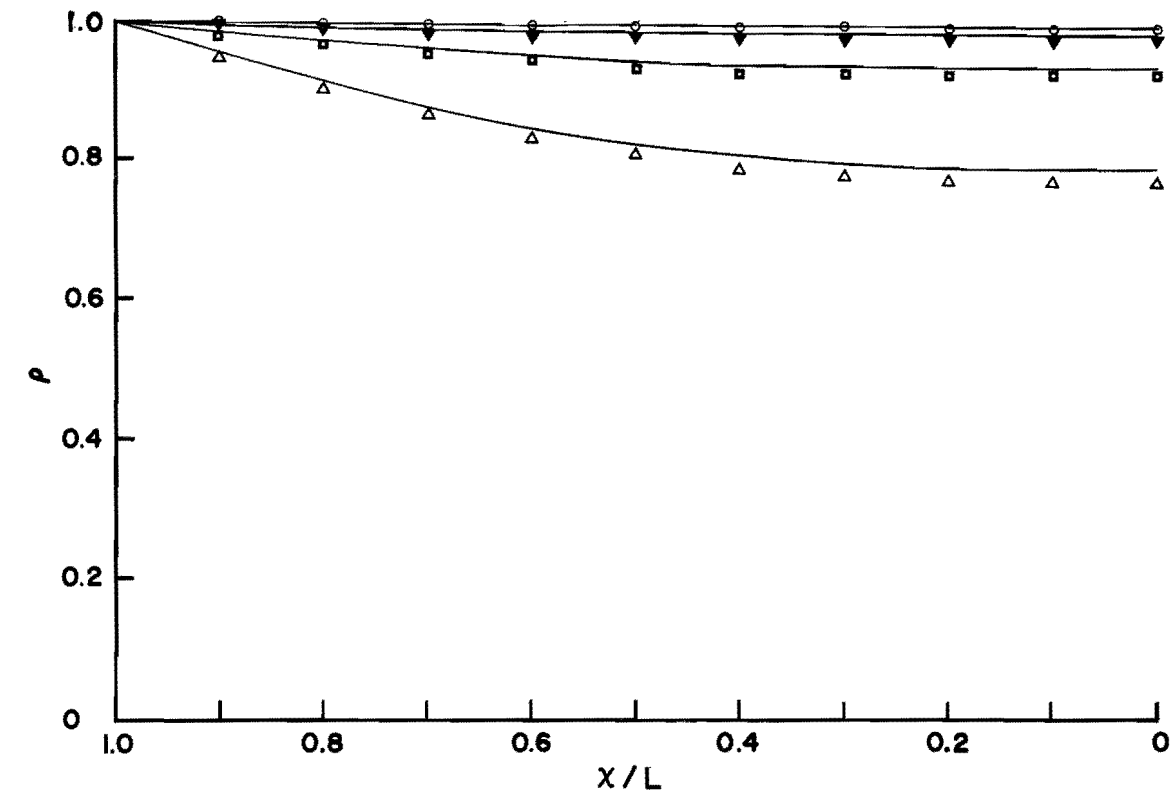


FIGURE 12. AMPLITUDE AND PHASE ANGLE VS x/L FOR A COASTAL AQUIFER WITH A NO-FLOW BOUNDARY CONDITION AT $x = 0$ AND A LINEARLY VARYING PERMEABILITY: $K = 0.1(1+x)$ FT/SEC.

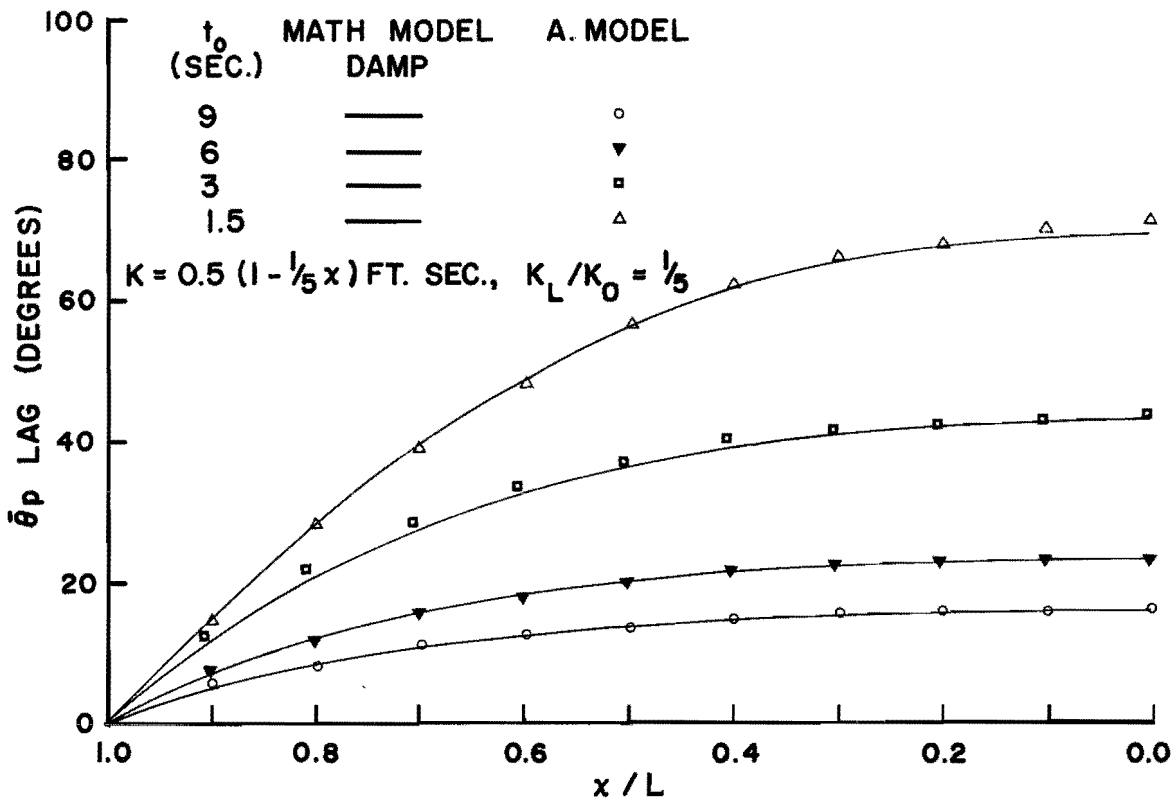
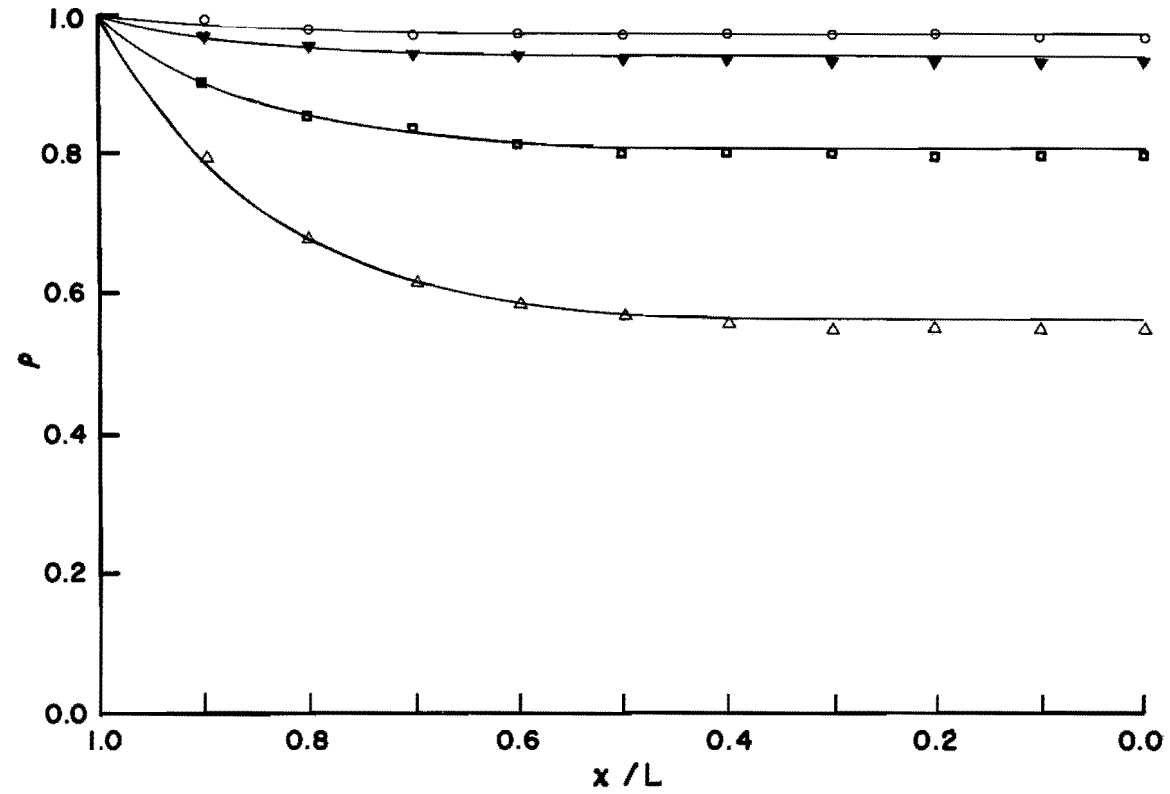


FIGURE 13. AMPLITUDE AND PHASE ANGLE VS x/L FOR A COASTAL AQUIFER WITH A NO-FLOW BOUNDARY CONDITION AT $x = 0$ AND A LINEARLY VARYING PERMEABILITY: $K = 0.5(1 - (1/5)x)$ FT/SEC.

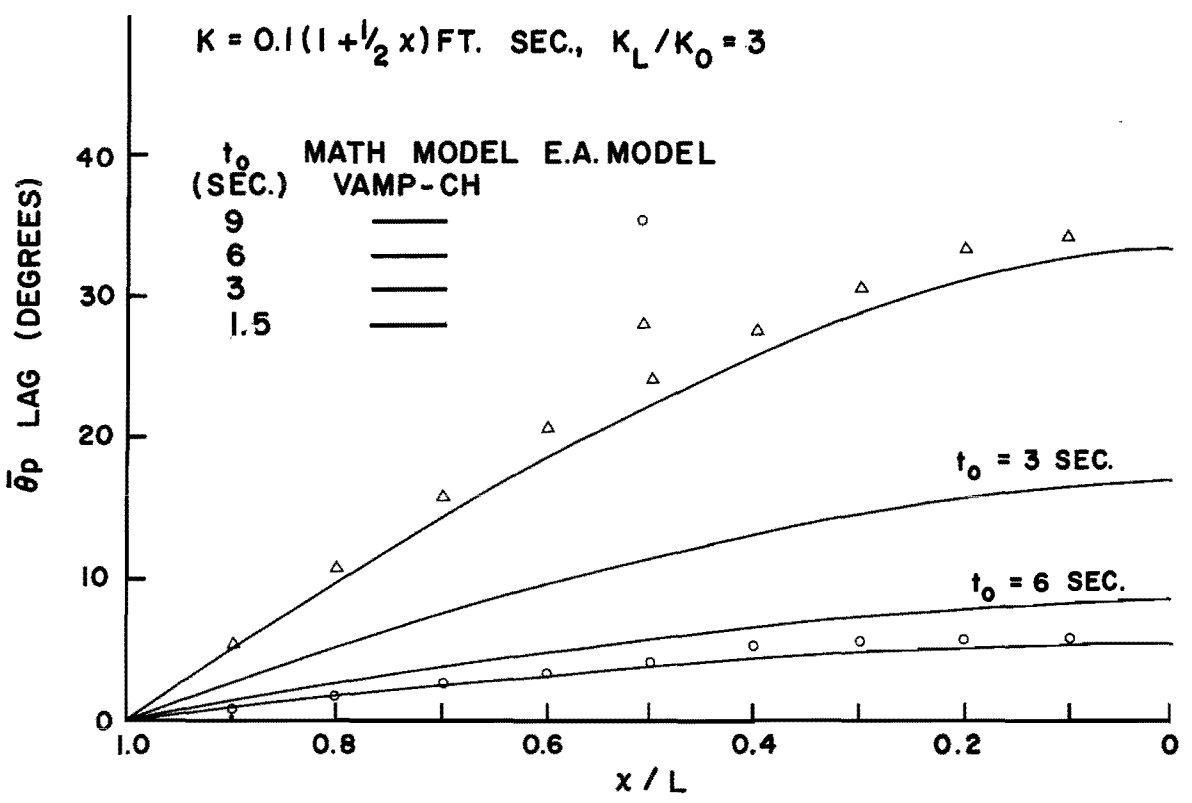
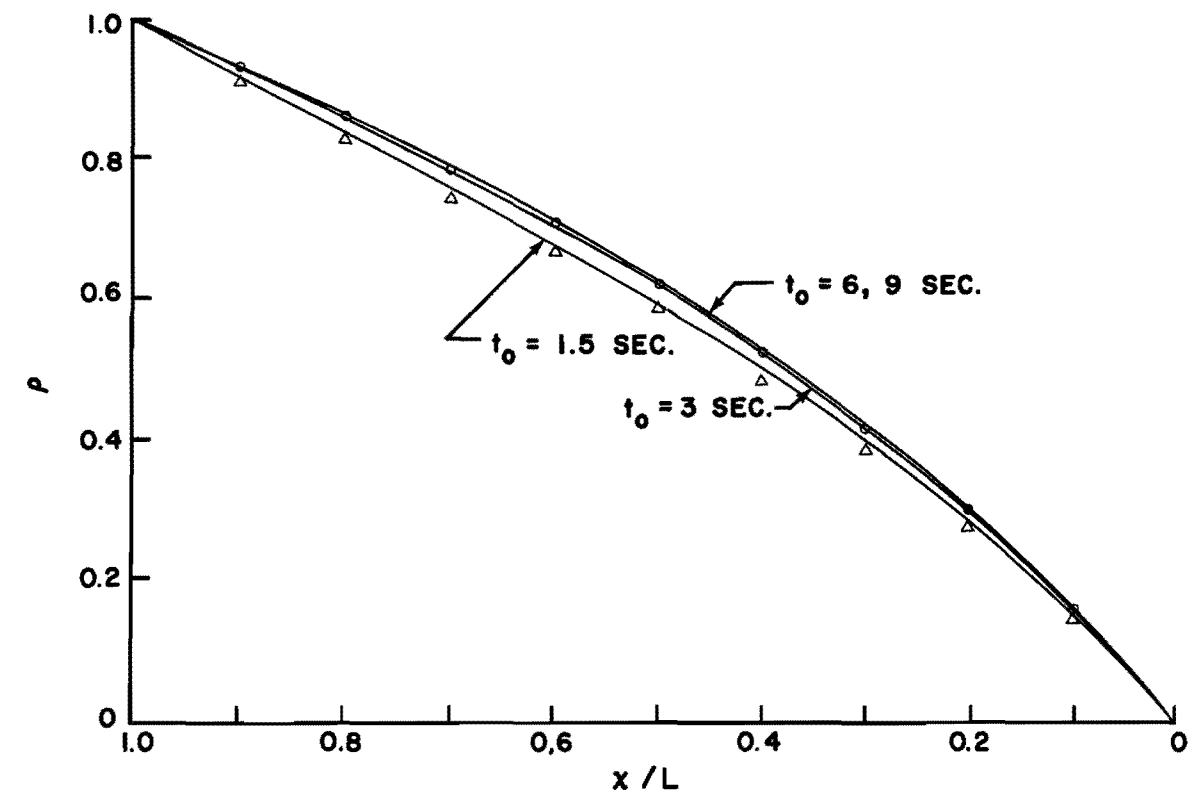
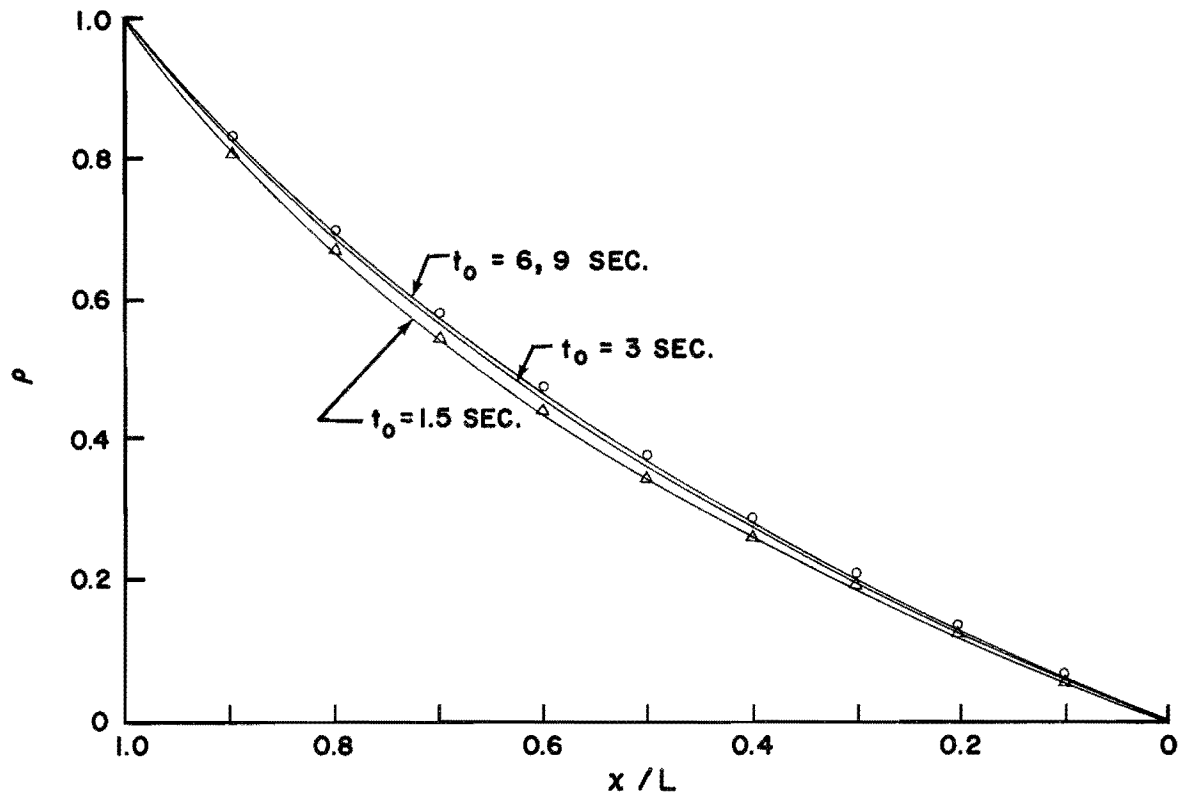


FIGURE 14. AMPLITUDE AND PHASE ANGLE VS x/L FOR A COASTAL AQUIFER WITH A CONSTANT HEAD BOUNDARY CONDITION AT $x = 0$ AND A LINEARLY VARYING PERMEABILITY: $K = 0.1(1 + (1/2)x)$ FT/SEC.



$K = 3.0 (1 - \frac{1}{6}x)$ FT/SEC, $K_L / K_0 = \frac{1}{3}$

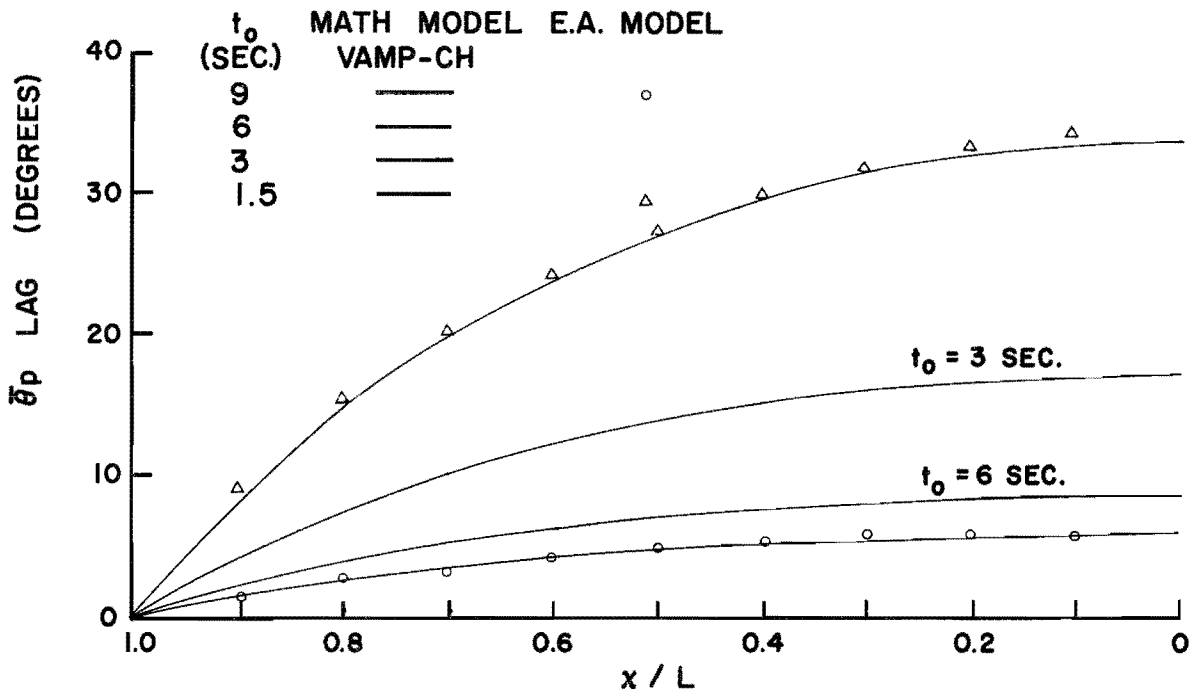


FIGURE 15. AMPLITUDE AND PHASE ANGLE VS x/L FOR A COASTAL AQUIFER WITH A CONSTANT-HEAD BOUNDARY CONDITION AT $x = 0$ AND A LINEARLY VARYING PERMEABILITY: $K = 0.3(1 - (1/6)x)$ FT/SEC.

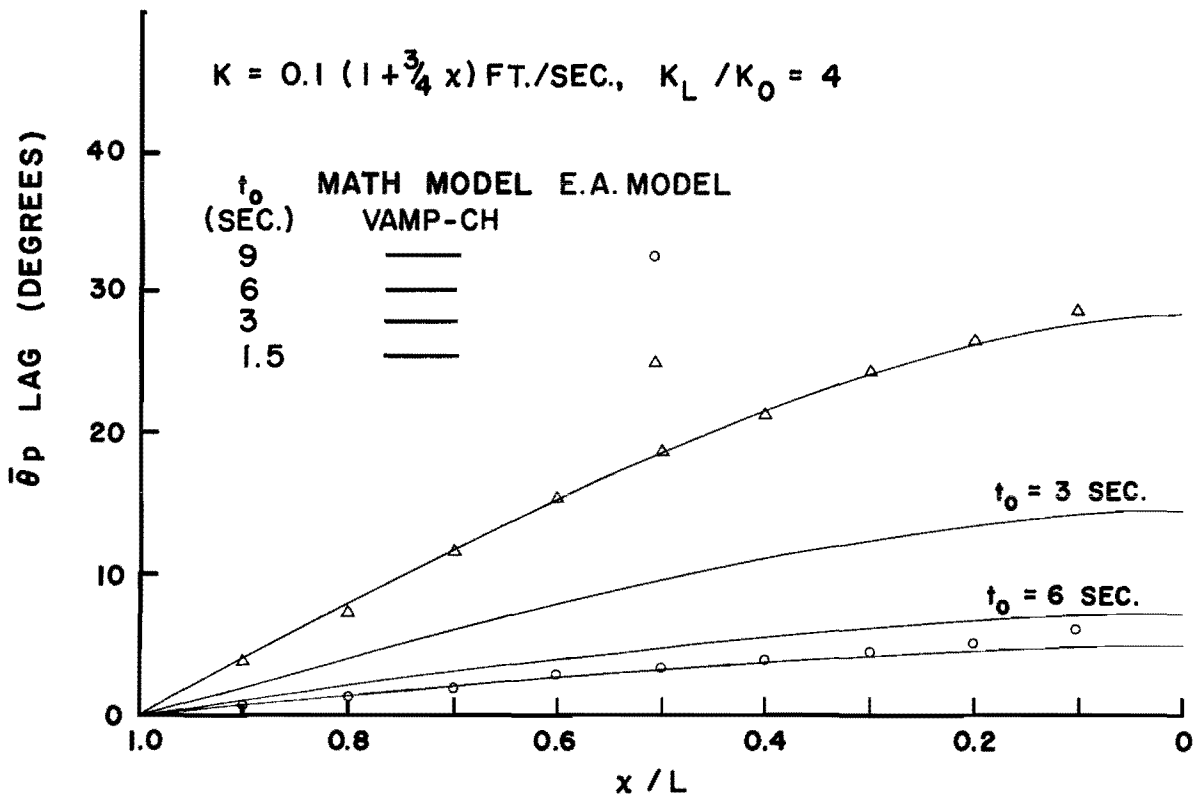
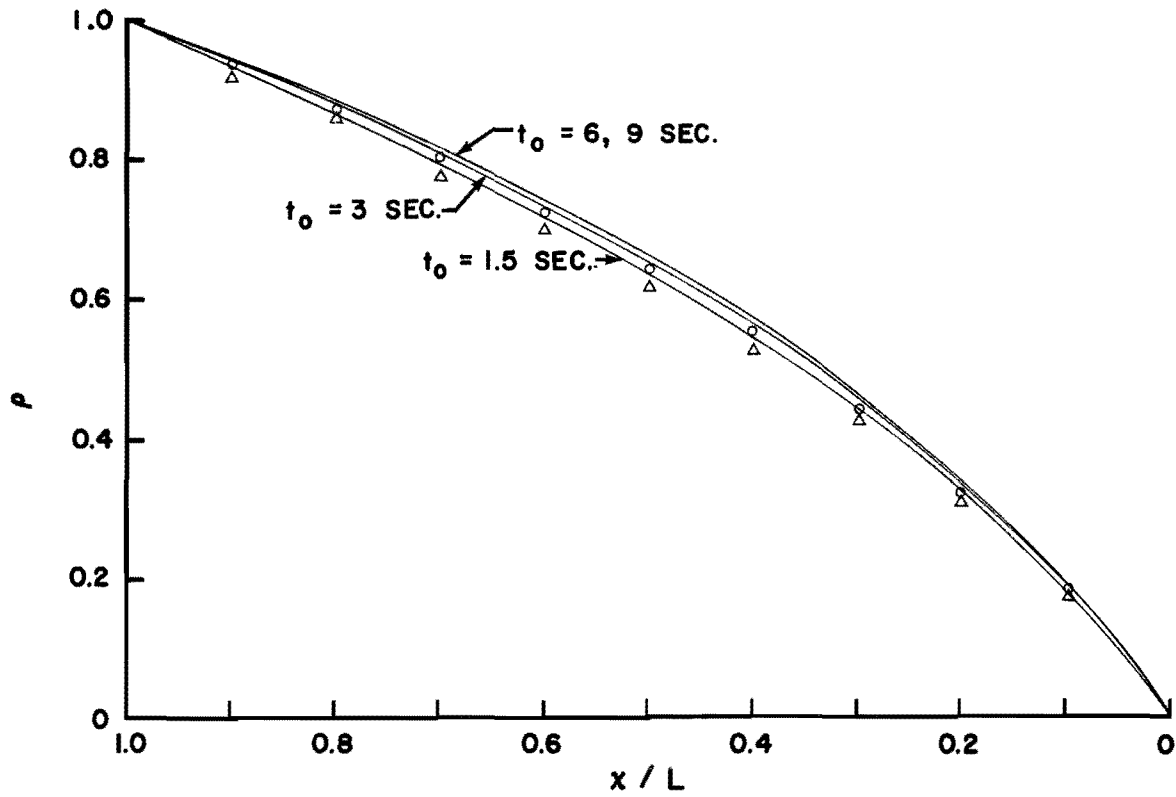


FIGURE 16. AMPLITUDE AND PHASE ANGLE VS x/L FOR A COASTAL AQUIFER WITH A CONSTANT-HEAD BOUNDARY CONDITION AT $x = 0$ AND A LINEARLY VARYING PERMEABILITY: $K = 0.1(1+(3/4)x)$ FT/SEC.

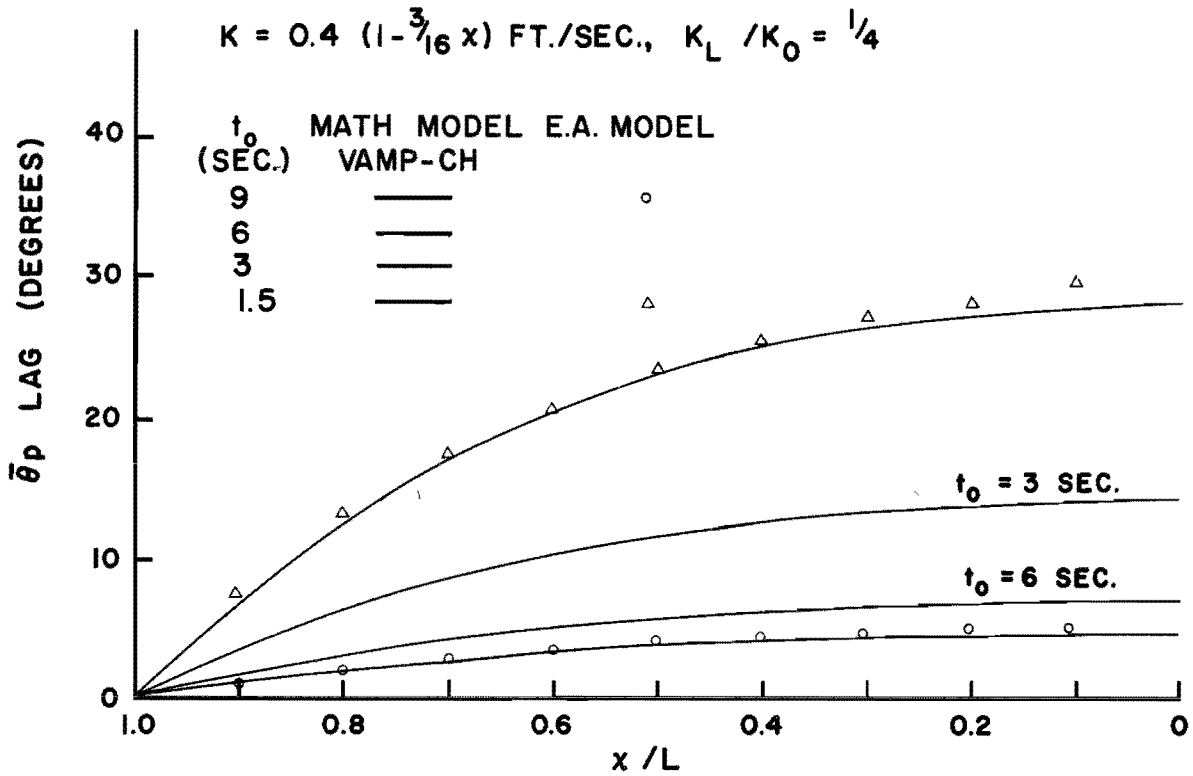
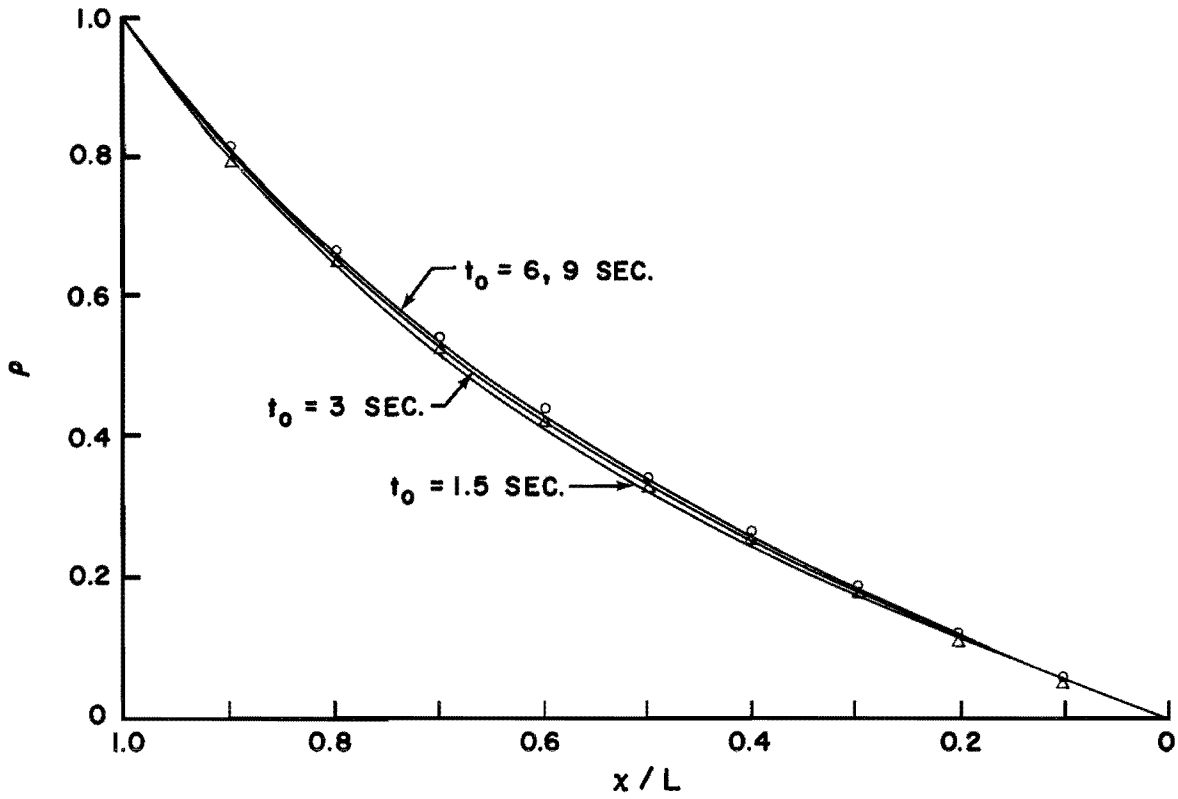


FIGURE 17. AMPLITUDE AND PHASE ANGLE VS x/L FOR A COASTAL AQUIFER WITH A CONSTANT-HEAD BOUNDARY CONDITION AT $x = 0$ AND A LINEARLY VARYING PERMEABILITY: $K = 0.4(1 - (3/16)x)$ FT/SEC.

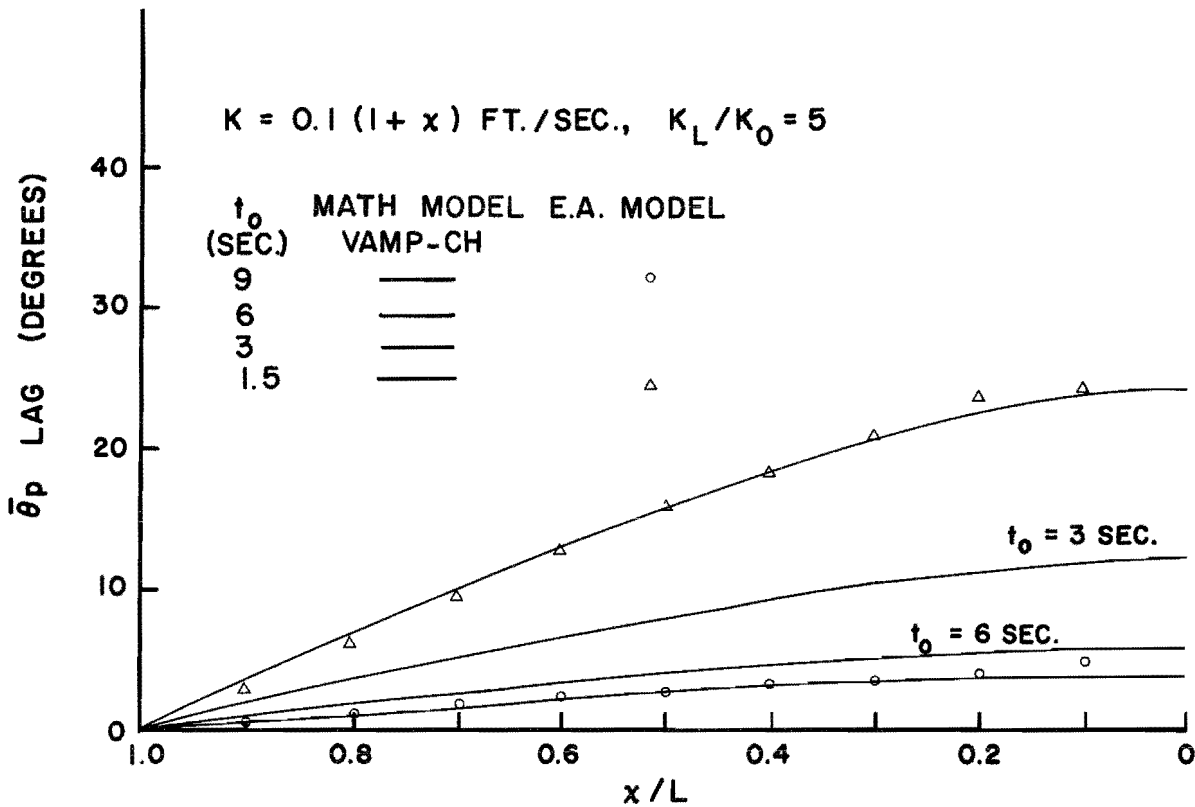
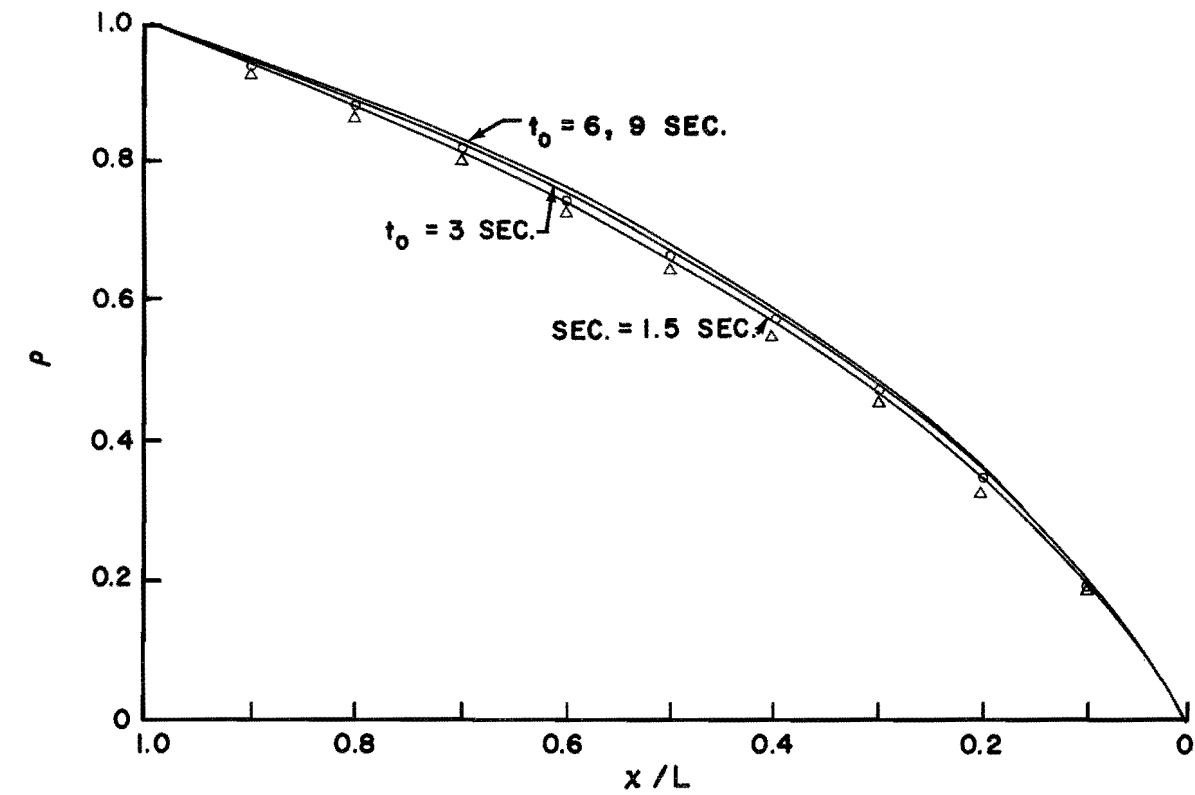


FIGURE 18. AMPLITUDE AND PHASE ANGLE $\forall x/L$ FOR A COASTAL AQUIFER WITH A CONSTANT-HEAD BOUNDARY CONDITION AT $x = 0$ AND A LINEARLY VARYING PERMEABILITY: $K = 0.1(1+x)$ FT/SEC.

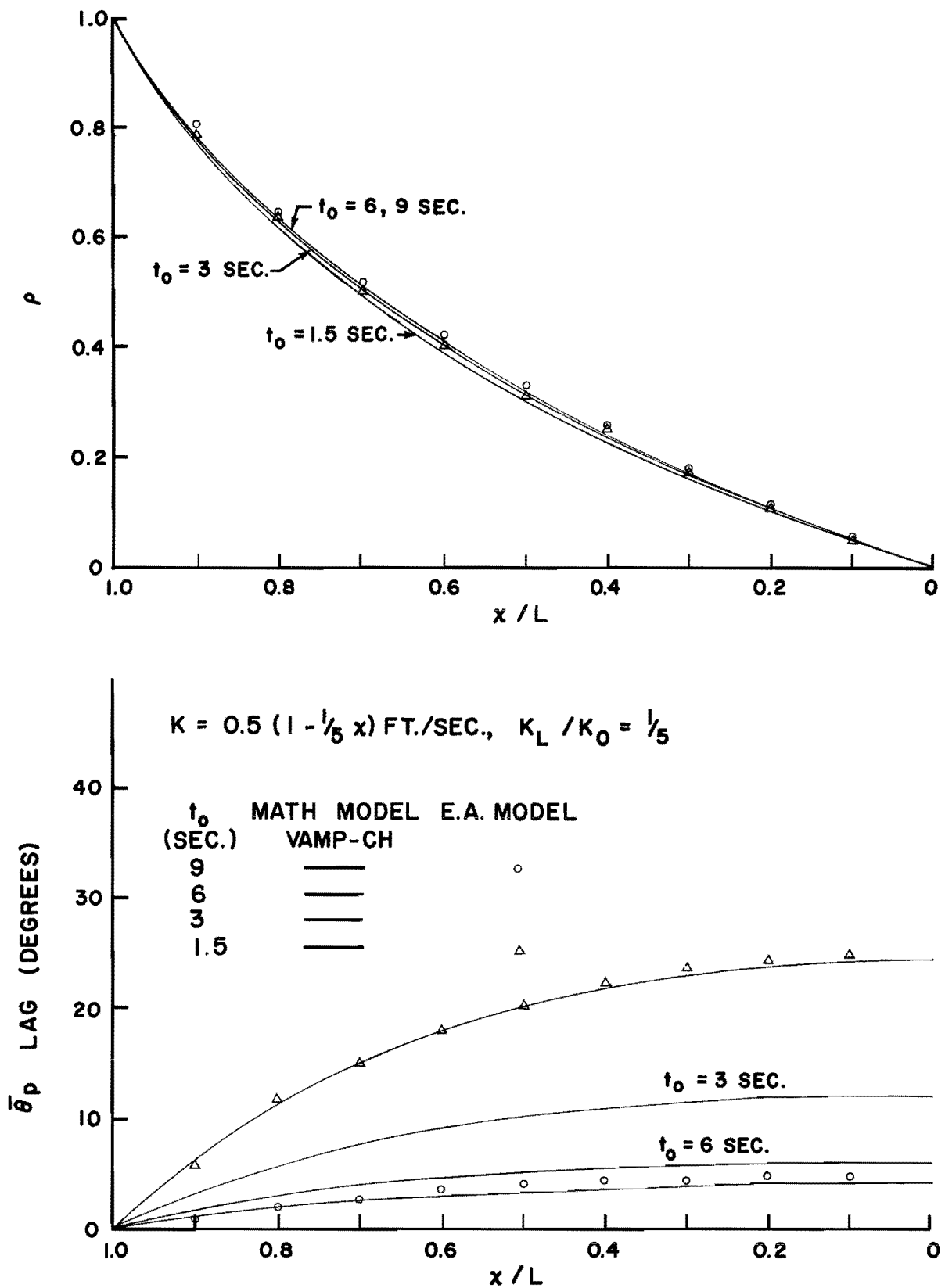


FIGURE 19. AMPLITUDE AND PHASE ANGLE $\bar{\theta}_p$ VS x/L FOR A COASTAL AQUIFER WITH A CONSTANT-HEAD BOUNDARY CONDITION AT $x = 0$ AND A LINEARLY VARYING PERMEABILITY: $K = 0.5(1 - (1/5)x)$ FT./SEC.

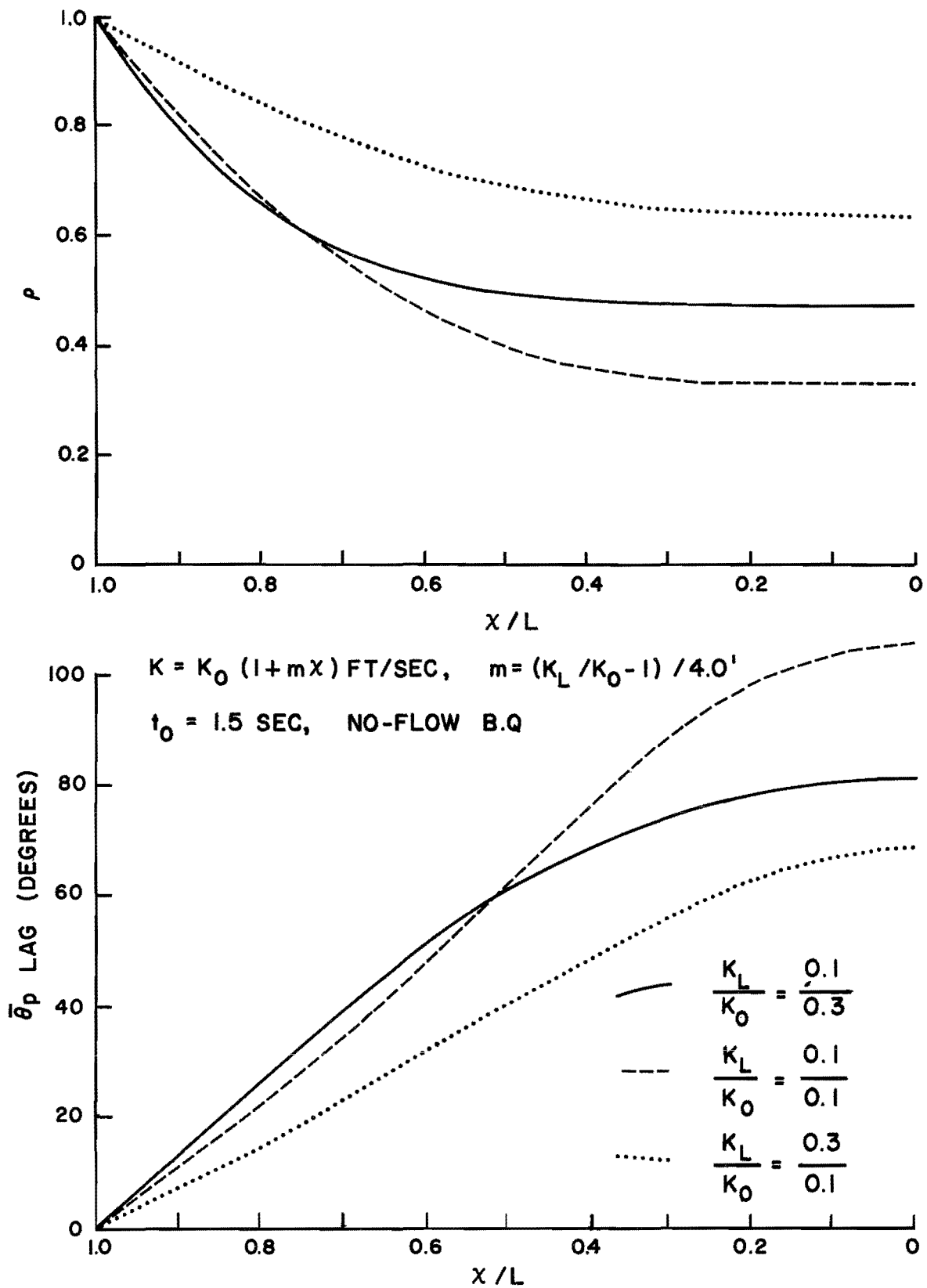


FIGURE 20. COMPARISON OF MATH MODEL RESULTS FOR AQUIFERS HAVING $K = 0.1(1+mx)$ FT/SEC: $m = 1/2, 0, -1/6$, FOR $t_0 = 1.5$ SEC AND A NO-FLOW BOUNDARY CONDITION.

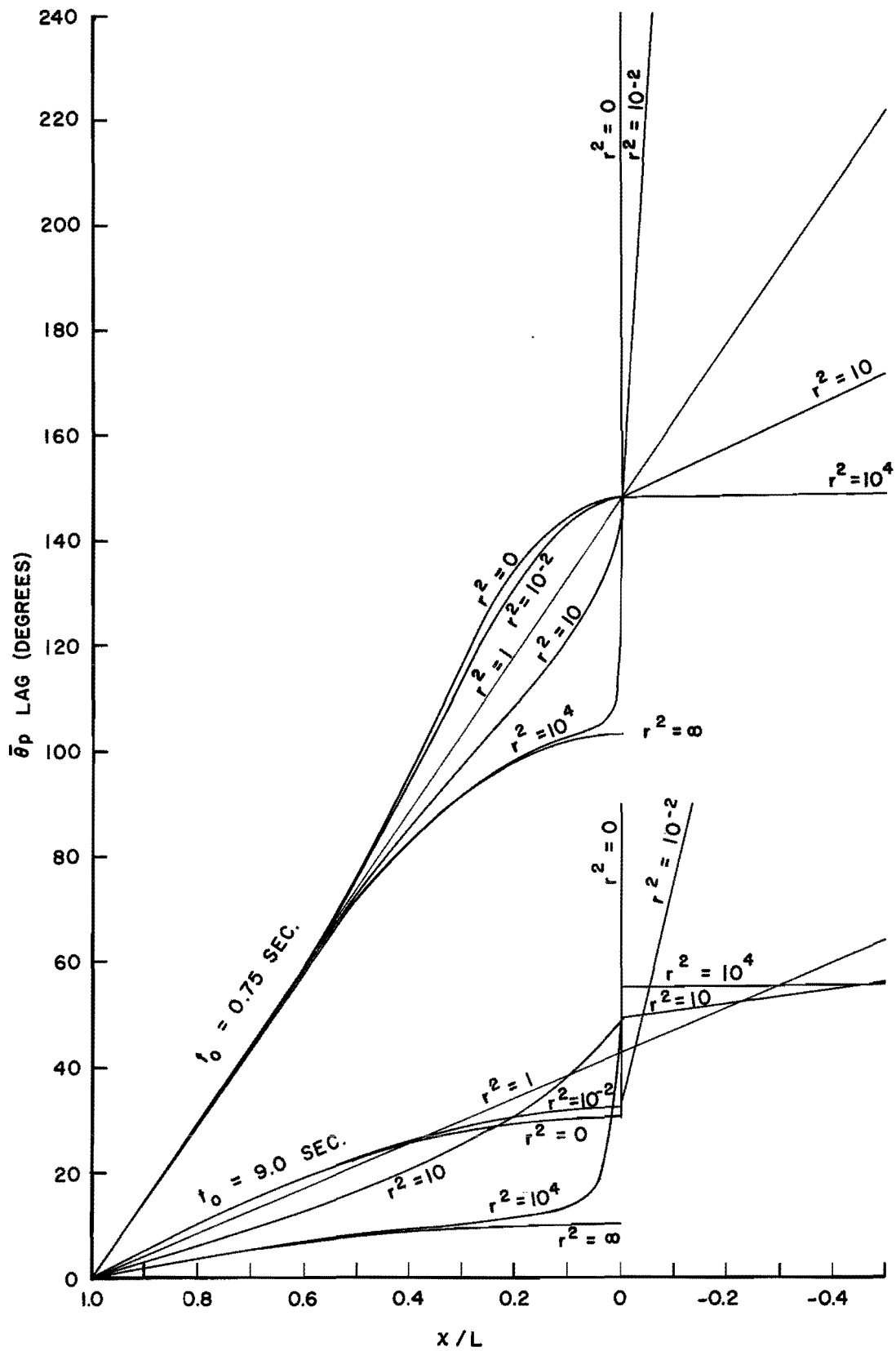
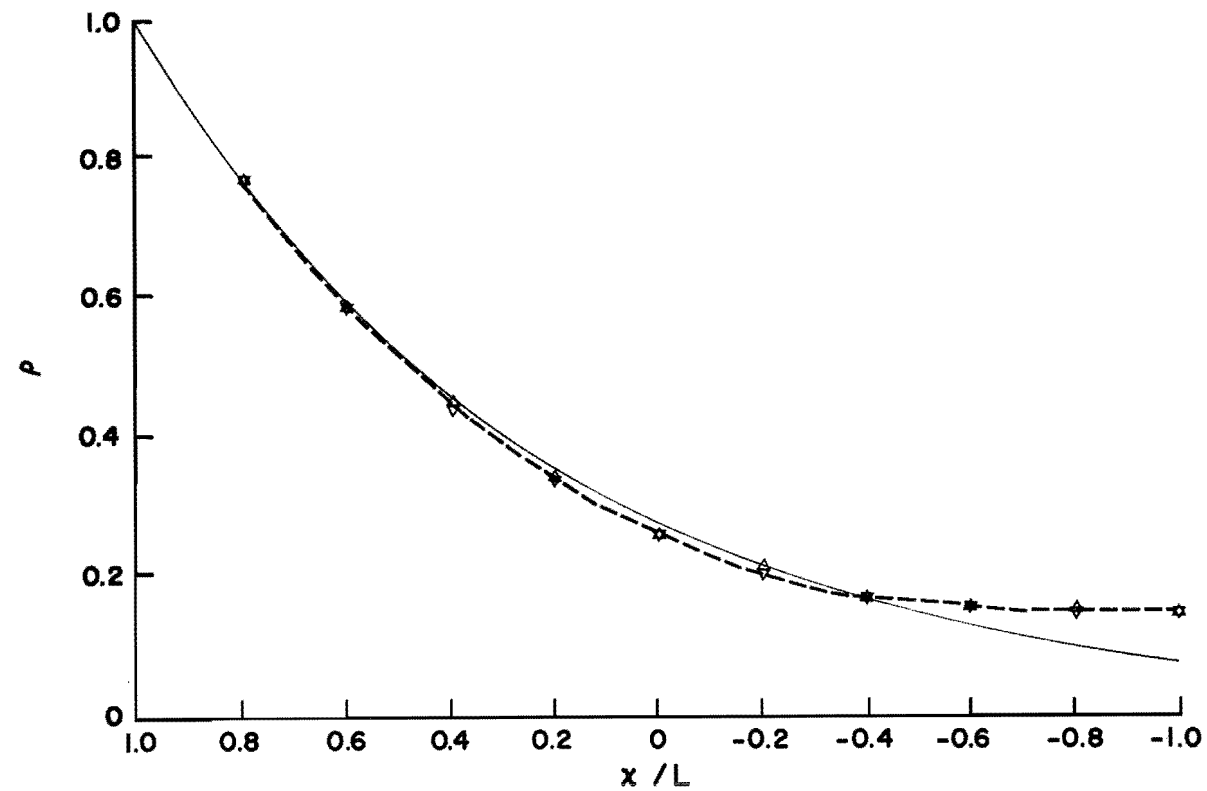


FIGURE 21. A COMPARISON OF THE PHASE ANGLE VS POSITION RELATION FOR SEVERAL VALUES OF r AND t_0 FOR THE DISCONTINUOUS PERMEABILITY MODEL.



— DAMP: $r^2 = 1.0$, i.e. SEMI-INFINITE AQUIFER
 --- DAMP: $r^2 = 0$, i.e. FINITE AQUIFER, LENGTH $2L$

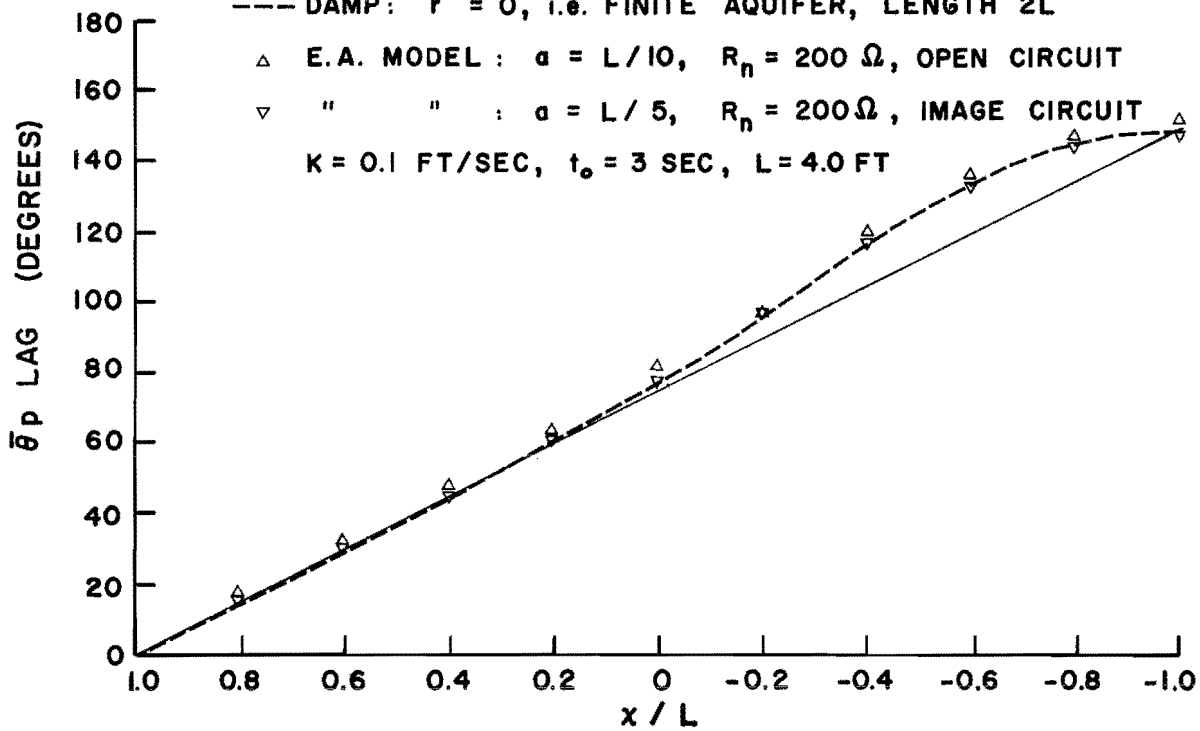


FIGURE 22. COMPARISON OF ELECTRIC ANALOGS HAVING AN IMAGE CIRCUIT AND AN OPEN CIRCUIT TO SIMULATE NO-FLOW BOUNDARY CONDITIONS.

values were common to all calculations: $D = \epsilon/\bar{z} = .01$, $a = 0.4$ ft., $L = 4.0$ ft., $C = .01\mu\text{f}$. The length L and the tidal periods were selected to facilitate direct comparisons of the results obtained in the reported study with those from future tests using the Hele-Shaw flow analog. However, the results can be projected to give the response of an aquifer characteristic of real field conditions. That is, if $a = 750$ ft., $S = .002$, $\bar{z} = 200$ ft., and $K = 1000$ ft/day for each 0.1 ft/sec used in the above calculations, then the amplitude and phase angle curves for the 3 sec and 1.5 sec period tides will represent the response of this characteristic aquifer to the diurnal and semi-diurnal tidal components, respectively.

The computer programs are included as Appendix B. DAMP (1 and 2), or *discontinuous aquifer-model permeability*, was the program used to evaluate equations (8b), (8d), and (10b), (10c) for regions 1 and 2, respectively, while VAMP, or *variable aquifer-model permeability*, was the program used to evaluate equations (18b) and (18c). The designations NF and CH indicate the no-flow and the constant-head boundary conditions, respectively. For the latter boundary condition, equations (18b) and (18c) are valid provided all the "1" subscripts are replaced with "0" subscripts, *i.e.*, only zero-order functions are required.

The solutions to the modified Bessels equation can be expressed as

$$K_{\nu}(i^{1/2}x) = \text{ker}_{\nu}x + i\text{kei}_{\nu}x$$

$$I_{\nu}(i^{1/2}x) = \text{ber}_{\nu}x + i\text{bei}_{\nu}x.$$

Hence, for VAMP, sub-routines were written for $\text{ber}_{\nu}x$, $\text{bei}_{\nu}x$, $\text{ker}_{\nu}x$, and $\text{kei}_{\nu}x$, using the first twenty terms of their respective series expansions. The functions M_{ν} , θ_{ν} , and N_{ν} , ϕ_{ν} were subsequently evaluated as the modulus and argument of the complex quantities K_{ν} and I_{ν} . The series expansions failed to converge to the correct value for arguments greater than about five,¹ as a result of the rapid in-

¹This does not limit the use of the program for field data, since real tidal components have periods of sufficient length to keep the argument less than five.

crease in the size of each successive term in the series and the limited capacity of the computer to represent such large numbers (*i.e.*, e^{170} is the maximum for the IBM 360 computer).

DISCUSSION OF THE RESULTS AND THE CONCLUSIONS

There is generally good agreement between the results of the mathematical and the electric analog models shown in Figures 3 through 6 and 8 through 19. This good agreement verifies the computer programs DAMP and VAMP. But more important, the good agreement verifies the mathematical models as representing the response of the two given non-homogeneous aquifers to tidal changes since such resistance-capacitance circuits have been shown, by Williams, *et al.* (1970), to model periodic flows in a porous media, provided the appropriate diffusion coefficient is used to determine the time scale factor.

An examination of the discontinuous aquifer model results shown in Figures 3 through 6 indicates clearly the discontinuity in the permeability since the slope of both the amplitude and the phase angle curves exhibit a discontinuous change at $x = 0$. In comparing results for the extreme values of r used (Figures 3 and 6), the steepness of both the amplitude and the phase angle curves is seen to increase across the discontinuity when $r^2 = 0.5$ because of the increased resistance to flow in region 2 of the aquifer. Also, the phase angle curves become slightly concave downwards in region 1 as $x = 0$ is approached from the coast, indicating that some positive reflection occurs as the disturbance moves into the less permeable or shallower region 2. However, when $r^2 = 1.5$, the steepness of both the amplitude and the phase angle curve decreases discontinuously when passing from region 1 into region 2. The phase angle curve becomes slightly concave upwards in region 1 as $x = 0$ is approached, indicating a partial negative reflection as the disturbance moves into the more permeable or deeper region 2. The variation of phase angle with position in region 2 is linear for both cases, as it should be for a semi-infinite aquifer.

The amplitude ρ , determined by the electric analog, is as much as 10 to 15 percent greater than that predicted by the mathematical model for the range $-1 \leq x/L \leq -0.3$ for the longest tidal period of

9 seconds. This error appears to increase as r increases, *i.e.*, as the resistance to flow in region 1 increases relative to that in region 2, and becomes evident in the amplitude *vs* position curves for a tidal period of 6 seconds when $r^2 > 1$. This error is most likely the result of modeling an aquifer of infinite extent in the x -direction by a resistance-capacitance circuit of finite length. In particular, the longer period fluctuations penetrate further into the aquifer model and the end of the finite length analog circuit provides a no-flow boundary and a subsequent partial positive reflection which increases the amplitude of the free surface fluctuation above that predicted by the mathematical model. When $r^2 > 1.0$, region 2 offers relatively less resistance to the flow than region 1, thereby permitting the shorter period fluctuations to penetrate further into region 2 with a resulting increase in the amount of energy reflected from the open-circuit end of the analog model.

Figure 7 indicates that the significant factor in the accuracy of the electric analog model for the semi-infinite aquifer is the extension, to $x = -2L$, of the fine grid spacing, $a = L/10$, when measurements are required for $x > -L$. Also, no significant difference in the accuracy is observed on extending the circuit from $x = -4L$ to $x = -8L$ with "lumped" components, *i.e.*, $a = L$, when $a = L/10$ is used only to $x = -L$. However, when $a = L/10$ is used to $x = -2L$, then extending the circuit to $x = -4L$ with lumped parameters reduced the error between prediction and measurement to approximately one-third of that observed for the circuit of the same length but using $a = L/10$ to $x = -L$. The extension of the circuit from $x = -4L$ to $x = -10L$, with lumped components and where $a = L/10$ for $x \geq -2L$ is seen to have relatively little influence on the amplitudes but does noticeably improve the agreement of the measured phase angles with the mathematical model predictions.

From the above discussion it is clear that the accuracy of the electric analog for the semi-infinite aquifer depends on both the finite difference grid spacing¹ and the length of the circuit. The rule for

¹It can be shown that errors caused by discretizing the problem space depend upon the grid spacing and the fourth and higher order derivatives of the solution function and are zero if these higher derivatives are zero. Since $h(x, t)$ has non-vanishing higher derivatives these errors are not zero for the tidal response problem. See Karplus, 1953.

extending the circuit is simply to add resistors and capacitors out to a point where changes in the voltage can no longer be detected. Since the decay in amplitude at a distance of one penetration length, *i.e.*, $\lambda = \sqrt{\frac{4 K_2 t_0}{\epsilon'}}$ for a semi-infinite aquifer is $1 - e^{-2\pi}$ or about 99.8 percent, it would seem reasonable that a circuit of length equivalent to or greater than one penetration length would be more than adequate. Penetration lengths for the tidal periods tested varied from 7.0' to 41.5' and are recorded in Table 3. The overall circuit length for region 2 was

TABLE 3. PENETRATION LENGTHS FOR SEMI-INFINITE AQUIFER IN REGION 2.

r ²	K ₂ FT/SEC	35.5 √K ₂ ^{**} FT/SEC ^{1/2}	λ ₂ (FT)				
			t ₀ = .75 SEC	t ₀ = 1.5 SEC	t ₀ = 3 SEC	t ₀ = 6 SEC	t ₀ = 9 SEC
.5	.05	7.92	7.03	9.7	14.06	19.4	23.8 10%
.8	.08	10.02	8.9	12.3	17.80	24.6 8%	30.3 13%
1.25	.125	12.58	11.18	15.3	22.36 ^{***} 17%	30.6 16%	37.6 17%
1.50	.150	13.80	12.22	16.85	24.44 17%	33.7 16%	41.5 17%
1.00	.100	11.20	9.94	13.75	19.88	27.5	33.6

$$** \lambda_2 = \sqrt{4\pi z_2 K_2 t_0 / \epsilon'} = (35.5 \sqrt{K_2}) \sqrt{t_0}$$

*** IN THE COLUMNS RECORDING THE PENETRATION LENGTH, λ, THE UPPER NUMBER IS λ AND THE LOWER NUMBER IS THE PERCENTAGE ERROR BETWEEN THE PREDICTED AND MEASURED AMPLITUDES.

equivalent to $10L = 40'$. Thus, it seems likely that the errors in the amplitude-position curves mentioned above are basically the result of not using the spacing of $a = L/10 = 0.4'$ for $x < -2L$. It is of interest to note that when $\lambda \geq 20'$, measured amplitudes begin to exceed predicted amplitudes in the neighborhood of $x = -L$. This implies that for the semi-infinite aquifer, no significant error will result from the circuit configuration if $a \leq \lambda/50$ and the circuit length is equivalent to 2λ ; furthermore, "lumped" components, *i.e.*, $a = \lambda/5$, may be used to extend the circuit beyond $x = .4\lambda$ if measurements are restricted to $x \geq -.2\lambda$.

Figures 8 through 13, representing the linearly varying permeability model with a no-flow boundary condition, reveal that a greater

attenuation of the tidal fluctuation is produced by an aquifer with permeability that increases rather than decreases with distance from the coast, *i.e.*, when $K_L/K_0 < 1$ (see also Fig. 20). This is the result of having a disproportionately greater portion of the energy attenuated in the less permeable region near the coastline. The phase angles at any given position are likewise greater when the permeability increases rather than decreases with distance from the coast. The phase angle curves for the case $K_L/K_0 < 1$ are generally concave downwards, while those for the case $K_L/K_0 > 1$ are concave downwards over the interior half of the aquifer but have a point of inflection at about $x/L = 0.5$. This point of inflection shifts towards the coastline as the ratio K_L/K_0 becomes smaller for a given tidal period (*e.g.* compare curves in Figs. 8, 10, and 12 for $t_0 = 1.5$ seconds), as well as when the tidal period becomes larger and the ratio K_L/K_0 remains fixed. This shift is the result of the reflected fluctuation being able to penetrate more closely to the coastline because of the relatively less resistive medium in the vicinity of the boundary for the former condition and because of increased energy in the longer period fluctuation for the latter condition.

The effect of the variable permeability when a constant-head boundary condition is applied is clearly visible in the amplitude curves of Figures 14 through 19. When the permeability increases with distance from the coast, these curves are concave upward, indicating a decreasing rate of attenuation as the tidal-generated fluctuation propagates into the interior of the aquifer. When the permeability decreases with distance from the coast, the amplitude curves are concave downward and the rate of attenuation increases as the fluctuation propagates into the interior.

The phase angle curves are generally concave downward, have no points of inflection, and give phase angles which are smaller than those for the no-flow boundary condition. The phase angles at the interior boundary are essentially equal regardless of whether the permeability increases or decreases, provided the change is linear and between the same extreme values of K .

The constant-head boundary produces a negative reflection and would represent a node in a standing-wave system, whereas the no-flow

boundary produces a positive reflection and would correspond to an anti-node in the same standing-wave system. Equations (8d) and (10c) have been used as bases for studying the effect on the phase angle of the partial positive and negative reflections which exist between these two limiting conditions of a positive reflection ($r^2 = 0$) and a negative reflection ($r^2 = \infty$), and the results are seen in Figure 21. From this figure, for $t_0 = 0.75$ seconds, it is clear that partial positive and negative reflections are characterized by phase-angle *vs* position curves which are concave downward and concave upward, respectively, in the neighborhood of the reflecting boundary (see also Fig. 3 to 6). In the limiting case of a complete negative reflection, the point of inflection is located at the reflecting boundary and the phase angle curve is entirely concave downward (see also Fig. 14 to 19). The shift of the point of inflection toward the coastline with increasing period for a positive reflection is evident on a comparison of the curves for $t_0 = .75$ sec and $t_0 = 9$ sec but having the same values of $r^2 < 1$.

It is worth noting that in the variable permeability model the incremental change used for $K(x)$ was 10 percent, and that errors of less than 10 percent between measured and predicted values of amplitude and phase angle were observed.

In light of the results as discussed above, the following conclusions are made:

1. The mathematical model developed for the one-dimensional semi-infinite coastal aquifer having a discontinuous change in permeability, or in both permeability and depth for the free surface aquifer, at a distance L from the coastline is valid provided that the assumptions delineated for equation (2) are satisfied. The mathematical model expressed by equations (8) and (10) and the corresponding computer program, DAMP 1 and 2, may be used to study the response of this aquifer to sinusoidal *tides* of a given period t_0 . In particular:

i. The steepness of both the amplitude and the phase-angle curves increase or decrease discontinuously at the section where the permeability decreases or increases discontinuously.

ii. A partial positive ($r^2 < 1$) or negative ($r^2 > 1$) reflection of energy takes place at the discontinuity. This partial

reflection is characterized by the curvature of the phase angle *vs* position curve in the neighborhood ($x/L \geq 0$) of the reflecting boundary: concave downward for a positive reflection and concave upward for a negative reflection. In the limiting case of a complete negative reflection, the point of inflection coincides with the reflecting boundary and the entire phase angle *vs* position curve is downward in region 1.

2. The mathematical model developed for the one-dimensional, finite coastal aquifer (confined or unconfined) of length L having a permeability which varies linearly with distance from the coastline is valid, provided the assumptions delineated for equation (2) are satisfied. The mathematical model as expressed by equation (18) and the corresponding computer program VAMP-CH¹ or VAMP-NF may be used to study the response of this aquifer to sinusoidal *tidal* fluctuations of period t_0 . In particular:

i. The amplitude *vs* position curves for a constant-head boundary condition are concave downward for a permeability which decreases with distance from the coast and are concave upward for a permeability which increases with distance from the coast.

ii. The amplitude *vs* position curves for a no-flow boundary condition flatten out more rapidly and indicate greater attenuation when the permeability increases rather than decreases with distance from the coast.

iii. The phase angles at a constant-head boundary are essentially the same regardless of whether the permeability increases or decreases, provided the change is linear and between the same extreme values of K .

iv. The phase angle *vs* position curves for the no-flow boundary condition are concave downward near the reflecting boundary with a point of inflection which shifts towards the coast when either the tidal period increases or the ratio K_L/K_0 decreases. This effect is most pronounced when $K_L/K_0 > 1$. When a constant-head boundary condition is maintained these curves are concave downward over their

¹If the constant-head boundary condition is used, all the first order functions must be replaced with zero order functions in equation (18).

entire range.

3. In the electric analog model of the semi-infinite aquifer, no significant error will result from the circuit configuration if $a \leq \lambda/50$ and the circuit length is equivalent to 2λ where λ is the tidal penetration length; furthermore, "lumped" components, *i.e.*, $a = \lambda/5$, may be used to extend the circuit beyond $x = -.4\lambda$ if measurements are restricted to $x \geq -.2\lambda$.

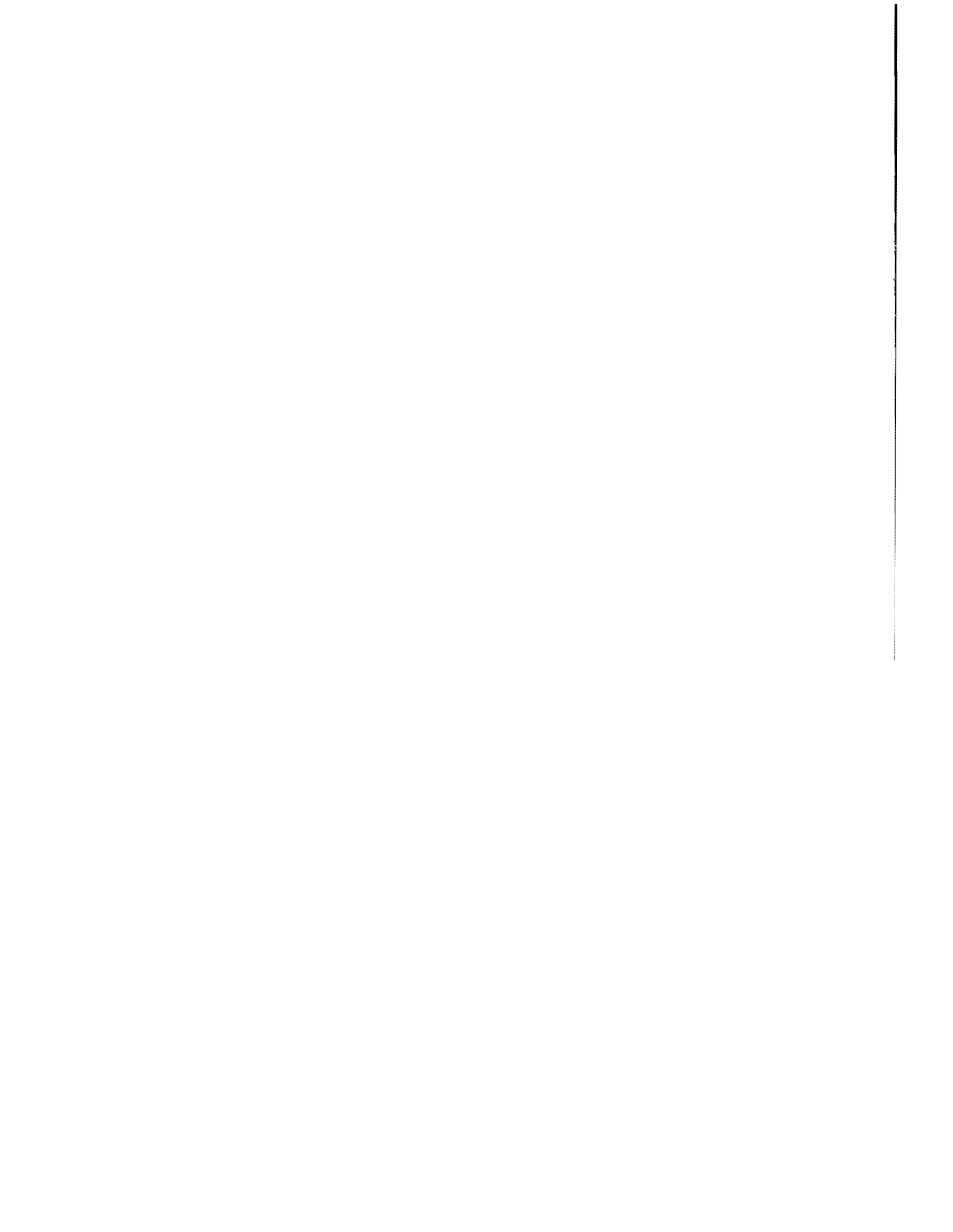
ACKNOWLEDGEMENTS

The authors would like to thank Mr. Ronald N. Wada for his assistance in the initial stages of writing the computer program and Drs. L. S. Lau and D. C. Cox for their helpful comments regarding the preparation of the manuscript.

REFERENCES

- Karplus, W. J. 1958. *Analog simulation*. McGraw-Hill Book Company, Inc., New York.
- McCracken, D. A. 1967. *Fortran IV manual*. John Wiley & Sons, Inc., New York, 4th printing.
- McLachlan, N. W. 1934. *Bessel functions for engineers*. Oxford University Press, London.
- Sneddon, I. N. 1969. *Special functions of mathematical physics and chemistry*. Oliver and Boyd, Edinburgh and London.
- Walton, W. C. and T. A. Prickett. 1963. "Hydrogeologic electric analog computers." *ASCE Journal of Hydraulic Division*. HY-6. pp. 67-91.
- Williams, John A., Ronald N. Wada, and Ru-yih Wang. 1970. *Model studies of tidal effects on ground water hydraulics*. Technical Report No. 39. Water Resources Research Center, University of Hawaii.
- Young, Andrew and Alan Kirk. 1964. Title of chapter - "Royal Society Mathematical Tables," In *Bessel Functions, Part IV, Kelvin Functions*. Royal Society, University Press, Cambridge. Vol. 10.

APPENDICES

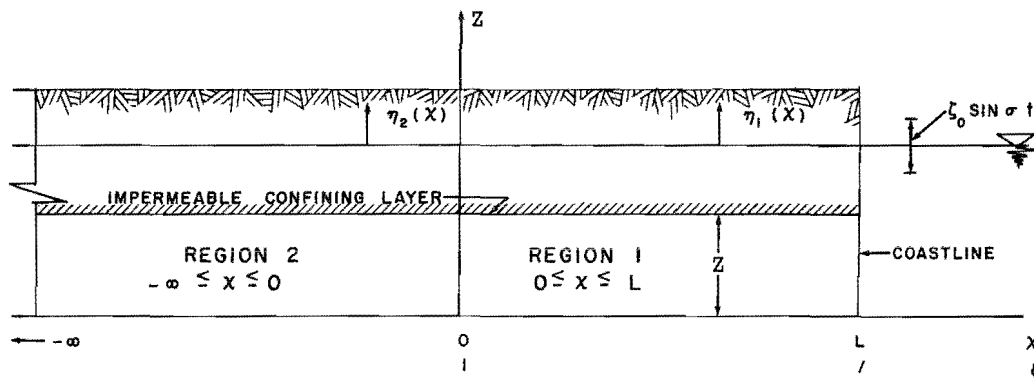
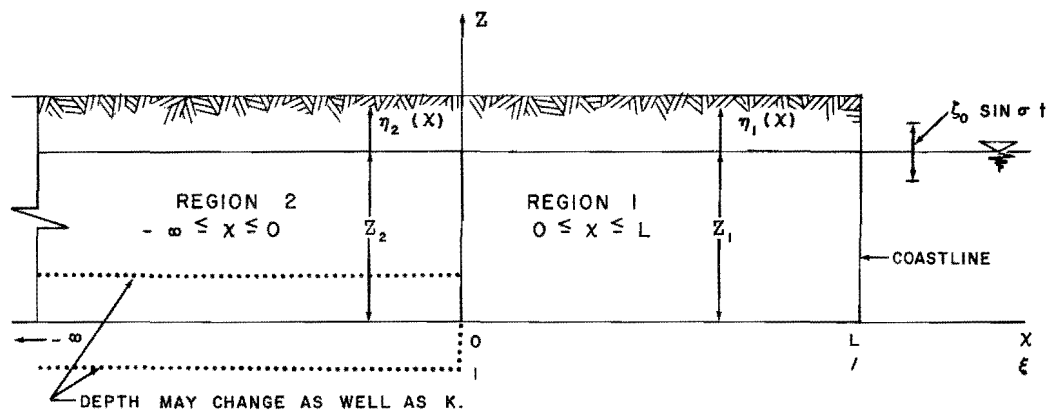


APPENDIX A. LIST OF SYMBOLS.

a	grid spacing in finite difference representation of the equations
a_{11}, \dots, a_{22}	constants of integration
A	coefficient composed of a product of zero and first order Kelvin functions
A_0, \dots, A_4	coefficients composed of combinations of circular and hyperbolic functions
b_{11}, \dots, b_{22}	constants of integration
B	coefficient composed of a product of zero and first order Kelvin functions
C	cosine, capacitance, and a coefficient composed of a product of zero and first order Kelvin functions
C_1, C_2	complex constants of integration
Ch	hyperbolic cosine
D	coefficient composed of a product of zero and first order Kelvin functions
D	coefficient expressing storage per unit volume of aquifer
e	base of natural logarithms
h	piezometric head
i	$\sqrt{-1}$
I_ν	Kelvin function of the first type of order ν
K, K_1, K_2	Darcy coefficient of permeability; in region 1; in region 2
K_L, K_0	Darcy coefficient of permeability at the coast; at the interior boundary
K_4	time scale factor for electric analog model
K_ν	Kelvin function of the second type of order ν
l	aquifer length in transformed coordinate system
L	aquifer length

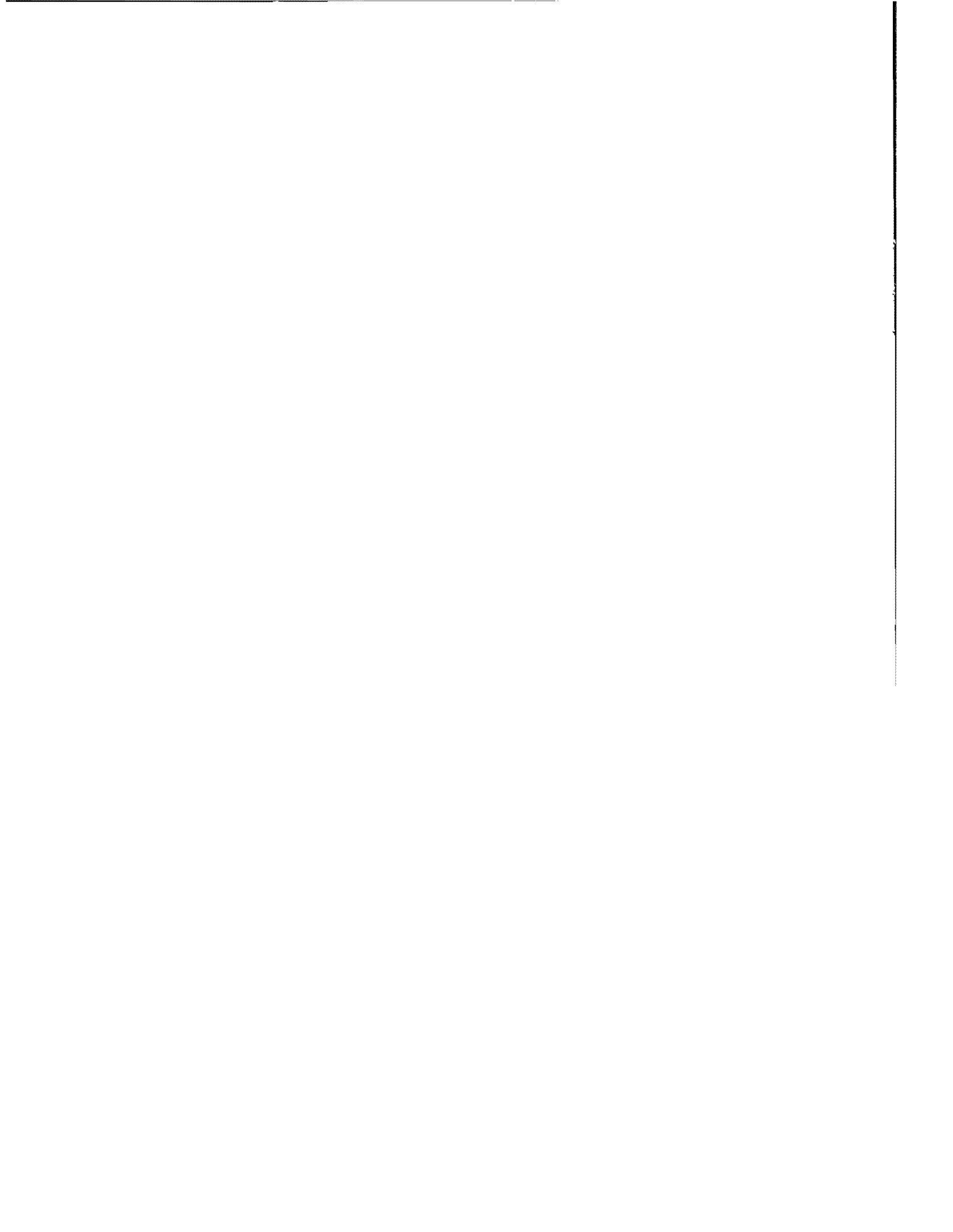
m', m	rate at which the permeability and the normalized permeability, respectively, change with position
M_U	modulus of $I_U(i^{1/2}x)$
n	integer
N	integer--total number of elements in finite difference representation of equations
N_U	modulus of $K_U(i^{1/2}x)$
r	square root of ratio of transmissibility in region 2 to that in region 1
R, R_1, \dots, R_N	electrical resistance
R	real part of
Sh	hyperbolic sine
S, S_s	storage and specific storage
t	time variable
t_0	period of the sinusoidal tide
T, T_1, T_2	transmissibility
w_0	specific weight of fluid
x, x_n	horizontal position variable; continuous and discretized
z	elevation of the free surface
$\bar{z}, \bar{z}_1, \bar{z}_2$	average elevation of the free surface and aquifer thickness
α	compressibility of porous media, coefficient combining aquifer properties and tidal period
A_0, A_1, A_2	coefficients composed of combinations of circular and hyperbolic functions
$\beta_0, \beta_1, \beta_2$	coefficients composed of combinations of circular and hyperbolic functions
$\varepsilon', \varepsilon$	apparent porosity, porosity
ζ_0	amplitude of tide
η	space varying part of piezometric head
θ_U	argument of $I_U(i^{1/2}x)$
θ_p	phase angle

λ	penetration length--the distance, normal to the coast, in a semi-infinite aquifer, to the point where fluctuations in h are in phase with the tide at the coastline.
ξ	transformed space variable
ρ	dimensionless amplitude
σ	angular frequency of tide
ϕ_0	argument of $K_0(i^{1/2}x)$
ψ_1, ψ_2	coefficients containing aquifer properties and tidal period
$\psi, \bar{\psi}, \bar{\psi}_1$	coefficients containing aquifer properties and tidal period



NOTE: FOR DISCONTINUOUS PERMEABILITY MODEL: $-\infty \leq x \leq L$ AND $r^2 = K_2 \bar{z}_2 / K_1 \bar{z}_1$
 FOR LINEARLY VARYING PERMEABILITY MODEL: $0 \leq x \leq L$ AND $K(x) = K_0(1 + mx)$
 WITH $\partial h / \partial x = 0$ OR $h = \text{CONSTANT}$ AT $x = 0$.

FIGURE A-1. SKETCH DEFINING THE AQUIFER MODELS ANALYZED.



APPENDIX B

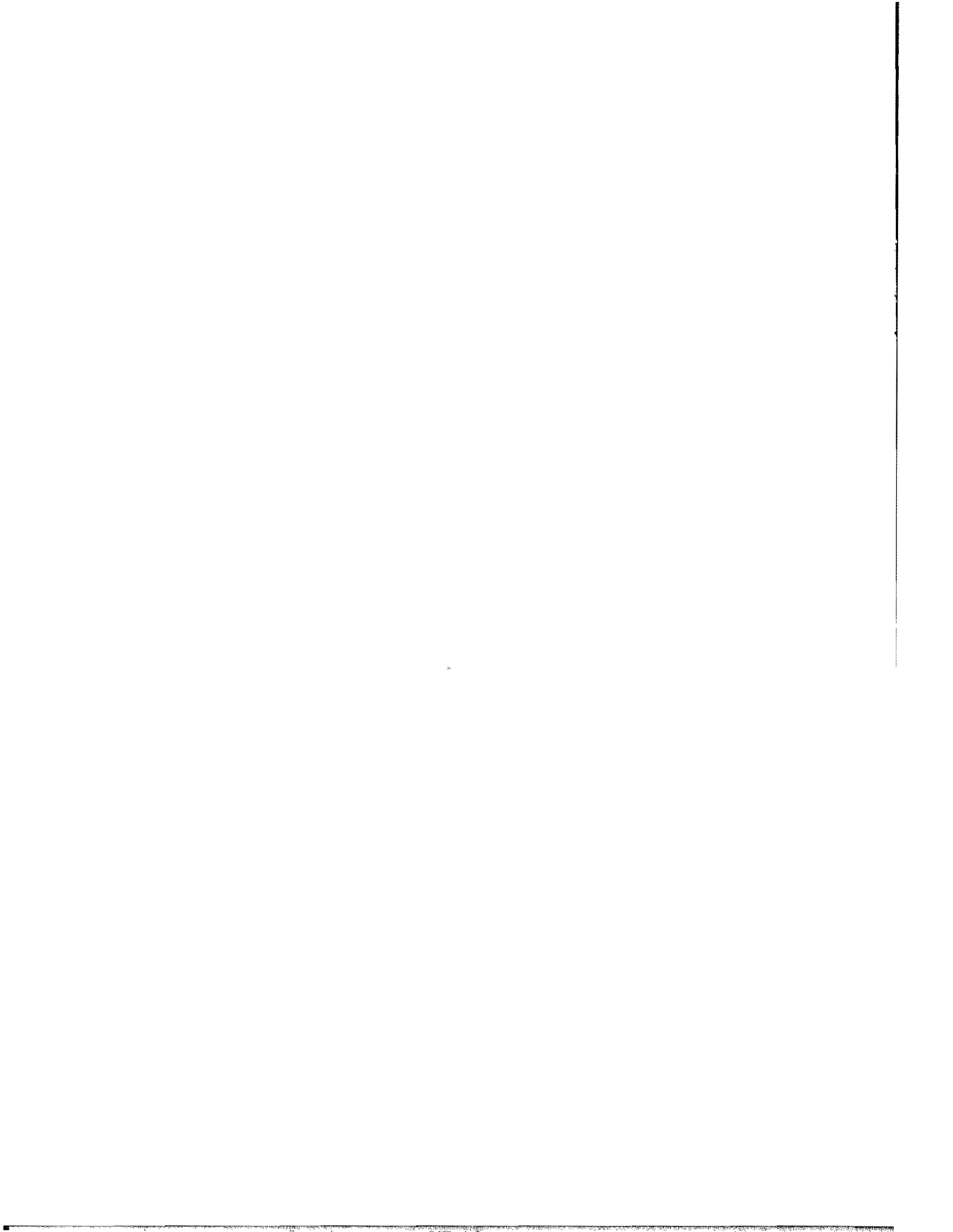
Computer programs and sample output for:

$$\text{DAMP - (1) - } K_1 = 0.1 \text{ ft/sec, } r^2 = 1/2$$

$$\text{DAMP - (2) - } K_1 = 0.1 \text{ ft/sec, } r^2 = 1/2$$

$$\text{VAMP - NF - } K_L/K_0 = 1/3, K_0 = 0.3 \text{ ft/sec}$$

$$\text{VAMP - CH - } K_L/K_0 = 1/3, K_0 = 0.3 \text{ ft/sec}$$



```

C      DAMP - REGION 1
10 READ (5, 1) PERIOD, CK1, AL1, R2
1  FORMAT (F5.2, F10.7, F6.3, F9.3)
   IF (PERIOD .EQ. 12.00) STOP
C      ARG1 = (SIGMA*EPSI) / (CK1*Z1) = (SIGMA*D) / CK1
C      ALPHA1 = (SQRT(ARG1/2.0)) * AL1
C      EPSI = PORCSITY
C      SIGMA = FREQUENCY = (2.0*PI)/(PERIOD) RAD/SEC
C      CK = PERMEABILITY
C      L1 = THE LENGTH OF REGION 1
C      R = ((K2*Z2)/(K1*Z1))**0.5  Z = DEPTH
C      R = SQRT(R2)
      SIGMA = 6.2831583/PERIOD
      D = 0.01
      ARG1 = (SIGMA*D) / CK1
      ALPHA1 = (SQRT(ARG1/2.0)) * AL1
      WRITE (6, 2) CK1, R2, PERIOD, ARG1
2  FORMAT (1H1,5HK1 = ,F9.6,4H FPS,2X,5HR2 = ,F7.3/1H0,9HPERIOD = ,
1      F5.2,4H SEC,2X,7HARG1 = ,F5.3/1H0,8HLOCATION,2X,
2      9HAMPLITUDE,2X,11HPHASE ANGLE)
C      X = LOCATION (DIMENSIONLESS)
C      DEGREE = PHASE ANGLE
C      CALCULATE AND PRINT THE AMPLITUDES AND PHASE ANGLES FOR VALUES OF X
      TENX = 10.0
20 X = TENX/10.0
      CA = COS(ALPHA1)
      CAX = CCS(ALPHA1*X)
      SA = SIN(ALPHA1)
      SAX = SIN(ALPHA1*X)
      CHA = COSH(ALPHA1)
      CHAX = CCOSH(ALPHA1*X)
      SHA = SINH(ALPHA1)
      SHAX = SINH(ALPHA1*X)
      AOX = (CAX**2) + (SHAX**2)
      AOL = (CA**2) + (SHA**2)
      A4X = (SAX**2) + (SHAX**2)
      A4L = (SA**2) + (SHA**2)
      A0 = AOX*AOL
      A1 = (2.0*CHAX*SHAX*AOL) + (2.0*CHA*SHA*AOX)
      A2 = (4.0*CHAX*CHA*SHAX*SHA) + (A4X*AOL) + (A4L * AOX)
      A3 = (2.0*CHAX*SHAX*A4L) + (2.0*CHA*SHA*A4X)
      A4 = A4X*A4L
      RHO1 = (A0 + A1*R + A2*(R**2) + A3*(R**3) + A4*(R**4))
      RHO2 = (AOL + 2.0*R*CHA*SHA + (R**2)*A4L) ** 2
      RHO = SQRT(RHO1/RHO2)
      TAO = CAX*CHAX*SA*SHA - CA*CHA*SAX*SHAX
      TA1 = CAX*SA*SHAX*SHA + CAX*CHAX*CHA*SA - CA*SAX*SHAX*SHA -
3      CA*CHA*CHA*SAX
      TA2 = CAX*CHA*SA*SHAX - CA*CHA*SAX*SHA
      TEO = SAX*SHAX*SA*SHA + CAX*CHAX*CA*CHA
      TB1 = CAX*CA*CHAX*SHA + CAX*CA*CHA*SHAX + CHA*SAX*SA*SHAX +
4      CHAX*SAX*SA*SHA
      TB2 = CAX*CA*SHAX*SHA + CHAX*CHA*SAX*SA
      TAM = (TA0 + TA1*R + TA2*(R**2.0)) / (TE0 + TB1*R + TB2*(R**2.0))
      THETA = ATAN(TAM)
      DEGREE = THETA * (360/6.2831853)

```

```

WRITE (6, 3) X, RHO, DEGREE
3 FORMAT (1H0,F4.2,7X,F7.5,4X,F10.5)
C X IS PRINTED UNDER LOCATION HEADING
C RHO IS PRINTED UNDER AMPLITUDE HEADING
C DEGREE IS PRINTED UNDER PHASE ANGLE HEADING
IF (X .EQ. 0.0) GO TO 10
TENX = TENX - 1.0
GO TO 20
END

```

OUTPUT - DAMP REGION 1

```

K1 = 0.100000 FPS R2 = 0.500
PERIOD = 3.00 SEC ARG1 = 0.209
LOCATION  AMPLITUDE  PHASE ANGLE
1.00      1.00000     -0.00000
0.90      0.87817      7.72643
0.80      0.77250     15.53953
0.70      0.68136     23.42622
0.60      0.60322     31.35088
0.50      0.53662     39.24757
0.40      0.48010     47.01573
0.30      0.43216     54.52057
0.20      0.39128     61.60020
0.10      0.35592     68.07764
0.0       0.32463     73.77243

```

```

C      DAMP - REGION 2
10 READ (5, 1) PERIOD, CK1, AL1, R2
   1 FORMAT (F5.2, F10.7, F6.3, F9.3)
   IF (PERIOD .EQ. 12.00) STOP
C      ARG1 = (SIGMA*EPSI) / (CK1*Z1) = (SIGMA*D) / CK1
C      ARG2 = ARG1 / R2
C      ALPHA1 = (SQRT(ARG1/2.0)) * AL1
C      ALPHA2 = (SQRT(ARG2/2.0)) * AL1
C      EPSI = POROSITY
C      SIGMA = FREQUENCY = (2.0*PI) / PERIOD   RAD/SEC
C      CK = PERMEABILITY
C      AL1 = THE LENGTH OF REGION 1
C      R = ((K2*Z2)/(K1*Z1))**.5      Z = DEPTH
C      R2 = R**2
C      R = SQRT(R2)
C      SIGMA = 6.2831583 / PERIOD
C      D = 0.01
C      ARG1 = (SIGMA*D) / CK1
C      ARG2 = ARG1 / R2
C      ALPHA1 = (SQRT(ARG1/2.0)) * AL1
C      ALPHA2 = (SQRT(ARG2/2.0)) * AL1
   WRITE (6, 2) CK1, R2, PERIOD, ARG2
   2 FORMAT (1H1,5HK1 = ,F9.6,4H FPS,2X,5HR2 = ,F7.3/1H0,9HPERIOD = ,
   1      F5.2,4H SEC,2X,7HARG2 = ,F5.3/1H0,8HLOCATION,2X,
   2      9HAMPLITUDE,2X,11HPHASE ANGLE)
C      X = LOCATION (DIMENSIONLESS)
C      DEGREE = PHASE ANGLE
C      CALCULATE AND PRINT THE AMPLITUDES AND PHASE ANGLES FOR VALUES OF X
   TENX = 0.0
20 X = TENX/10.0
   CA1 = COS(ALPHA1)
   SA1 = SIN(ALPHA1)
   A2X = ALPHA2 * X
   CA2X = COS(A2X)
   SA2X = SIN(A2X)
   CHA1 = COSH(ALPHA1)
   SHA1 = SINH(ALPHA1)
   RHO1 = (2.7183)**(A2X)
   RHO2 = ((CA1**2 + SHA1**2) + (2.C*R*CHA1*SHA1)
   3      + (R**2)*(SA1**2 + SHA1**2)) ** (0.5)
   RHO = (RHO1) / (RHO2)
   TAM1 = (CA2X*SA1*SHA1 - CA1*CHA1*SA2X)
   4      + R*(CA2X*CHA1*SA1 - CA1*SA2X*SHA1)
   TAM2 = (CA2X*CA1*CHA1 + SA2X*SA1*SHA1)
   5      + R*(CA2X*CA1*SHA1 + CHA1*SA2X*SA1)
   TAM = (TAM1) / (TAM2)
   THETA = ATAN(TAM)
   DEGREE = THETA * (360/6.2831853)
   WRITE (6, 3) X, RHO, DEGREE
   3 FORMAT (1H0,F5.2,6X,F7.5,4X,F10.5)
C      X IS PRINTED UNDER LOCATION HEADING
C      RHO IS PRINTED UNDER AMPLITUDE HEADING
C      DEGREE IS PRINTED UNDER PHASE ANGLE HEADING
   IF (X .EQ. -1.0) GO TO 10
   TENX = TENX - 1.0
   GO TO 20

```

END

OUTPUT - DAMP REGION 2

K1 = 0.100000 FPS R2 = 0.500
PERIOD = 3.00 SEC ARG2 = 0.419

LOCATION	AMPLITUDE	PHASE ANGLE
0.0	0.32463	73.77243
-0.10	0.27033	84.26086
-0.20	0.22511	-85.25060
-0.30	0.18745	-74.76215
-0.40	0.15609	-64.27371
-0.50	0.12998	-53.78529
-0.60	0.10824	-43.29694
-0.70	0.09013	-32.80850
-0.80	0.07506	-22.32005
-0.90	0.06250	-11.83163
-1.00	0.05204	-1.34314


```

C      VAMP - NF
C      THIS PROGRAM IS USED TO CALCULATE THE AMPLITUDE AND THE PHASE
C      ANGLE FOR COASTAL AQUIFER WITH LINEAR INCREASE OR DECREASE IN
C      PERMEABILITY, NO FLOW AT INTERNAL BOUNDARY
C      DOUBLE PRECISION AL, CL, CKL, CKO, M, CD, PERIOD, SIGMA, ALPHA,
1      TENX, X, XI, P, PB, P1, BEROP, BEIOP, A12, A1, A2, CKROP,
2      CKIOP, A32, A3, A4, BER1PB, BEI1PB, B12, B1, B2, CKR1PB,
3      CKI1PB, B32, B3, B4, BEROP1, BEIOP1, C12, C1, C2, CKROP1,
4      CKIOP1, C32, C3, C4, A, B, C, D, RI, RXI, RL, RCL, R, RHO,
5      SCA, SINA, AS, SCB, SINB, BS, SCC, SINC, CS, SCD, SIND, DS,
6      TS, COSA, AC, COSB, BC, CESC, CC, COSD, DC, TC, TAM, THETAP
7      , DEGREE
C      AL = THE LENGTH BETWEEN INTERIOR BOUNDARY AND COASTLINE
C      CKL = THE PERMEABILITY AT (X) = L      (FT/SEC)
C      CKO = THE PERMEABILITY AT (X) = 0      (FT/SEC)
C      SIGMA = FREQUENCY
C      X = (X) / L      THE RELATIVE LOCATION FROM INTERIOR BOUNDARY
C      P = PSI
C      PB = PSI BAR
C      P1 = PSI BAR1
C      BEROP = BERO FUNCTION WITH ARGUMENT P
C      BEIOP = BEIO FUNCTION WITH ARGUMENT P
C      CKROP = KERO FUNCTION WITH ARGUMENT P
C      CKIOP = KEIO FUNCTION WITH ARGUMENT P
C      RHO = AMPLITUDE
C      DEGREE = PHASE ANGLE
10     READ (5, 20) CKO, CKL
20     FORMAT (2D15.7)
      IF (CKL .EQ. 0.0000000D 00) STOP
      AL = 4.0
      CL = CKL / CKO
      M = (CL - 1.0) / AL
      CD = 0.01
      PERIOD = 3.0
1      SIGMA = 6.2831853 / PERIOD
      ALPHA = (SIGMA * CD) / (M * M * CKO)
      WRITE (6, 30) CKO, CKL, PERIOD, ALPHA
30     FORMAT (1H1, 5HKO = , D13.7, 4X, 5HKL = , D13.7/1H0, 9HPERIOD = ,
4      D9.3, 4X, 8HALPHA = , D10.4/1H0, 8HLOCATION, 4X, 9HAMPLITUDE,
5      7X, 11HPHASE ANGLE)
      TENX = 20.0
2      X = TENX / 20.0
      XI = 1.0 + (M * AL * X)
      P = DSQRT(4.0 * ALPHA * XI)
      PB = DSQRT(4.0 * ALPHA)
      P1 = DSQRT(4.0 * ALPHA * CL)
      CALL CALBER (BEROP, P)
      CALL CALBEI (BEIOP, P)
      A12 = (BEROP * BEROP) + (BEIOP * BEIOP)
      A1 = DSQRT(A12)
      A2 = DATAN(BEIOP / BEROP)
      IF (BEROP .LT. 0.0 .AND. BEIOP .GT. 0.0) A2 = A2 + 3.1415927
      IF (BEROP .LT. 0.0 .AND. BEIOP .LT. 0.0) A2 = A2 + 3.1415927
      IF (BEROP .GT. 0.0 .AND. BEIOP .LT. 0.0) A2 = A2 + 6.2831853
      CALL CALKER (CKROP, P)
      CALL CALKEI (CKIOP, P)

```

```

A32 = (CKROP * CKROP) + (CKIOP * CKIOP)
A3 = DSQRT(A32)
A4 = DATAN(CKIOP / CKROP)
IF (CKROP .LT. 0.0 .AND. CKIOP .GT. 0.0) A4 = A4 + 3.1415927
IF (CKROP .LT. 0.0 .AND. CKIOP .LT. 0.0) A4 = A4 + 3.1415927
IF (CKROP .GT. 0.0 .AND. CKIOP .LT. 0.0) A4 = A4 + 6.2831853
CALL CABER1 (BER1PB, PB)
CALL CABE11 (BEI1PB, PB)
B12 = (BER1PB * BER1PB) + (BEI1PB * BEI1PB)
B1 = DSQRT(B12)
B2 = DATAN(BEI1PB / BER1PB)
IF (BER1PB .LT. 0.0 .AND. BEI1PB .GT. 0.0) B2 = B2 + 3.1415927
IF (BER1PB .LT. 0.0 .AND. BEI1PB .LT. 0.0) B2 = B2 + 3.1415927
IF (BER1PB .GT. 0.0 .AND. BEI1PB .LT. 0.0) B2 = B2 + 6.2831853
CALL CAKER1 (CKR1PB, PB)
CALL CAKE11 (CKI1PB, PB)
B32 = (CKR1PB * CKR1PB) + (CKI1PB * CKI1PB)
B3 = DSQRT(B32)
B4 = DATAN(CKI1PB / CKR1PB)
IF (CKR1PB .LT. 0.0 .AND. CKI1PB .GT. 0.0) B4 = B4 + 3.1415927
IF (CKR1PB .LT. 0.0 .AND. CKI1PB .LT. 0.0) B4 = B4 + 3.1415927
IF (CKR1PB .GT. 0.0 .AND. CKI1PB .LT. 0.0) B4 = B4 + 6.2831853
CALL CALBER (BEROP1, P1)
CALL CALBEI (BEIOP1, P1)
C12 = (BEROP1 * BEROP1) + (BEIOP1 * BEIOP1)
C1 = DSQRT(C12)
C2 = DATAN(BEIOP1 / BEROP1)
IF (BEROP1 .LT. 0.0 .AND. BEIOP1 .GT. 0.0) C2 = C2 + 3.1415927
IF (BEROP1 .LT. 0.0 .AND. BEIOP1 .LT. 0.0) C2 = C2 + 3.1415927
IF (BEROP1 .GT. 0.0 .AND. BEIOP1 .LT. 0.0) C2 = C2 + 6.2831853
CALL CALKER (CKROP1, P1)
CALL CALKEI (CKIOP1, P1)
C32 = (CKROP1 * CKROP1) + (CKIOP1 * CKIOP1)
C3 = DSQRT(C32)
C4 = DATAN(CKIOP1 / CKROP1)
IF (CKROP1 .LT. 0.0 .AND. CKIOP1 .GT. 0.0) C4 = C4 + 3.1415927
IF (CKROP1 .LT. 0.0 .AND. CKIOP1 .LT. 0.0) C4 = C4 + 3.1415927
IF (CKROP1 .GT. 0.0 .AND. CKIOP1 .LT. 0.0) C4 = C4 + 6.2831853
A = A1 * C3 * B1 * B3
B = B12 * C3 * A3
C = C1 * A1 * B32
D = C1 * B1 * A3 * B3
RI = ((A2 - B2) - (A4 - B4))
RXI = (B32 * A12) + (B12 * A32)
$ - (2.0 * B1 * B3 * A1 * A3 * DCCS(RI))
RL = ((C2 - B2) - (C4 - B4))
RCL = (B32 * C12) + (B12 * C32)
$ - (2.0 * B1 * B3 * C1 * C3 * DCCS(RL))
R = RXI / RCL
RHO = DSQRT(DABS(R))
SCA = ((A2 - B2) - (C4 - B4))
SINA = DSIN(SCA)
AS = A * SINA
SCB = (A4 - C4)
SINB = DSIN(SCB)
BS = B * SINB

```

```

SCC = (A2 - C2)
SINC = DSIN(SCC)
CS = C * SINC
SCD = ((A4 - B4) - (C2 - B2))
SIND = DSIN(SCD)
DS = D * SIND
TS = -AS + BS + CS - DS
COA = DCOS(SCA)
AC = A * COA
COB = DCOS(SCB)
BC = B * COB
COC = DCOS(SCC)
CC = C * COC
COD = DCOS(SCD)
DC = D * COD
TC = -AC + BC + CC - DC
TAM = TS / TC
THETAP = DATAN(TAM)
IF (TS .GT. 0.0 .AND. TC .GT. 0.0) THETAP = THETAP - 6.2831853
IF (TS .GT. 0.0 .AND. TC .LT. 0.0) THETAP = THETAP - 3.1415927
IF (TS .LT. 0.0 .AND. TC .LT. 0.0) THETAP = THETAP - 3.1415927
DEGREE = THETAP * (360.0 / 6.2831853)
WRITE (6, 40) X, RHO, DEGREE
40 FORMAT (1H0, D9.3, D15.6, D16.6)
IF (TENX .EQ. 0.0) GO TO 3
TENX = TENX - 1.0
GO TO 2
3 PERIOD = PERIOD + 3.0
IF (PERIOD .EQ. 6.0) GO TO 10
GO TO 1
END

```

```

C SUBROUTINE CALKER (BKER, Z)
  THIS PROGRAM CALCULATES THE KERO FUNCTION
  DOUBLE PRECISION Z, RF, RFM1, S, S1, Y, SUM, BER, BEI, R, R2, X,
1  TERM, W, BKER, XX, TI2, TIP12, TIM12
  RF = 1.0
  RFM1 = 1.0
  S = 0.0
  S1 = 0.0
  Y = 1.0
  SUM = 0.0
  CALL CALBER (BER, Z)
  CALL CALBEI (BEI, Z)
  W = ((0.1159 - DLOG(Z)) * BER) + ((1.0 / 4.0) * 3.1415927 * BEI)
  DO 3 I = 2, 30, 2
  R = I
  RF = RF * R
  RFM1 = RFM1 * (R - 1.0)
  R2 = (RF * RFM1) ** 2
  S = S + (1.0 / R)
  S1 = S1 + (1.0 / (R - 1.0))
  X = (0.500 * Z) ** (2.0 * R)
  Y = Y * (-1.0)

```

```

    TERM = (X * Y * (S + S1)) / R2
    SUM = SUM + TERM
    BKER = W + SUM
    IF (DABS(TERM) .LE. 1.0E-10) GO TO 4
3  CONTINUE
4  RETURN
    END

```

```

C  SUBROUTINE CALKEI (BKEI, Z)
    THIS PROGRAM CALCULATES THE KEIO FUNCTION
    DOUBLE PRECISION RF, RFM1, S, S1, Y, SUM, BER, BEI, R, R2, X,
1   TERM, W, BKEI, XX, Z
    RF = 1.0
    RFM1 = 1.0
    S = 1.0
    S1 = 0.0
    Y = 1.0
    SUM = (Z/2)**2
    CALL CALBER (BER, Z)
    CALL CALBEI (BEI, Z)
    W = ((0.1159 - DLOG(Z)) * BEI) - ((3.1415927 * BER) / 4.0)
    DO 3 I = 3, 31, 2
    R = I
    RF = RF * R
    RFM1 = RFM1 * (R - 1.0)
    R2 = (RF * RFM1)**2
    S = S + (1.0 / R)
    S1 = S1 + (1.0 / (R - 1.0))
    X = (Z/2)**(2.0*R)
    Y = Y * (-1.0)
    TERM = (X * Y * (S + S1)) / R2
    SUM = SUM + TERM
    BKEI = W + SUM
    IF (DABS(TERM) .LE. 1.0E-10) GO TO 4
3  CONTINUE
4  RETURN
    END

```

```

C  SUBROUTINE CAKER1 (BKER1, Z)
    THIS PROGRAM CALCULATES THE KER1 FUNCTION
    DOUBLE PRECISION Z, RF, RPIF, S, S1, SUM, BER1, BEI1, W, Y, R,
1   THETA, X, TERM, THETA1, SUM1, PTS, BKER1
    RF = 1.0
    RPIF = 1.0
    S = 0.0
    S1 = 1.0
    SUM = 0.0
    CALL CABER1 (BER1, Z)
    CALL CABE11 (BEI1, Z)
    W = ((0.1159 - DLOG(Z)) * BER1) + ((1.0 / 4.0) * 3.1415927 * BEI1)
    DO 3 I = 1, 20
    Y = (-1.0) ** (1 + I)

```

```

R = I
THETA = 0.250 * (1.0 + (2.0 * R)) * 3.1415927
RF = RF * R
RP1F = RP1F * (R + 1.0)
S = S + (1.0 / R)
S1 = S1 + (1.0 / (R + 1.0))
X = (0.5 * Z) ** (1.0 + (2.0 * R))
TERM = 0.500 * ((X * Y * (S + S1) * DCOS(THETA)) / (RF * RP1F))
SUM = SUM + TERM
THETA1 = 0.250 * 3.1415927
SUM1 = ((-1.0) / Z) * DCOS(THETA1)
PTS = (-0.250 * Z) * DCCS(THETA1)
BKER1 = W + SUM1 + PTS + SUM
IF (DABS(TERM) .LE. 1.0E-10) GO TO 4
3 CONTINUE
4 RETURN
END

```

```

C SUBROUTINE CAKE11 (BKE11, Z)
  THIS PROGRAM CALCULATES THE KE11 FUNCTION
  DOUBLE PRECISION Z, RF, RP1F, S, S1, SUM, BER1, BE11, W, Y, R,
1   THETA, X, TERM, THETA1, SUM1, PTS, BKE11
  RF = 1.0
  RP1F = 1.0
  S = 0.0
  S1 = 1.0
  SUM = 0.0
  CALL CABER1 (BER1, Z)
  CALL CABE11 (BE11, Z)
  W = ((0.1159 - DLOG(Z)) * BE11) - ((1.0 / 4.0) * 3.1415927 * BER1)
  DO 3 I = 1, 20
  Y = (-1.0) ** (1 + I)
  R = I
  THETA = 0.250 * (1.0 + (2.0 * R)) * 3.1415927
  RF = RF * R
  RP1F = RP1F * (R + 1.0)
  S = S + (1.0 / R)
  S1 = S1 + (1.0 / (R + 1.0))
  X = (0.5 * Z) ** (1.0 + (2.0 * R))
  TERM = 0.500 * ((X * Y * (S + S1) * DSIN(THETA)) / (RF * RP1F))
  SUM = SUM + TERM
  THETA1 = 0.250 * 3.1415927
  SUM1 = ((-1.0) / Z) * DSIN(THETA1)
  PTS = (-0.250 * Z) * DSIN(THETA1)
  BKE11 = W + SUM1 - PTS - SUM
  IF (DABS(TERM) .LE. 1.0E-10) GO TO 4
3 CONTINUE
4 RETURN
END

```

```

C SUBROUTINE CALBER (BER, X)
  THIS PROGRAM CALCULATES THE BERO FUNCTION

```

```

DOUBLE PRECISION TIPI2, TI2, XX, Y, X, TERM, BER
BER = 1.0
TERM = 1.0
DO 3 I = 1, 100
TI2 = (2 * I) ** 2
TIPI2 = ((2 * I) - 1) ** 2
XX = ((0.25) * (X ** 2)) ** 2
Y = ((-1) * XX) / (TI2 * TIPI2)
TERM = TERM * Y
BER = BER + TERM
IF (DABS(TERM) .LE. 1.0E-07) GO TO 4
3 CONTINUE
4 RETURN
END

```

```

C
SUBROUTINE CALBEI (BEI, X)
THIS PROGRAM CALCULATES THE BEI0 FUNCTION
DOUBLE PRECISION TI2, TIM12, XX, Y, X, TERM, BEI
TERM = 0.25 * (X ** 2)
BEI = 0.25 * (X ** 2)
DO 3 I = 1, 100
TI2 = (2 * I) ** 2
TIM12 = ((2 * I) + 1) ** 2
XX = ((0.25) * (X ** 2)) ** 2
Y = ((-1) * XX) / (TI2 * TIM12)
TERM = TERM * Y
BEI = BEI + TERM
IF (DABS(TERM) .LE. 1.0E-07) GO TO 4
3 CONTINUE
4 RETURN
END

```

```

C
SUBROUTINE CABER1 (BERS1, X)
THIS PROGRAM CALCULATES THE BER1 FUNCTION
DOUBLE PRECISION BER1, TERM1, BER2, TERM2, X, FTI2, FTIM1, XX,
1 Y1, STI, STIP2, STIP12, Y2, BERS1
BER1 = 1.0
TERM1 = 1.0
BER2 = ((0.5 * X) ** 2) / 2.0
TERM2 = ((0.5 * X) ** 2) / 2.0
DO 3 I = 1, 100
FTI2 = (2 * I) ** 2
FTIP1 = (2 * I) + 1
FTIM1 = (2 * I) - 1
XX = (0.5 * X) ** 4
Y1 = ((-1.0) * XX) / (FTI2 * FTIP1 * FTIM1)
TERM1 = TERM1 * Y1
BER1 = BER1 + TERM1
STI = (2 * I)
STIP12 = ((2 * I) + 1) ** 2
STIP2 = (2 * I) + 2
Y2 = ((-1.0) * XX) / (STI * STIP12 * STIP2)

```

```

TERM2 = TERM2 * Y2
BER2 = BER2 + TERM2
BERS1 = (BER1 + BER2) * ((-X) / (2 * SQRT(2.0)))
IF (DABS(TERM1) .LE. 1.0D-07 .OR. DABS(TERM2) .LE. 1.0D-07)
  2GO TO 4
3 CONTINUE
4 RETURN
END

```

```

C SUBROUTINE CABE11 (BERS1, X)
  THIS PROGRAM CALCULATES THE BE11 FUNCTION
  DOUBLE PRECISION BER1, TERM1, X, BER2, TERM2, FTI2, FTIP1, FTIM1,
1  XX, Y1, STI , STIP12, STIP2, Y2, BERS1
  BER1 = 1.0
  TERM1 = 1.0
  BER2 = ((-1.0) * ((0.5 * X) ** 2)) / 2.0
  TERM2 = ((-1.0) * ((0.5 * X) ** 2)) / 2.0
  DO 3 I = 1, 100
  FTI2 = (2 * I) ** 2
  FTIP1 = (2 * I) + 1
  FTIM1 = (2 * I) - 1
  XX = (0.5 * X) ** 4
  Y1 = ((-1.0) * XX) / (FTI2 * FTIP1 * FTIM1)
  TERM1 = TERM1 * Y1
  BER1 = BER1 + TERM1
  STI = (2 * I)
  STIP12 = ((2 * I) + 1) ** 2
  STIP2 = (2 * I) + 2
  Y2 = ((-1.0) * XX) / (STI * STIP12 * STIP2)
  TERM2 = TERM2 * Y2
  BER2 = BER2 + TERM2
  BERS1 = (BER1 + BER2) * (X / (2 * SQRT(2.0)))
  IF (DABS(TERM1) .LE. 1.0D-07 .OR. DABS(TERM2) .LE. 1.0D-07)
  2GO TO 4
3 CONTINUE
4 RETURN
END

```

OUTPUT - VAMP NF

```

KO = 0.3000000D 00    KL = 0.1000000D 00
PERIOD = 0.300D 01    ALPHA = 0.2513D 01

LOCATION    AMPLITUDE    PHASE ANGLE
0.100D 01    0.100000D 01    -0.810611D-15
0.950D 00    0.935486D 00    -0.573245D 01
0.900D 00    0.885169D 00    -0.112010D 02
0.850D 00    0.846213D 00    -0.163584D 02

```

0.8000 00	0.816327D 00	-0.211657D 02
0.7500 00	0.793638D 00	-0.255955D 02
0.7000 00	0.776618D 00	-0.296334D 02
0.6500 00	0.764020D 00	-0.332767D 02
0.6000 00	0.754837D 00	-0.365324D 02
0.5500 00	0.748261D 00	-0.394145D 02
0.5000 00	0.743648D 00	-0.419417D 02
0.4500 00	0.740493D 00	-0.441353D 02
0.4000 00	0.738402D 00	-0.460176D 02
0.3500 00	0.737068D 00	-0.476106D 02
0.3000 00	0.736260D 00	-0.489356D 02
0.2500 00	0.735803D 00	-0.500126D 02
0.2000 00	0.735569D 00	-0.508599D 02
0.1500 00	0.735464D 00	-0.514943D 02
0.1000 00	0.735428D 00	-0.519313D 02
0.5000-01	0.735420D 00	-0.521844D 02
0.0	0.735420D 00	-0.522662D 02


```

C      VAMP-CH
C      THIS PROGRAM IS USED TO CALCULATE THE AMPLITUDE AND THE PHASE
C      ANGLE FOR COASTAL AQUIFER WITH LINEAR INCREASE OR DECREASE IN
C      PERMEABILITY, CONSTANT HEAD AT INTERNAL BOUNDARY
C      DOUBLE PRECISION AL, CL, CKL, CKO, M, CD, PERIOD, SIGMA, ALPHA,
1      TENX, X, XI, F, PB, P1, BEROP, BEIOP, A12, A1, A2, CKROP,
2      CKICP, A32, A3, A4, BEROPB, BEIOPB, B12, B1, B2, CKROPB,
3      CKIOPB, B32, B3, B4, BEROP1, BEIOP1, C12, C1, C2, CKROP1,
4      CKIOP1, C32, C3, C4, A, B, C, D, FI, RXI, RL, RCL, R, RHO,
5      SCA, SINA, AS, SCB, SINB, BS, SCC, SINC, CS, SCD, SIND, DS,
6      TS, COSA, AC, COSB, BC, COSC, CC, COSD, DC, TC, TAM, THETAP
7      , DEGREE
C      AL = THE LENGTH BETWEEN INTERIOR BOUNDARY AND COASTLINE
C      CKL = THE PERMEABILITY AT (X) = L      (FT/SEC)
C      CKO = THE PERMEABILITY AT (X) = 0      (FT/SEC)
C      SIGMA = FREQUENCY
C      X = (X) / L      THE RELATIVE LOCATION FROM INTERIOR BOUNDARY
C      P = PSI
C      PB = PSI BAR
C      P1 = PSI BAR1
C      BEROP = BERO FUNCTION WITH ARGUMENT P
C      BEIOP = BEIO FUNCTION WITH ARGUMENT P
C      CKROP = KERO FUNCTION WITH ARGUMENT P
C      CKIOP = KEIO FUNCTION WITH ARGUMENT P
C      RHO = AMPLITUDE
C      DEGREE = PHASE ANGLE
10     READ (5, 20) CKO, CKL
20     FORMAT (2D15.7)
      IF (CKL .EQ. 0.00000000) STOP
      AL = 4.0
      CL = CKL / CKO
      M = (CL - 1.0) / AL
      CD = 0.01
      PERIOD = 3.0
1     SIGMA = 6.2831853 / PERIOD
      ALPHA = (SIGMA * CD) / (M * M * CKO)
      WRITE (6, 30) CKO, CKL, PERIOD, ALPHA
30     FORMAT (1H1, 5HKO = , D13.7, 4X, 5HKL = , D13.7/1H0, 5HPERIOD = ,
8     D9.3, 4X, 8HALPHA = , D10.4/1H0, 8HLOCATION, 4X, 5HAMPLITUDE,
9     7X, 11HPHASE ANGLE)
      TENX = 20.0
2     X = TENX / 20.0
      XI = 1.0 + (M * AL * X)
      P = DSQRT(4.0 * ALPHA * XI)
      PB = DSQRT(4.0 * ALPHA)
      P1 = DSQRT(4.0 * ALPHA * CL)
      CALL CALBER (BEROP, P)
      CALL CALBEI (BEIOP, P)
      A12 = (BEROP * BEROP) + (BEIOP * BEIOP)
      A1 = DSQRT(A12)
      A2 = DATAN(BEIOP / BEROP)
      IF (BEROP .LT. 0.0 .AND. BEIOP .GT. 0.0) A2 = A2 + 3.1415927
      IF (BEROP .LT. 0.0 .AND. BEIOP .LT. 0.0) A2 = A2 + 3.1415927
      IF (BEROP .GT. 0.0 .AND. BEIOP .LT. 0.0) A2 = A2 + 6.2831853
      CALL CALKER (CKROP, P)
      CALL CALKEI (CKIOP, P)

```

```

A32 = (CKROP * CKROP) + (CKIOP * CKIOP)
A3 = CSQRT(A32)
A4 = DATAN(CKIOP / CKROP)
IF (CKROP .LT. 0.0 .AND. CKIOP .GT. 0.0) A4 = A4 + 3.1415927
IF (CKRCP .LT. 0.0 .AND. CKIOP .LT. 0.0) A4 = A4 + 3.1415927
IF (CKROP .GT. 0.0 .AND. CKIOP .LT. 0.0) A4 = A4 + 6.2831853
CALL CALBER (BEROPB, PB)
CALL CALBEI (BEIOPB, PB)
B12 = (BEROPB * BEROPB) + (BEIOPB * BEIOPB)
B1 = CSQRT(B12)
B2 = DATAN(BEIOPB / BEROPB)
IF (BERCPB .LT. 0.0 .AND. BEIOPB .GT. 0.0) B2 = B2 + 3.1415927
IF (BEROPB .LT. 0.0 .AND. BEIOPB .LT. 0.0) B2 = B2 + 3.1415927
IF (BERCPB .GT. 0.0 .AND. BEIOPB .LT. 0.0) B2 = B2 + 6.2831853
CALL CALKER (CKROPB, PB)
CALL CALKEI (CKIOPB, PB)
B32 = (CKROPB * CKROPB) + (CKIOPB * CKIOPB)
B3 = CSQRT(B32)
B4 = DATAN(CKIOPB / CKROPB)
IF (CKROPB .LT. 0.0 .AND. CKIOPB .GT. 0.0) B4 = B4 + 3.1415927
IF (CKROPB .LT. 0.0 .AND. CKIOPB .LT. 0.0) B4 = B4 + 3.1415927
IF (CKRCPB .GT. 0.0 .AND. CKIOPB .LT. 0.0) B4 = B4 + 6.2831853
CALL CALBER (BEROP1, P1)
CALL CALBEI (BEIOP1, P1)
C12 = (BERCP1 * BERCP1) + (BEIOP1 * BEIOP1)
C1 = CSQRT(C12)
C2 = DATAN(BEIOP1 / BEROP1)
IF (BEROP1 .LT. 0.0 .AND. BEIOP1 .GT. 0.0) C2 = C2 + 3.1415927
IF (BEROP1 .LT. 0.0 .AND. BEIOP1 .LT. 0.0) C2 = C2 + 3.1415927
IF (BEROP1 .GT. 0.0 .AND. BEIOP1 .LT. 0.0) C2 = C2 + 6.2831853
CALL CALKER (CKRO1, P1)
CALL CALKEI (CKIO1, P1)
C32 = (CKRCP1 * CKRCP1) + (CKIO1 * CKIO1)
C3 = CSQRT(C32)
C4 = DATAN(CKIO1 / CKRO1)
IF (CKRCP1 .LT. 0.0 .AND. CKIO1 .GT. 0.0) C4 = C4 + 3.1415927
IF (CKRCP1 .LT. 0.0 .AND. CKIO1 .LT. 0.0) C4 = C4 + 3.1415927
IF (CKRCP1 .GT. 0.0 .AND. CKIO1 .LT. 0.0) C4 = C4 + 6.2831853
A = A1 * C3 * B1 * B3
E = B12 * C3 * A3
C = C1 * A1 * B32
D = C1 * B1 * A3 * B3
RI = ((A2 - B2) - (A4 - B4))
RXI = (B32 * A12) + (B12 * A32)
$ - (2.0 * B1 * B3 * A1 * A3 * DCOS(RI))
RL = ((C2 - B2) - (C4 - B4))
RCL = (B32 * C12) + (B12 * C32)
$ - (2.0 * B1 * B3 * C1 * C3 * DCOS(RL))
R = RXI / RCL
R+C = DSGRT(DABS(R))
SCA = ((A2 - B2) - (C4 - B4))
SINA = DSIN(SCA)
AS = A * SINA
SCB = (A4 - C4)
SINB = DSIN(SCB)
ES = B * SINB

```

```

SCC = (A2 - C2)
SINC = DSIN(SCC)
CS = C * SINC
SCD = ((A4 - B4) - (C2 - B2))
SIND = DSIN(SCD)
DS = D * SIND
TS = -AS + BS + CS - DS
CCSA = DCCS(SCA)
AC = A * CCSA
COSB = DCCS(SCB)
BC = B * CCSB
COSC = DCCS(SCC)
CC = C * CCSC
CCSD = DCCS(SCD)
DC = D * CCSD
TC = -AC + BC + CC - DC
TAM = TS / TC
THETAP = DATAN(TAM)
IF (TS .GT. 0.0 .AND. TC .GT. 0.0) THETAP = THETAP - 6.2831853
IF (TS .GT. 0.0 .AND. TC .LT. 0.0) THETAP = THETAP - 3.1415927
IF (TS .LT. 0.0 .AND. TC .LT. 0.0) THETAP = THETAP - 3.1415927
DEGREE = THETAP * (360.0 / 6.2831853)
WRITE (6, 40) X, RHC, DEGREE
40 FFORMAT (1F0, D9.3, D15.6, D16.6)
IF (TENX .EQ. 0.0) GO TO 3
TENX = TENX - 1.0
GO TO 2
3 PERIOD = PERIOD + 3.0
IF (PERIOD .EQ. 6.0) GO TO 10
GO TO 1
END

```

```

C SUBROUTINE CALKER (BKER, Z)
  THIS PROGRAM CALCULATES THE KERO FUNCTION
  DOUBLE PRECISION Z, RF, RFM1, S, S1, Y, SUM, BER, BEI, R, R2, X,
1  TERM, W, BKER, XX, TI2, TIP12, TIM12
  RF = 1.0
  RFM1 = 1.0
  S = 0.0
  S1 = 0.0
  Y = 1.0
  SUM = 0.0
  CALL CALBER (BER, Z)
  CALL CALBEI (BEI, Z)
  W = ((0.1159 - DLG(Z)) * BER) + ((1.0 / 4.0) * 3.1415927 * BEI)
  DO 3 I = 2, 30, 2
  R = I
  RF = RF * R
  RFM1 = RFM1 * (R - 1.0)
  R2 = (RF * RFM1) ** 2
  S = S + (1.0 / R)
  S1 = S1 + (1.0 / (R - 1.0))
  X = (0.500 * Z) ** (2.0 * R)
  Y = Y * (-1.0)

```

```

    TERM = (X * Y * (S + S1)) / R2
    SUM = SUM + TERM
    BKER = W + SUM
    IF (DABS(TERM) .LE. 1.0D-10) GO TO 4
3 CONTINUE
4 RETURN
END

```

```

C   SUBROUTINE CALKEI (BKEI, Z)
    THIS PROGRAM CALCULATES THE KEIO FUNCTION
    DOUBLE PRECISION RF, RFM1, S, S1, Y, SUM, BER, BEI, R, R2, X,
1   TERM, W, BKEI, XX, Z
    RF = 1.0
    RFM1 = 1.0
    S = 1.0
    S1 = 0.0
    Y = 1.0
    SUM = (Z/2)**2
    CALL CALBER (BER, Z)
    CALL CALBEI (BEI, Z)
    W = ((0.1159 - DLG(Z)) * BEI) - ((3.1415927 * BER) / 4.0)
    DO 3 I = 2, 31, 2
    R = I
    RF = RF * R
    RFM1 = RFM1 * (R - 1.0)
    R2 = (RF * RFM1)**2
    S = S + (1.0 / R)
    S1 = S1 + (1.0 / (R - 1.0))
    X = (Z/2)**(2.0*R)
    Y = Y * (-1.0)
    TERM = (X * Y * (S + S1)) / R2
    SUM = SUM + TERM
    BKEI = W + SUM
    IF (DABS(TERM) .LE. 1.0D-10) GO TO 4
3 CONTINUE
4 RETURN
END

```

```

C   SUBROUTINE CALBER (BER, X)
    THIS PROGRAM CALCULATES THE BERO FUNCTION
    DOUBLE PRECISION TI12, TI2, XX, Y, X, TERM, BER
    BER = 1.0
    TERM = 1.0
    DO 3 I = 1, 100
    TI2 = (2 * I) ** 2
    TI12 = ((2 * I) - 1) ** 2
    XX = ((0.25) * (X ** 2)) ** 2
    Y = ((-1) * XX) / (TI2 * TI12)
    TERM = TERM * Y
    BER = BER + TERM
    IF (DABS(TERM) .LE. 1.0D-07) GO TO 4
3 CONTINUE

```

```
4 RETURN
END
```

```
C
SUBROUTINE CALBEI (BEI, X)
THIS PROGRAM CALCULATES THE BEIC FUNCTION
DOUBLE PRECISION TI2, TIM12, XX, Y, X, TERM, BEI
TERM = 0.25 * (X ** 2)
BEI = 0.25 * (X ** 2)
DO 3 I = 1, 100
TI2 = (2 * I) ** 2
TIM12 = ((2 * I) + 1) ** 2
XX = ((0.25) * (X ** 2)) ** 2
Y = ((-1) * XX) / (TI2 * TIM12)
TERM = TERM * Y
BEI = BEI + TERM
IF (DABS(TERM) .LE. 1.0D-07) GO TO 4
3 CONTINUE
4 RETURN
END
```

OUTPUT - VAMP CH

```
KC = 0.30000000 00    KL = 0.10000000 00
PERIOD = 0.3000 01    ALPHA = 0.25130 01
LOCATION      AMPLITUDE      PHASE ANGLE
0.1000 01    0.1000000 01    0.0
0.9500 00    0.9093290 00    -0.2194040 01
0.9000 00    0.8276990 00    -0.4153980 01
0.8500 00    0.7534420 00    -0.5506970 01
0.8000 00    0.6853020 00    -0.7475350 01
0.7500 00    0.6223120 00    -0.8877810 01
0.7000 00    0.5637120 00    -0.1013020 02
0.6500 00    0.5089010 00    -0.1124590 02
0.6000 00    0.4573910 00    -0.1223670 02
0.5500 00    0.4087850 00    -0.1311260 02
0.5000 00    0.3627560 00    -0.1388260 02
0.4500 00    0.3190290 00    -0.1455450 02
0.4000 00    0.2773750 00    -0.1513510 02
```

C.3500 00	C.237556D 00	-C.156306D 02
C.3000 00	C.199526D 00	-C.160465D 02
C.2500 00	C.163018C 00	-C.163878D 02
C.2000 00	C.127948D 00	-C.166589D 02
C.1500 00	C.942028C-01	-C.168639D 02
C.1000 00	C.616863C-01	-C.170063D 02
C.5000-01	C.303112C-01	-C.170896D 02